OULU 2012
C 417

ACTA

UNIVERSITATIS OULUENSIS

Jari Ruuska

SPECIAL MEASUREMENTS AND CONTROL MODELS FOR A BASIC OXYGEN FURNACE (BOF)

UNIVERSITY OF OULU GRADUATE SCHOOL;
UNIVERSITY OF OULU, FACULTY OF TECHNOLOGY,
DEPARTMENT OF PROCESS AND ENVIRONMENTAL ENGINEERING

ACTA UNIVERSITATIS OULUENSIS
C Technica 417

JARI RUUSKA

SPECIAL MEASUREMENTS AND CONTROL MODELS FOR A BASIC OXYGEN FURNACE (BOF)

Academic dissertation to be presented with the assent of the Doctoral Training Committee of Technology and Natural Sciences of the University of Oulu for public defence in Kuusamonsali (Auditorium YB210), Linnanmaa, on 11 May 2012, at 12 noon

UNIVERSITY OF OULU, OULU 2012

Acta Univ. Oul. C 417, 2012

Supervised by
Professor Kauko Leiviskä

Reviewed by
Professor Lauri Holappa
Doctor Matti Luomala

ISBN 978-951-42-9801-1 (Paperback)
ISBN 978-951-42-9802-8 (PDF)

ISSN 0355-3213 (Printed)
ISSN 1796-2226 (Online)

Cover Design
Raimo Ahonen

JUVENES PRINT
TAMPERE 2012

Ruuska, Jari, Special measurements and control models for a basic oxygen furnace (BOF).
University of Oulu Graduate School; University of Oulu, Faculty of Technology, Department of Process and Environmental Engineering, P.O. Box 4300, FI-90014 University of Oulu, Finland
Acta Univ. Oul. C 417, 2012

Abstract

The target in this thesis was to study selected special measurements in a basic oxygen furnace (BOF) and develop a model to predict the steel temperature at the end of the oxygen blow. Furthermore, the work aimed at increasing knowledge on measurements and phenomena in the converter and in this way improve the possibility of more efficient monitoring and control of the process.

Special measurements were investigated to obtain more knowledge about their usability in running the converter process. Analysing the measurement results also led to new process knowledge. The usage of a Radio Wave Interferometer (RWI) was seen as beneficial as it makes it possible to see the rising trend of the liquid surface level in advance and to perform some corrective actions to avoid excessive foaming and possible splashing out from the converter. Acoustic measurement could also detect trends in advance, but it was found to be sensitive to disturbing noise from the surroundings. Splashing measurement gives information about the current state of the slag but not advance information. Nevertheless, the measurements revealed several factors that usually increase splashing. It would be best to use the knowledge from two different measurements, for example RWI and splashing measurement, to predict increasing splashing, which causes significant iron losses.

The development of the models for end temperature prediction and additional materials provided a lot of knowledge about the factors affecting the temperature. Factors that were used in grouping were the BOF number, heat size and end carbon content. However, there were many heats that did not satisfy the target. Furthermore, there is a need for additional research into temperature progress and its control in BOF. It would also be useful to study the effect of additional materials more systematically.

There are other factors, such as the oxygen flow rate and lance height, which affect the temperature that are not included in the models. Some of the factors are measurable and some are not. There is still a need for more research in this area. This work strengthens the impression that the converter process is a complex one. It was noticed; as always in process development, that continuous monitoring and efforts are required to observe the changes in process conditions, raw materials or running practices. Otherwise, the benefit of the improvements and models will be lessened. However, it would be possible to set acknowledged routines and warnings into the improved monitoring system to help the operators notice the need for system tuning. A monitoring system would provide financial benefits in terms of having fewer reblowings, better yield and better quality of final product. Savings in raw materials can also be attained as the controllability of the process becomes better. As the monitoring system contains a database of guidelines, it would form a good basis for new employees to become familiar with the process and thus facilitate their training.

Keywords: basic oxygen furnace, monitoring, RWI, splashing, temperature model, temperature sensor

Ruuska, Jari, Teräskonvertterin erikoismittaukset ja ohjausmallit.
Oulun yliopiston tutkijakoulu; Oulun yliopisto, Teknillinen tiedekunta, Prosessi- ja ympäristötekniikan osasto, PL 4300, 90014 Oulun yliopisto
Acta Univ. Oul. C 417, 2012
Oulu

Tiivistelmä

Tämän opinnäytteen tarkoitus oli tutkia teräskonvertterin valittuja erikoismittauksia ja kehittää malli ennustamaan teräksen lämpötilaa happipuhalluksen lopussa. Työn tarkoituksena oli lisätä tietämystä mittauksista ja ilmiöistä konvertterissa ja tällä tapaa lisätä mahdollisuuksia prosessin tehokkaampaan monitorointiin ja ohjaukseen.

Erikoismittauksia tutkittiin lisätietämyksen saamiseksi niiden käytettävyydestä konvertteriprosessin ajossa. Mittausten analysointi tuotti myös uutta prosessitietämystä. Radioaaltointerferometrin (RWI) käyttö koettiin hyödylliseksi, koska on mahdollista havaita kuonan pinnankorkeuden nousu ennakkoon ja suorittaa joitakin korjaavia toimenpiteitä liiallisen kuohumisen ja lopulta roiskumisen estämiseksi ulos konvertterista. Äänimittaus voi myös havaita trendin ennakkoon, mutta huomattiin sen olevan herkkä ympäristön häiriöäänille. Roiskemittaus antaa tietoa kuonan sen hetkisestä tilasta, mutta ei ennakkoon. Mittaukset toivat kuitenkin esiin useita tekijöitä, jotka yleensä lisäävät roiskumista. Olisi parasta käyttää kahden eri mittauksen tietoa, RWI ja roiskemittaus, ennustettaessa lisääntyvää roiskumista, joka aiheuttaa huomattavia rautahäviöitä.

Loppulämpötilan ennustamiseen kehitetyn mallin ja lisäainemallin kehittäminen antoi paljon tietoa tekijöistä, jotka vaikuttavat lämpötilaan. Tekijät, joita käytettiin ryhmittelyssä, olivat konvertterinumero, panoskoko ja loppuhiilipitoisuus. Mallin soveltamisesta huolimatta jäi edelleen useita sulatuksia, jotka eivät osuneet tavoitteeseen. On edelleen tarve teräskonvertterin lämpötilakäyttäytymisen ja sen hallinnan lisätutkimukselle konvertterissa. Myös lisäaineiden vaikutusta lämpötilaan olisi hyödyllistä tutkia systemaattisemmin.

On edelleen muita tekijöitä, esimerkiksi hapen virtausnopeus ja lanssin korkeus, jotka vaikuttavat lämpötilaan, mutta jotka eivät ole mukana malleissa. Osa näistä tekijöistä on mitattavia suureita ja osa ei. Lisätutkimukselle on edelleen tilaa tällä alueella. Tämä työ vahvistaa edelleen käsitystä, että konvertteriprosessi on monimutkainen. Huomattiin, kuten aina prosessikehityksessä, että jatkuvaa kehitystyötä pitää tehdä prosessiolosuhteiden, raaka-aineiden ja ajopraktiikoiden muutosten huomaamiseksi. Muuten parannusten ja mallien antama hyöty heikkenee. Monitorointijärjestelmään olisi mahdollista kehittää rutiineja ja varoituksia operaattorien avuksi, jotta he huomaisivat järjestelmävirityksen tarpeen. Monitorointijärjestelmä toisi taloudellista hyötyä, mm. lisäpuhallusten vähentymisen, lopputuotteen paremman saannon ja laadun muodossa. Raaka-ainesäästöjä voidaan saavuttaa prosessin ohjattavuuden parantuessa. Monitorointijärjestelmän sisältäessä sääntötietokannan, se luo hyvän pohjan uusille työntekijöille tutustua prosessiin ja näin heidän koulutuksensa onnistuisi helpommin.

Asiasanat: lämpötila-anturi, lämpötilamalli, monitorointi, roiskuminen, RWI, teräskonvertteri

Acknowledgements

The research work reported in this thesis was done in the Control Engineering Laboratory of the University of Oulu. I want to express my gratitude to all the people who have supported me during the work. In particular, I wish to thank my supervisor, Professor Kauko Leiviskä, for his valuable guidance and feedback during the research.

I am most grateful to the reviewers of this thesis, Professor Lauri Holappa and Matti Luomala, D.Sc. (Tech).

I would like to thank the personnel of Ruukki Raahe steelworks for their great help during this research; especially I want to thank Seppo Ollila, my co-author in the papers, and Jarmo Lilja. I want to thank the personnel of Control Engineering Laboratory; special thanks are addressed to Aki Sorsa. In addition, special thanks go to Jarmo Keski-Säntti.

The work was financed mostly by Tekes and Ruukki. I am grateful that I had the opportunity to work on two very interesting projects concerning the BOF. I would also like to acknowledge the support from Tekniikan edistämissäätiö.

I would also like to thank my parents, Oili and Esko, who have supported me throughout my life. Finally, I thank my family, my wife Minna, who has been patient and supportive during my research, and my children, Joonas and Laura, just for being around.

Abbreviations

120B1, 105B2	120 tons heat size of BOF1 and 105 tons heat size of BOF2
BOF	Basic oxygen furnace
C-%	Carbon content at the end of the blow
e	Error
FeSi0	Ferrosilicon addition of 0 kilograms after drop sensor
FeSi38-200	Ferrosilicon addition of 38–200 kilograms after drop sensor
FeSi200+	Ferrosilicon addition of over 200 kilograms after drop sensor
FeSi/Heat	Ferrosilicon amount divided by heat size
Heat105k	BOF heat size 105 tons
HeatBig	$\geq$ 120 tons hot metal
HeatSmall	< 120 tons hot metal
Lime/Heat	Amount of lime divided by heat size
OGT_slope	Off-gas temperatures slope between 100 and 200 seconds
OGT	Off-gas temperature at 100 seconds
S	Slope [°C/s]
Scrap/Heat	Amount of scrap divided by heat size
Si*Lime/Heat	Lime divided by heat size
ScrapLight < 50%	Amount of light scrap from total scrap is less than 50%
Si/Mn	Content of silicon divided by manganese in the pig iron
TC	Calculated end temperature
TDS	Temperature when the drop sensor is used
TEB	Target temperature at the end of the blow
tDS	Moment of the drop sensor from the beginning of the blow
tEB	Total blowing time

Contents

1 Introduction

1.1 Background

The results introduced in this thesis come mainly from two research projects, KONVERTO and KONTROL. Both of them were joint research projects financed by TEKES (the Finnish funding agency for technology and innovation) and steel companies. These projects started in the year 2000 and ended in 2005. The work for this thesis was mainly done during the period between 2000 and 2007. The aim of KONVERTO was to develop the dynamic control of a basic oxygen furnace (BOF) and to increase the knowledge of measurements and process control. The target was to develop models for temperature and additional material models for a BOF. The aim of KONTROL was to develop heat control by improving the usability of current measurements and by testing new measurements. At the same time, knowledge about the phenomena in the converter process was increased. Since these projects, there has been an increase in the knowledge and experience of measurements and process control. One target of this thesis is to illustrate how the current and new potential measurements and models could be utilised in a monitoring system. The thesis also includes some newly analysed results from project material that has not been published earlier.

1.2 Research problem

A BOF is a complex process with hazardous features, for example because of the high temperature, dust and vibration. There are many chemical reactions and physical phenomena within a BOF, which are not fully understood by the users. It is difficult to get direct measurements from the vessel. Therefore, indirect measurements and models are often used to predict the status in the vessel. The models are not precise because of the limited amount of measurements and the complex and unknown interactions between the variables.

It would be useful to get more accurate and reliable direct measurements from the BOF. This would also bring new knowledge of the process. Models need to be further developed and their adaptation needs to be discussed. This would improve the monitoring and control of the BOF by combining the different types of information: measurements, models and expert knowledge.

1.3 Research assumptions

To achieve efficient monitoring of the BOF and to build up a monitoring system, the following are the minimum requirements. New measurements are needed to be able to identify the state of the process and to reveal the changes and disturbances in operation. An example of one such measurement is the Radio Wave Interferometer (RWI). By using an RWI, it would be possible to monitor the slag surface and get information early enough about a slag rise to avoid splashing and therefore possible loss of the product. These measurements need new computational tools to systematise the usage of the information and to gain the best possible benefit. New statistical models are needed to obtain better knowledge of the process behaviour from the history data and to help the user to run the process in a more efficient way. A model update and adaptation are required as the raw materials and process parameters change from time to time. Without them the models would end up being almost useless.

These improvements in the monitoring system can also be used in control to a certain extent. For example, if the models for carbon content, temperature and additional materials are accurate enough, it would be possible to let the system automatically stop the blow or add the required additional material to achieve the desired temperature at the targeted carbon content. However, it is highly recommended that the user makes the decisions concerning the blow-end.

1.4 Hypotheses

This thesis was built upon the following three hypotheses:

- There are new efficient and reliable measurements available and their usage requires new computerised tools. This thesis deals with an acoustic measurement, a splashing measurement and a RWI measurement and shows how these measurements must be analysed so that they provide new information on process behaviour.
- The existing models need to be updated and used in an adaptive way. This thesis concentrates mainly on how the blow-end temperature model could be improved. This model has an important role in deciding on the end-point of the heat. Furthermore, an additional material model is developed.
- New measurements and improved models must be integrated into a new monitoring system where it is possible to utilise information, process data and

expert knowledge in a more effective way. This leads to several advantages: better quality, increased production and better predictability. The basic principles of using new measurements and models in monitoring are also outlined in this thesis. Detailed design and testing of this system are, however, outside the scope of this thesis.

1.5 Author's contribution

Several publications have been published on this research. The author has been the main writer in all of these publications and has done the majority of the model development and analyses. The development of blow-end temperature and additional material models was also carried out by the author. The analyses of the acoustic and splashing measurements were carried out by the author. The RWI measurement was tested by the personnel of both the plant and the RWI supplier. They carried out some analyses concerning the RWI measurement. Some further analyses were carried out by the author. The ideas for the proposed monitoring system originated from the author. The contribution of the plant personnel to the publications was their expert knowledge about the plant. The contribution of the thesis supervisor was to advise the author. In addition, some research assistants were employed for data mining and data processing.

1.6 Structure of the thesis

Chapter 1 is a brief introduction to the research problem and hypothesis for this thesis. In Chapter 2, the process description is given and Chapter 3 introduces some new special measuring methods for the BOF together with the analysis of their applicability based on the author's findings. In addition, comments on their availability for the monitoring task are made. Chapter 4 describes the efforts and stages employed in improving the existing blow-end temperature model. The development of model for additional materials is discussed as well. Chapter 5 discusses the results and outlines the monitoring system that takes advantage of the main results provided in the previous chapters. Chapter 6 is a brief conclusion of the work.

2 Process description

2.1 History of steelmaking

Steel has been known and used for over five thousand years even though it was not produced in liquid state until about 1700 A.D. The direct reduction of iron ores by carbonaceous fuel to steel was practiced in ancient times, but liquid processing was not known until the development of the crucible process. Iron sponge or cemented wrought iron, coal, and flux materials were melted in a crucible, producing small quantities of liquid steel. The air-blown converter invented by Bessemer in 1856 is considered to be the first modern steelmaking process. In 1878, the Thomas process, a modified Bessemer process, was developed to permit the treatment of high phosphorus pig iron. In the Thomas process, phosphorus was oxidised in what is called an “after blow” after most of the carbon was removed from the bath. The Siemens-Martin (SM) process, commonly referred to as the open-hearth process, was developed almost simultaneously with the Thomas process. The open-hearth process utilises regenerative heat transfer to preheat air used in a burner, and it is able to generate sufficient heat to refine solid steel scrap and pig iron in a reverberatory furnace. (Pehlke 1973)

Around the 1950s, steelmaking was mainly based on open-hearth (Siemens-Martin) technology. Hot metal and scrap were charged into large horizontal furnaces where burners provided energy for scrap melting. Oxygen lances were used to improve burner efficiency and to remove carbon and silicon from the hot metal. The open-hearth process is allothermic and thus external energy had to be supplied to the furnace. Typical tap-to-tap times were eight hours for two hundred tonnes of liquid steel. In 1952, Voest introduced the oxygen steelmaking (LD) process in Austria. The Austrian process appeared to be economically attractive because large-scale production of pure oxygen (tonnage oxygen) was feasible. (Boom 2003) Two main factors behind the development of the LD process to replace the open-hearth furnaces are as follows: the investment costs are substantially lower and the productivity is much higher. The development of secondary metallurgy treatments since the 1970s also made it possible to produce high quality steel grades via the LD process. Subsequently, SM furnaces rapidly disappeared and the LD process emerged as the major steelmaking technology for

the reforming of blast furnace hot metal. (Krieger 2003) For scrap-based steelmaking, the EAF (electric arc furnace) has become dominant.

2.2 The oxygen steelmaking process

The oxygen steelmaking process in its simplest form (Fig. 1) is performed in a converter vessel with a basic refractory lining and a waste gas cleaning system. The vessel is tilted in order to charge predetermined and weighed amounts of liquid hot metal and solid scrap. Gaseous oxygen is blown vertically onto the metal bath until the estimated composition and temperature are achieved. Fluxes such as burned lime and dolomite are added from bins on the top of the vessel to regulate the process while iron ore is added as a coolant. In normal cases, steel samples are taken and steel bath temperatures are measured from the tilted converter only after the end of the blow. Blowing is also possible by means of some special equipment, such as the sub lance. In the latter case, the converter can stay upright and uninterrupted. When the blow has ended, the vessel is tilted to the other side and steel is tapped through a tap hole into a steel ladle. Slag is then tapped into a slag pot and the converter is ready for the next batch.

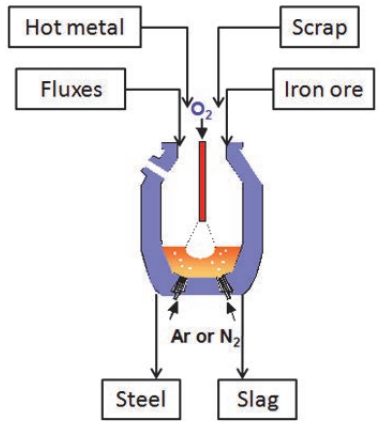

Fig. 1. The oxygen steelmaking process.

Specific aims for the oxygen steelmaking process include precisely described end point values for steel weight, temperature and composition. Carbon, phosphorus and sulphur and often also nitrogen, manganese and hydrogen concentrations need to be within the target windows. As continuous casting started to emerge in

the 1960s, the end point requirements became even more critical. Typical end point temperatures rose by 50 °C to 1650–1700 °C or even higher depending on the steel grade and the subsequent process stages. Also, sulphur limits had to be lowered to prevent crack formation and thus hot metal desulphurisation became a necessity. The new process also required better phosphorus removal and the oxygen content in the liquid steel became far more critical. Moreover, it became more critical to get the batch blown ready at the right time for the following process phases. (Boom 2003)

2.3 Understanding the oxygen steelmaking process

The fundamentals of the oxygen steelmaking process are written in several textbooks, for example Lange (1981), Deo & Boom (1993), Oeters (1994) and Turkdogan (1996). More general, technological descriptions are given, for example, in books by Fruehan (1998) and Béranger (1996).

Scrap is charged into the converter vessel first, followed by the liquid hot metal. Scrap is added to compensate for the surplus of heat generated by the oxidation of elements dissolved in iron such as silicon, carbon, manganese and titanium, and by the oxidation of iron into the slag phase. The basis of the oxygen steelmaking process is the jet of oxygen blown with high pressure onto a mixture of hot metal and scrap through a lance. The design of the lance nozzle started with a single-hole straight nozzle and led to multi-hole lances such as the six-hole lance of Sumitomo. (Higuchi & Tago 2001) The flow characteristics of the oxygen and the distribution of momentum over the liquid steel bath leading to a deep cavity, a dimple or heavy splashes were modelled in Molloy (1970). A new aspect was the restricted time available for melting the scrap: blowing times were in the order of twenty minutes or less.

From the thermodynamics of the oxygen steelmaking process, it can be seen that, at the beginning, the oxygen blown onto the hot metal preferably reacts with the dissolved silicon, forming SiO_2 that floats on the surface of the hot metal. From kinetics, it is expected that a part of the oxygen blown reacts with the dissolved carbon and iron atoms. The formation of CO gas occurs instantaneously on process ignition. Burned lime is added to neutralise the acid slag, which initially includes a liquid mixture of Fe_mO_n and SiO_2. (Boom 2003)

Numerous chemical reactions take place in a basic oxygen furnace. The description of the main chemical reactions is given, for example, in (Brooks & Coley 2002) and they are listed in Table 1. The main reactions are dissolution of

oxygen into the metal from O_2gas (1), decarburisation through dissolved oxygen (5), and oxidation of Fe, [Si], [Mn], [P], [V] and [Ti] (6–9). Solid or liquid oxides are formed as reaction products during blowing, and they are bound with the lime added at the start of blowing to form a liquid slag in the converter. Due to intensive CO gas formation (5), droplets of liquid metal are introduced into the slag, which tends to foam. Thus, the slag in a BOF during O_2blowing is actually an emulsion of liquid slag and metal droplets, foaming due to the influence of gas bubbles. The emulsion is also a favourable site for reactions. For instance, a significant fraction of carbon oxidation can occur in the metal droplets in emulsion although the majority takes place in the impact zone of the oxygen jets.

Table 1. The main chemical reactions in a Basic Oxygen Furnace. Taken from Brooks & Coley 2002: 838.

Oxygen pick up by the metal:	
$O_2(g) = 2\underline{O}$	(1)
$(FeO) = \underline{Fe} + \underline{O}$	(2)
$(Fe_2O_3) = 2(FeO) + \underline{O}$	(3)
$CO_2(g) = CO(g) + \underline{O}$	(4)
Oxidation of elements in the metal:	
$\underline{C} + \underline{O} = CO(g)$	(5)
$\underline{Fe} + \underline{O} = (FeO)$	(6)
$\underline{Si} + 2\underline{O} = (SiO_2)$	(7)
$\underline{Mn} + \underline{O} = (MnO)$	(8)
$2\underline{P} + 5\underline{O} = (P_2O_5)$	(9)
Oxidation of compounds in the slag:	
$2(FeO) + ½O_2(g) = (Fe_2O_3)$	(10)
$2(FeO) + CO_2(g) = (Fe_2O_3) + CO$	(11)
Flux reactions:	
$MgO(s) = (MgO)$	(12)
$CaO(s) = (CaO)$	(13)
Gas reactions:	
$CO(g) + ½O_2(g) = CO_2$	(14)

Note: "_" metal phase and "( )" slag phase.

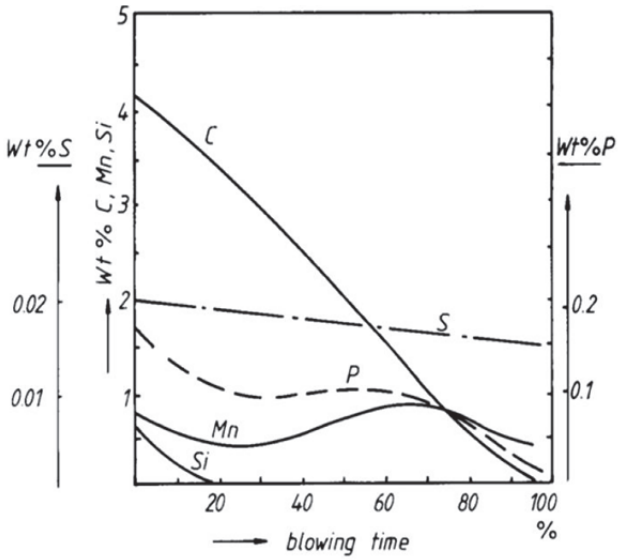

Fig. 2. The contents of elements during the blow (Hoorn 1976), (Deo & Boom 1993).

Fig. 2 shows the concentrations of elements in the melt during the blow according to Hoorn (1976) and Deo & Boom (1993). The rest of the oxygen is used to burn Fe into Fe_mO_n. During blowing, oxygen penetrates the metal droplets and can react with the CO gas. The total slag-gas system behaves as foam and rises quickly to the cone of the converter. Thus, the oxygen inflow and the reaction rates have to be adjusted so that foam is not spilled from the vessel. The spitting phenomenon is typically referred to as slopping. However, the terms spitting and splashing are also used depending on the material and author. Slopping frequently occurs even though the inner volume of the BOF is almost nine times larger than the volume of the quiescent metal and slag bath. (Boom 2003) Finnish researchers have developed a simulator in which it is possible to simulate the amounts of elements during the blow. The simulator is called ConSim. (Jalkanen 2007)

Several variations of blowing are known in converter steelmaking. In bottom blowing, oxygen is supplied from the bottom of the vessel to provide the necessary oxygen as well as additional stirring to improve the reaction kinetics. Such a blowing configuration is used, for example, in the Bessemer, Thomas, OBM, Q-BOP and LWS processes. A top-blowing converter using an oxygen lance is known as LD (after Linz & Donavitch, where the first industrial converters were established in the early 1950s) or BOF (Basic Oxygen Furnace). In the 1980s, LD converters were equipped with inert gas bottom stirring (LBE,

LD-KG, LD-AB, etc.). This is the most common converter type today. Additionally, there are other types of combined or mixed blowing converters. Principally, these can be divided into three main classes:

- oxygen top blow with inert stirring gas (nitrogen and argon) injection through the bottom,
- oxygen top blow with oxidising gas (such as air and CO_2) and inert gases from the bottom and
- combined oxygen top and bottom blowing with pure oxygen injection both through a top lance as well as through bottom tuyeres.

Fired blowing is a term used for processes where additional solid fuel is added into the vessel. Examples of fuels are coke, coal and compressed waste plastics. In an extreme variation of the oxygen steelmaking process (the Russian Z-BOP process), no hot metal is needed and 100% scrap is used. Also, post-combustion of CO to CO_2 can be utilised as an extra source of energy to melt more scrap. Special post-combustion lances in the upper half of the reactor are needed as secondary oxygen supply to guarantee that the gas mixture is fully combusted at the top of the converter vessel. Gas recovery can reduce energy consumption in combination with a reduction of CO and CO_2 emissions, respectively. (Boom 2003) An example of Finnish post-combustion research can be found from (Rautell 2000) and (Lassila 2004). In general, the controllability of the BOF deteriorates when post-combustion and extra fuel additions are applied. The BOF with increased scrap melting eventually lost the battle to the electric arc furnace, designed to melt 100% scrap.

With increasing understanding of the fundamentals of oxygen steelmaking, it became clear that separation of the process into different steps would be worthwhile. By performing the metallurgical operations under the most favourable thermodynamic and operational conditions, benefits are achieved in terms of better material yield and improved process reliability. The steps include, for example, sulphur and phosphorus removal from the hot metal before charging. However, it is notable that hot metal needs to be desiliconised before it can be dephosphorised. (Boom 2003) In addition, more secondary metallurgical processes are being used, such as vacuum degassing units, CAS-OB stations and ladle furnaces.

The economy of the BOF is determined to a great extent by the annual output. The availability of converter vessels is also an important factor when considering the economics of the process and is mostly governed by the life of the refractory

lining. One possibility to lengthen the campaign is slag splashing. (Russell 1993) In slag splashing, first the steel is drained from the BOF and molten slag is left in the vessel. Then an oxygen lance is used to splash the molten slag onto the walls of the BOF to form a protective coating. (Zhao, 2010) The influence of several variables were investigated by (Luomala *et al.* 2002) using a physical model. However, slag splashing has disadvantages in process control, especially on lance height control as the material gathers in the bottom. Height control is usually based upon sub-lance technology and has reached a high level of accuracy. To overcome the difficulties concerning lance height control, a laser measurement can be made to measure the molten bath.

2.4 Process control

The simplest form of process control is based upon a static process model. It consists of a set of balances for heat, oxygen, iron, and slag, combined with an equation of state. The latter describes the relationship between the Fe content in the slag, the actual contents of Mn and C in steel and the basicity of the slag. For dynamic process control, accurate information of the actual state of the blowing process is required. Ideally, continuous information on the steel, slag and gas compositions as well as the temperature would be available and used on-line for process supervision. Any deviation from the progress of the anticipated process could then be detected and, based upon the models, the oxygen supply could be adapted or additional flux could be added into the vessel. In a steelmaking converter, as well as in almost all processing devices, this is possible only in an ideal situation. In practice, the situation is totally different. Especially in this process, there are strong practical limitations for continuous measurements, for example vibration, dust, high temperature and liquid metal and slag phases. (Boom 2003)

Continuous chemical analysis of converter waste gases was introduced in 1975 to derive information on the decarburisation rate, dC/dt, and to estimate the prevailing carbon content (Kreijger *et al.* 1975). Measuring the outgoing gas volume and the oxygen flow rate enables the quantitative determination of key values such as the actual value of the CO/CO_2 partition. The gas composition is determined by measuring the heat conductivity, infrared absorption or mass spectrum. One challenge is the response time of the measurement system, typically creating a delay of 15 to 20 seconds. Dynamic control based on waste gas analysis has proven to be very useful in understanding the basic oxygen

furnace process. For carbon control, the existing dynamic control is sufficient, but for simultaneous control of the end point temperature it is not effective enough. It has been noticed that the decarburisation rate, dC/dt, behaves correspondingly with the off-gas temperature. As the off-gas temperature falls, the dC/dt also falls. (Boom 2003)

Along with continuous measurements (of the process parameters/variables), discrete measurements of steel composition and bath temperature can be used to improve the dynamic process control. A sub lance, a water-cooled lance parallel to the oxygen-blowing lance, is an example of this type of measurement system. It measures temperature and oxygen concentrations from the steel bath. The temperature difference between the inlet and outlet cooling water streams of the blowing lance or detection of the thermal expansion of the blowing lance's outer cylinder can be related to the slag height in the converter. Monitoring the weight of the converter during the process by load cells in the vessel bearing has been tested to detect the carbon removal from the charge. Acoustic measurements with a sonic meter (audiometer) trimmed to low frequencies have been widely used to monitor the vessel. An acoustic signal can be related to, for example, slag formation, slag foaming and decarburisation. Many researchers have tried to detect the dramatic drop in decarburisation rate at the end of the process. (Boom 2003)

An example of dynamic control used in BOF is given in Fig. 3. In the figure on the left, the off-gas temperature is presented for the whole blow. In the right-hand figure the calculated carbon content and calculated temperature are presented. From the right-hand figure it can be seen that the carbon content and temperature are calculated after employing the drop sensor, which is used to measure the temperature during the blow. By using the drop sensor, it is possible to calculate the carbon content and temperature and therefore to use the information to decide the correct time to end the blow. (Ollila & Lilja2004)

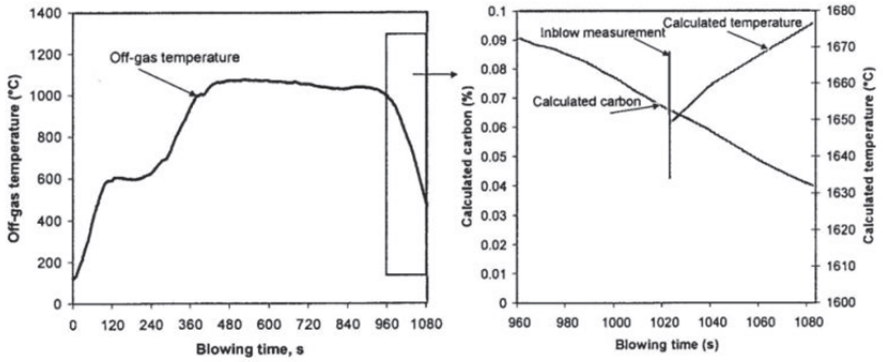

Fig. 3. Off-gas temperature, calculated carbon and temperature during blowing. (Ollila & Lilja 2004).

2.5 Development of the steelmaking process, case example: BOF

The continuous development of the process is always a reliable way to keep one's process competitive in many aspects; economically, technically, ecologically and metallurgically. The developer also needs to keep in mind process operators, and to make sure that their knowledge and working conditions are kept updated. (Guzela *et al.* 2003)

Since the introduction of the LD process, steelmaking practice has been improved over the whole process route. The economic and technological potential of steel quality can be achieved by installing new components in current production units. The cost-efficient production of high quality steel grades requires excellent equipment and a powerful process control system as well as operational standardisation of the process. The most important process stage is the metallurgical vessel of the process – the converter. In the converter there are extreme abnormal conditions such as high temperatures, mechanical impacts and many unforeseeable impacts. Converter engineering is challenging and is largely based on experience. From the metallurgical point of view, the ideal converter keeps the liquid steel in place and allows all necessary metallurgical reactions. Because of the high temperatures of approximately 1600–1700 °C that are involved, the optimum is a material, which withstands these extreme conditions without any wear. In practice, converters are steel vessels lined with refractory material lining. (Guzela *et al.* 2003)

Harsh conditions during steelmaking make it almost impossible to observe the process directly. Up to now no mathematical model has been available which describes this fully-coupled thermo-metallurgical-fluid dynamic process. Certainly parts of it are understood or described more or less correctly. The most interesting part, the metallurgical process, is well known since it has been investigated and improved since the very beginning. However, there is still a lot of research to do. For example, the positioning of tuyeres for bottom stirring is not fully optimised and a mathematical model for the oscillation of the vessel during the process is not available. (Guzela *et al.* 2003)

The mechanical part which keeps the liquid steel in place is a steel shell lined with refractory material. The behaviour of the steel shell is more or less known but it is still impossible to describe its temperature dependence including creep effects (in some detail). The interaction between the shell and the refractory material includes a lot of unknown factors. Several criteria for an optimum design of the converter vessel have been developed. One of the most important characteristics is the inner volume inside the refractory lining, which can be used for the steelmaking process. Basically this volume is to be maximised within the limits (space restriction) in order to have the maximal reaction volume for the metallurgical process. For comparison, the ratio between the reaction volume and the mass of the liquid steel is used. A typical LD converter shows a ratio of approx. 1.0 m^3/t. As there are demands for productivity to go up with minimum investment costs, this will cause an increase in the charging weight using the original vessel. In so doing, the ratio becomes smaller and smaller. One of the clearest consequences is heavy slopping, which typically occurs with specific volumes from 0.7 to 0.8 m^3/t. (Guzela *et al.* 2003) The specific volume of the BOFs at Ruukki Raahe is 0.7 m^3/t.

There is no specific standard available worldwide for metallurgical vessels like converters. In fact, a converter is not a pressure vessel according to its classical definition, because the internal pressure is caused by thermal expansion of the refractory and not by a fluid or gas inside the vessel. Many industrial applications have shown that in principle it is not absolutely necessary to apply a forced cooling system to the equipment, since cooling by natural air draft is sufficient. Nevertheless, cooling decreases the temperature of the equipment, which has a positive effect on creep deformation, refractory lifetime, as well as higher yield strength at the operating temperature. The base material for the vessel has been based on temperature-resistant pressure vessel steel from the very beginning. (Guzela *et al.* 2003)

A suspension system is also important equipment. Ideally the suspension system should not influence the behaviour of the vessel shell at all and it should run completely maintenance free. (Guzela *et al.* 2003)

Besides the design of the converter itself, converter technology consists of the following elements:

- slag cutting and inert gas bottom stirring for improved metallurgical process conditions
- integrated secondary metallurgy included in the converter
- computer-aided process automation and related sensors for increased quality, productivity and safety and decreased production costs
- proper tools and equipment for plant operation, maintenance and increased life cycles of refractories
- systems for increased environmental compatibility of waste materials. (Guzela *et al.* 2003)

Further development targets in converter technology for improving the economics are optimisation of logistics and plant operation and optimisation of process technology. To prove the value of a process automation system development, a couple of benefits can be mentioned: reblowings can be decreased and the correction times and waiting times for analysis reduced. Additional benefits are gained from reduced refractory consumption, which is a result of the shorter average tap-to-tap times. Smaller iron losses into slag by reduced re-blowings are another benefit. The increased hit rate for carbon and temperature at the end of the blow is one reason for this benefit. (Guzela *et al.* 2003)

2.6 Raahe Steel Works

The research discussed in this thesis has been carried out in co-operation with Ruukki Production, at their Raahe Steel Works in Raahe, Finland. The steel plant produces about 3 million tonnes of steel annually. The layout of the steel plant in 2005 is shown in Fig. 4.

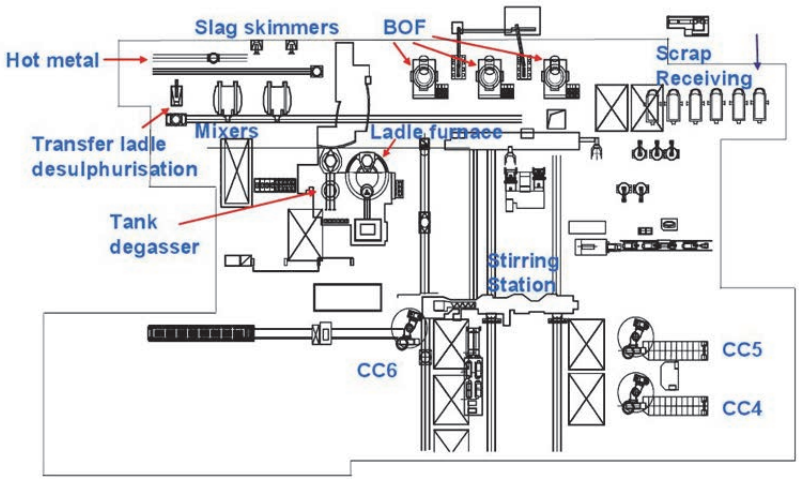

Fig. 4. Layout of steel plant at Ruukki Raahe Steel Works.(Lilja *et al.* 2006)

Hot metal comes from two blast furnaces via the desulphurisation station to the steel plant and is charged along with the scrap, slag formers and fluxes into the basic oxygen furnace, where it is converted into refined steel. After the secondary steelmaking processes, for example tank degassing, the steel is cast into slabs in continuous casting before going to hot rolling. The main task of the basic oxygen furnace is to decrease the carbon content of hot metal from ~4.5% to ~0.05%. Other tasks of the BOF process are to heat the melt from ~1350 °C to the target temperature (typically in the range 1650–1700 °C), to remove impurities (for example sulphur and phosphorus) and to melt the charged scrap. The converters in use at the Raahe plant are modified LD-KG-type combined blown converters. The melt is decarburised by the blown pure oxygen. Oxygen reacts with carbon generating mainly carbon monoxide. Inert gas (Ar or N_2) is blown through multi-hole nozzle bricks in the bottom. Stirring is used to keep the melt homogenous and to lower the oxygen level in relation to the carbon content at the blow-end. A simplified structure of a BOF is shown in Fig. 5.

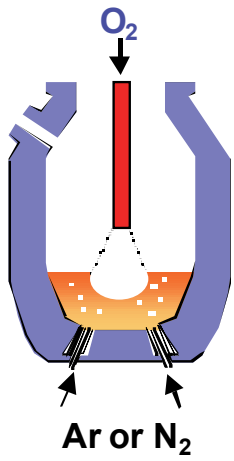

Fig. 5. Basic Oxygen Furnace. (Ruuska *et al.* 2003).

Many basic measurements and controls are needed to make any process – in this case the basic oxygen furnace – manageable. These measurements are not discussed in this thesis. The measurements, which were especially used during the progress of the thesis, are a drop sensor by means of which temperature and oxygen can be measured from the liquid steel (in use), an acoustic measurement (not in use currently), a radio wave interferometer (tested in the BOF) and a splashing measurement (in use). These measurements are applicable for the design of dynamic control. The drop sensor is dropped into the converter using a pipeline made for this purpose. The sensor is dropped using the control system of the converter. The result is displayed in the main operator interface and also recorded on a database. The error in temperature is assumed to be ±10 °C, due to using it in this kind of harsh environment. This estimate was made by the equipment supplier; no specific tests were done. For the acoustic measurement a microphone was mounted above the converter mouth opening and was directed to the gap area located between the mouth and the hood. The noise curve was displayed in a window in the main operator interface in the BOF control room. The signal was also recorded on a database. The splashing measurement is made by using a video cameras located under the converter. A snapshot captured from the video camera is utilised and converted into numerical form, which is then displayed to the operators in the control system. They are also recorded on a database. The tested RWI measurement was installed in a drop sensor pipeline (drop sensors were not in use during this test). The data was displayed and then

recorded on a database. There are also numerous models used to manage the production done in the BOF. The ones briefly presented here are the charging model, carbon, blow-end temperature and additional material models. The charging model is based on the formulas made by Healy & McBride (Healy & McBride 1977). In calculation the mass and energy balances are solved by using the following initial data: amount of scrap, analyses for all elements and the target values set for the heat, as well as target analysis and temperature. The carbon model calculates the carbon content based on the off-gas temperature, taking into account the off-gas temperature and carbon content at the end point of the previous heats. The carbon model has two components; the correlation between the off-gas temperature and carbon content at the end point and the slope of the decrease rate of the off-gas temperature. The model is updated by using the twenty previous acceptable heats. The existing blow-end temperature model was a constant slope, 0.54 °C, for all heats. There was no additional material model. The development of a blow-end temperature and additional material model is introduced in Chapters 4.2 and 4.3.

A lot of additional information is available on the development work done. The development of the drop sensor is reported for example in (Ollila *et al.* 1999). The continuous development of process control and performance are reported for example in (Ylönen *et al.* 1999a), (Ylönen *et al.* 1999b) and (Lilja *et al.* 2006). The BOF models are reported for example in (Ruuska *et al.* 2003), (Ollila & Lilja 2004), (Ruuska *et al.* 2004) and (Ruuska *et al.* 2005). Additionally, a significant number of diploma theses had earlier been done concerning the development of Ruukki's BOFs; Jämsä (1977) and Kivelä P. (1982) on developing a charging model, Kivelä S. (2000) on developing a carbon model and Laine (1998) and Roininen (1999) on developing the usage of drop sensors.

2.7 Other modelling and control approaches

Yang *et al.* (2002) developed an adaptive neuro-fuzzy phosphorus model. Kitamura *et al.* introduced a simulation model of dephosphorisation. Mizuta *et al.* (2000) developed a temperature control system. They had sub lance and off-gas measurements available. Jun *et al.* (2002) provided an intelligent control method for the BOF, where they combined a neural network, fuzzy inference and expert system with dynamic process control. It even contained models for coolant additions, the progress of carbon content and temperature. Viana & Castro (2004) presented a blowing model based on neural networks, which was found to

improve the hit rate of end point carbon and temperature. They presented their own neural networks for the required amount of oxygen and possible sinter coolant. Kim *et al.* (2005) introduced a hybrid concept of Case-Based Reasoning (CBR) and neural networks to control temperature in a BOF. Wang *et al.* (2006) presented multiple neural network models for oxygen blowing, coolant addition as well as for carbon and temperature. Fileti *et al.* (2006) developed a neural network model for carbon and temperature in a BOF. Han & Huang (2008) introduced an adaptive neural network fuzzy inference system (ANFIS) model based on kernel and greedy components to predict end point carbon and temperature in a BOF. Han & Wang (2011) presented a case-based reasoning (CBR) model to define the required volume of oxygen in a heat.

Birk *et al.* have presented results from physical modelling and control of dynamic foaming. They used an experimental setup including for example a water model and sonic meter. They also presented a foam height algorithm and validated it through experiments. (Birk *et al.* 2000), (Birk *et al.* 2001), (Birk *et al.* 2003)

Evestedt & Medvedev designed a model using BOF off-gas flow rate and pressure to estimate slag level. Using a change detector, which detects the changes in the model parameters, they developed a slopping warning system to give advance warning to the operator about slopping. The validation of the model was done using different measurements, for example sonic meter and camera signal. (Evestedt & Medvedev 2006), (Evestedt *et al.* 2007), (Evestedt & Medvedev 2009)

Kattenbelt's objective in her thesis was to develop a dynamic control strategy for a BOF to reduce the occurrence of slopping and to increase the production capacity by reducing the tap-to-tap time. However, as some important process variables could not be measured, it was necessary to develop a dynamic process model. (Stroomer-Kattenbelt 2008)

Kattenbelt and Roffel presented a hierarchical two-layer statistical slop prediction model, which uses the raw material input data and the physical properties of the slag. The first hierarchical layer predicts when slopping may occur during a heat. The second hierarchical layer predicts the probability of slopping. (Kattenbelt & Roffel 2008a)

Kattenbelt and Roffel have introduced a dynamic model for the main blow in a BOF using measured step responses. The measured step responses of the decarburisation rate and the accumulation rate of oxygen to step changes are presented in the oxygen flow rate, lance height, and the addition rate of iron ore

during the main blow. The model consists of an iron oxide and a carbon balance and an additional equation describing the influence of the lance height and the oxygen flow rate on the decarburisation rate. The decarburisation rate and the accumulation rate of oxygen are derived from the measured gas flow and composition of the off-gas. (Kattenbelt & Roffel 2008b)

Grethe *et al.* introduced BloCon, which is a modularised and adaptable BOF process model developed by Mannesmann Demag. BloCon is based on the metallurgical description of the BOF blowing process. It solves the heat and mass balances. It includes a possibility to calculate nearly all the possible charge materials. It also supports for example the use of bottom stirring, sonic measurement and a sub lance system. The implementation at Preussag Stahl AG is also presented. (Grethe *et al.* 1996)

A Finnish simulation program for the converter, ConSim, has been developed since the late 1980s. The program can simulate the amounts, compositions and temperatures of molten steel, slag and converter gas as a function of blown oxygen. (Jalkanen *et al.* 1998, Jalkanen, 2007)

Hahlin *et al.* introduced the MefCon system that was developed to predict the outgoing heat from a BOF. It is said to be easily adapted for all known converter processes. It requires an on-line off-gas analysis. The most important variables predicted for the endpoint are carbon content and temperature. (Hahlin *et al.* 1986), (Hahlin 1993), (Bergman & Hahlin 1997)

3 Special measurements and their use in analysing BOF behaviour

3.1 Radio wave interferometer

Radio wave interferometry (RWI) has been used for a long time as a space scanning method by astronomers. When radio waves move through two different materials, some changes in amplitude, phase and polarisation occur. RWI as a method does not cause any disturbances in the process. In BOFs, the measurement can be used to detect surface position and layer thicknesses. It can measure a distance from the surface with the accuracy of a fraction of a wavelength and separate the different layers of melt and slag and form a three-dimensional map of them. A 3D-map, however, requires three or four RWI units. (Malmberg & Bååth 1995), (Bååth L1996), Millman *et al.* 2001), (Bååth L 2003)

As RWI is used to measure surface distance and layer thicknesses in the BOF, it is required to have a line of sight into the vessel. Fig. 6 presents the arrangement of the vessel and hood and shows the position of the RWI unit. The RWI unit has a water-cooled moveable hood around it. Ahead of the measuring point there is a ceramic seal that is transparent to radio waves and acts as an effective window, through which the instrument can illuminate the inside of the converter. One problem that occurred was that the window was prone to skull formation and required cleaning. Some gas curtains and different hood access port designs were tried in order to prevent skulling. These trials reported only partial success against the skulling problem. (Millman *et al.* 2001) It is shown in Bååth (2003) that the measurement accuracy of the RWI method is good within the error estimated for the manual measurement and so it can be claimed to be at least as accurate as the manual method. RWI measurement has been also tested in EAFs (Malmberg & Bååth 1999).

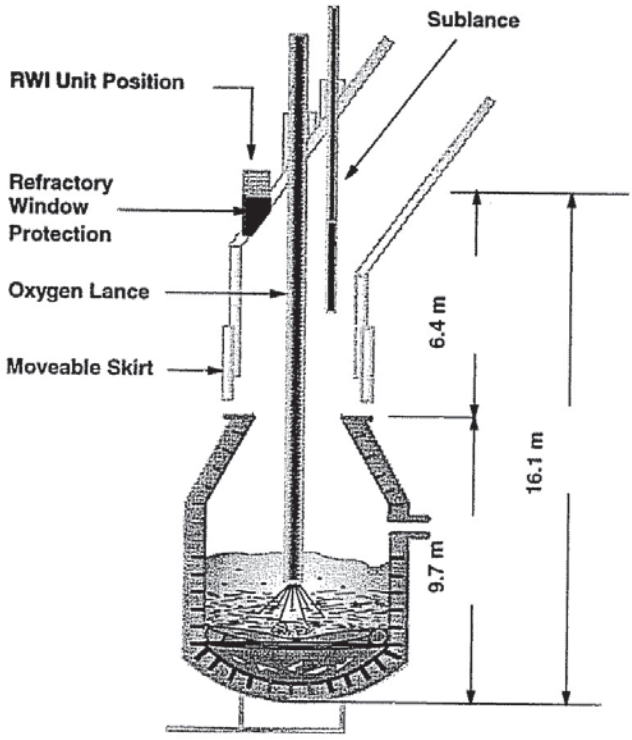

Fig. 6. Typical installation of RWI into a BOF (Millmann *et al.* 2001).

As presented by Ruuska *et al.* (2006a), an experiment was performed to measure the levels of slag and molten steel in one converter at Raahe Steel Works. The purpose was to determine the dynamic changes in the levels of slag and steel during blowing as well as the static levels after the blow. A RWI instrument was placed in the off-gas hood with direct visibility to the melt when the converter is in its upright position. The instrument was placed in the midpoint between the oxygen lance and the walls of the converter.

In way of an example, an interpretation of the data from a blow is presented (Fig. 7). This heat shows typical behaviour as all levels (slag, emulsions and steel) increase similarly at the start of the blow. This was interpreted as being caused by the blow of oxygen at the centre of the vessel, which pushes down the centre portion while the outer parts rise. First a flux is added, which causes a small addition to the volume of foam. The oxygen first reacts with silicon in the hot metal, forming SiO_2 in the slag. Within a few minutes this reaction has reduced all

the free silicon and then the oxygen will react with carbon to form carbon monoxide and carbon dioxide. The increased gas pressure will then form more substantial foam. It is worth noting that this is a very fast process; the slag level can rise by about one metre in ten seconds. Two additional surface levels are formed at this point of the process. These levels were interpreted as the top of the emulsion of iron droplets in the foaming slag and an additional thicker emulsion forming close to the steel surface. The top emulsion should, and does in this case, come almost to the top of the foam, producing a large reactive volume. The steel level moves upward at the start of the foam generation, possibly due to bubble formation in the steel. The emulsion level decreases towards the end of the blow, indicating that the gas evolution rate is reduced. As the samples are taken, blowing is turned off temporarily and the slag is cooled due to the sampling procedure, and thus temporarily collapses due to the gas released from the foam. A short re-blow was performed at the end to heat up the steel. The foam then collapses as it should when the oxygen flow is turned off and the lance is lifted. The collapse could take up to a minute depending on the remaining amount of carbon/oxygen after the blow. The vessel is then tilted for tapping and the instrument no longer has visibility to the melt.

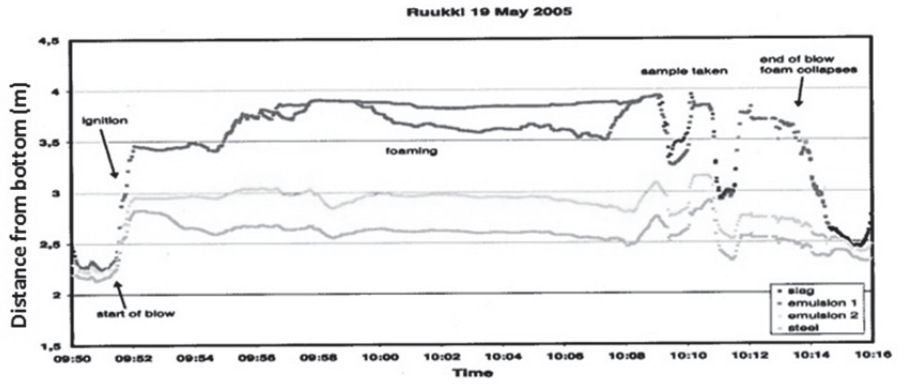

Fig. 7. An example heat in which RWI measurement is used. (Ruuska *et al.* 2006a).

From the example it can be seen that the slag and steel levels can be measured before and after the blow and that the slag and emulsion layers can be measured during the blow. The tests indicate that it is more problematic to measure the steel level during the blow, probably because the surface is disturbed due to turbulence.

Fig. 8 shows two example heats in which RWI and splashing measurements are used. From the figure, it can be seen that as the levels measured by RWI rise, splashing also occurs. Splashing is discussed in Chapter 3.3. Typically in the early stages of the heat (about 25–35% of the heat), when the levels of slag and steel are rising, nearly all the silicon has been consumed and the combustion turns almost fully to carbon oxidation, gas evolution is strongly intensified and heavy splashing occurs. (Kattenbelt & Roffel 2008a) In a later stage, another period of splashing occurs. Often this is the result of a change in lance height, the oxygen flow rate or an addition of material into the vessel. Also, it can result from the poor ignition of carbon oxidation, which again maybe due to several reasons. Typical reasons for poor ignition are an unsuccessful lance practice (which is however standardised in industry-scale vessels), a variation in the oxygen flow rate (which can occur for example as the pressure in the oxygen pipeline changes due to overload), too big an amount of added silicon in the early stages of the heat or the wrong scrap ratio (too much heavy scrap). More reasons for heavy splashing are given in Chapter 3.3 according to Ruuska *et al.* (2006b). Preventing splashing during this period of the heat is very important as the slag contains a lot of iron oxide. To summarise it can be stated that it is useful to keep process flows as stable as possible to prevent a process going into an oscillating state. RWI measurement can be said to have the potential to be a useful method in combination with other measurements and expertise to monitor splashing. Using RWI would make operation of BOF more effective as iron losses are smaller.

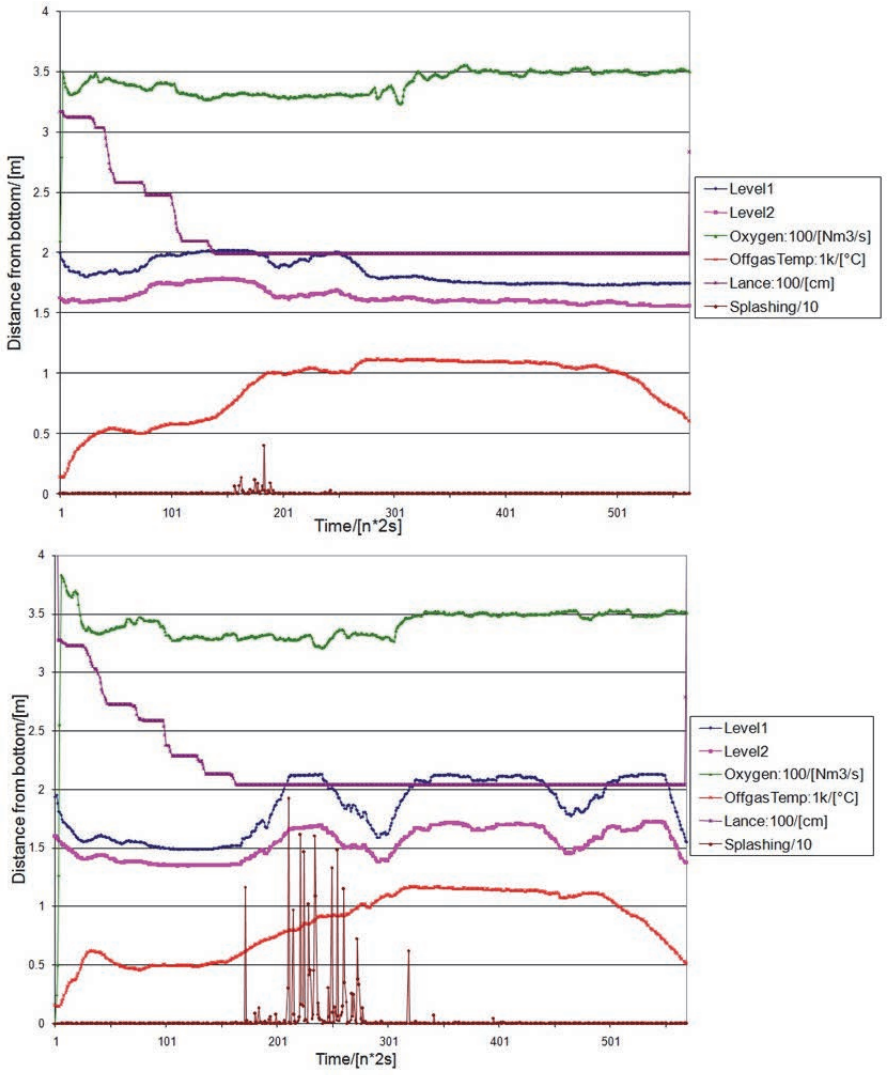

Fig. 8. Two example heats in which RWI and splashing measurements are used.

The usability of RWI depends on how repeatable the measurement is from one heat to another. Based on these measurements, it is difficult to verify because the placement of the measurement was very hazardous. The main observed weakness was the sensitivity to skulling; as the probe got dirty, the measurement became unreliable.

RWI measurement is not used for control in the basic oxygen furnace, but there is at least one industry-scale application in an EAF (Electric Arc Furnace) (Malmberg & Bååth 1999). Payback time is around one year as RWI is a continuous measurement and even a small improvement in yield gives significant annual savings.

3.2 Acoustic measurement

Acoustic measurement is used in several applications in a BOF. For example Graveland-Gisolf *et al.* (2003) used it as an indication of the foaminess of the BOF slag. Acoustic measurement correlated well with the amount of oxygen accumulated in the slag and with the amounts of dry and liquid slag. It can be used as an assisting tool when different kinds of slags are tested. Birk *et al.* (Birk *et al.* 2000, 2001, 2003) were able to develop a working foam level control for a BOF water model. The foam level was predicted by using processed acoustic measurement and the lance height was adjusted to get the foam to the desired level.

At Ruukki's Raahe steel works acoustic measurement has been in use in the BOFs since 2004. The frequency range of the measurement was incorrect as from time to time the incoming signal to process automation was cut off at 120 dB. It appeared that the signal from the sensor was transferred correctly, but in the process automation system the signal was cut off programmatically. After resetting the frequency range, the signal was correct. Fig. 9 shows the acoustic measurement before adjusting the frequency range and the signal after frequency range adjustment is presented in Fig. 10. The heats in Fig. 9 and Fig. 10 are different ones, but as the frequency range was adjusted correctly, the acoustic pressure did not reach 120 dB during the heat and the cut off problem did not occur thanks to this successful adjustment. Another problem was that the signal contained disturbances, which were assumed to be caused by the noise originating from the addition of lime. By averaging out the signal, it was possible to verify that the disturbance was caused by lime addition. This is shown in Fig. 11; the additions of lime have been marked with vertical lines. The maximum values of acoustic measurement are reached before the vertical lines, because the time stamp of the lime addition is fed into the process automation system as the lime addition ends.

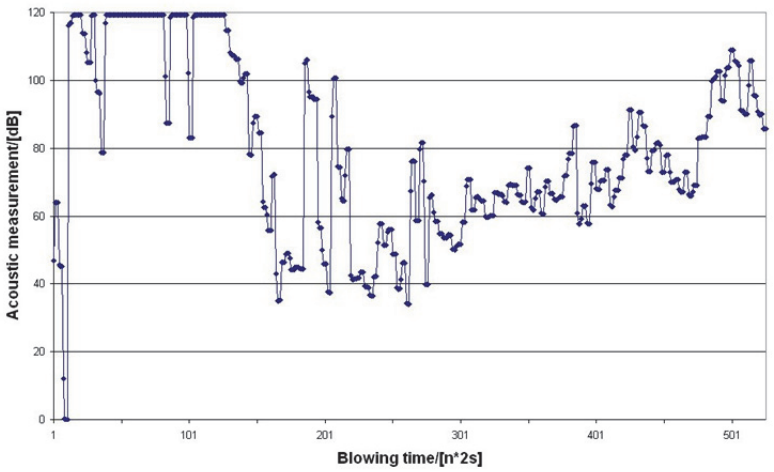

Fig. 9. Acoustic measurement before frequency range adjustment.

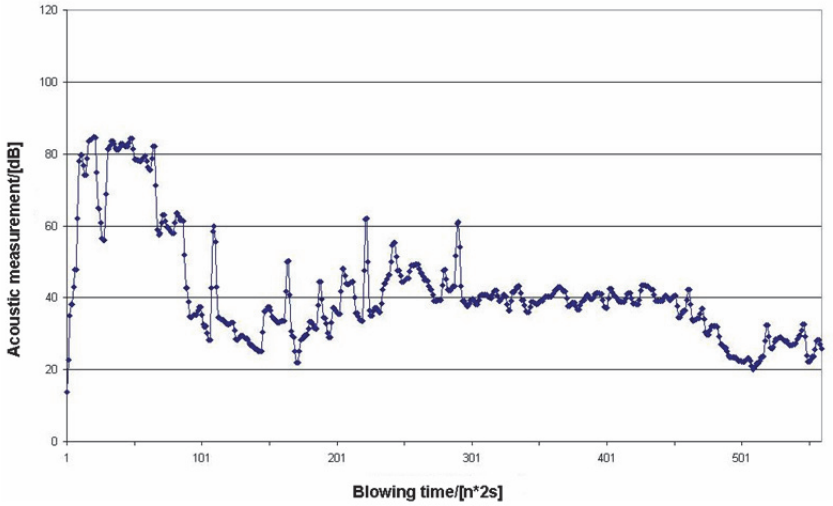

Fig. 10. Acoustic measurement after frequency range adjustment.

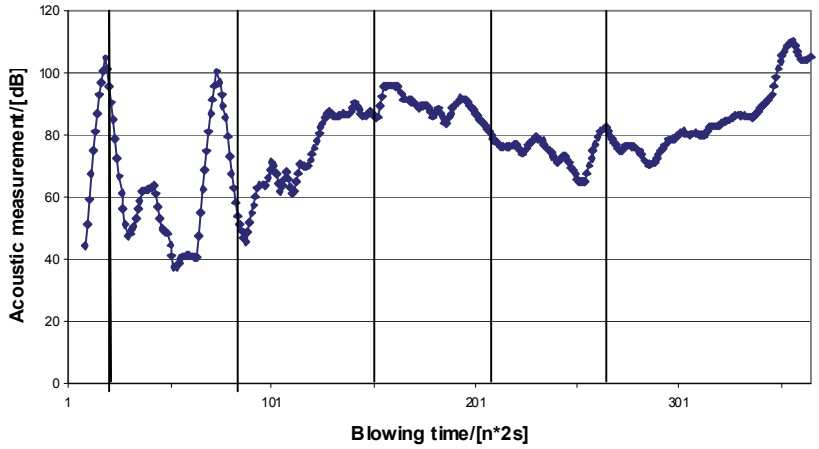

Fig. 11. Acoustic measurement with a moving average of ten measurements.

A suitable frequency range for acoustic measurement was originally chosen by the experts of the steel plant in 1997. The double-checking of the frequency range was done based on the prints from the original twenty-seven cases from eight different heats, in which the frequency range was changed. Seven cases were omitted from the study because the maximum value of the acoustic pressure was over 120 dB. The frequency was changed between 50 and 275 Hz. The microphone signal was filtered so that it recorded the signal between low and high frequency. It worked as a band-pass filter, for example the high pass frequency was 190 Hz and the low pass frequency was 210 Hz. It was desired that the difference between the lowest and highest value of acoustic pressure as big as possible. Table 2 shows the frequencies and minimum/maximum values of acoustic pressure for the twenty acceptable cases. In Fig. 12 the numerical difference between the minimum and maximum values can be seen. The five greatest differences in acoustic pressure are ranked from one to five in Table 2. Additionally, as big a numerical value for the frequency difference as possible was chosen. The frequency range of 230–275 Hz was selected for the band-pass filter of the microphone signal.

Table 2. The numerical values for choosing the band-pass filter.

Heat#	High pass freq/[Hz]	Low pass freq/[Hz]	Difference/[Hz]	dB_min	dB_max	dB_difference	Rank
2	235	275	40	21	100	79	3
2	180	200	20	11	55	44	
3	190	210	20	14	103	89	2
3	85	95	10	6	33	27	
3	180	200	20	8	60	52	
3	180	200	20	7	61	54	
4	180	200	20	14	41	27	
4	190	200	10	10	33	23	
4	190	200	10	7	33	26	
4	180	200	20	8	41	33	
5	190	200	10	11	51	40	
5	190	200	10	14	69	55	
6	190	200	10	13	68	55	
6	170	200	30	16	82	66	5
7	180	200	20	15	69	54	
7	190	200	10	15	69	54	
7	220	230	10	21	91	70	4
8	50	95	45	5	49	44	
8	230	275	45	21	111	90	1
8	170	190	20	9	56	47	

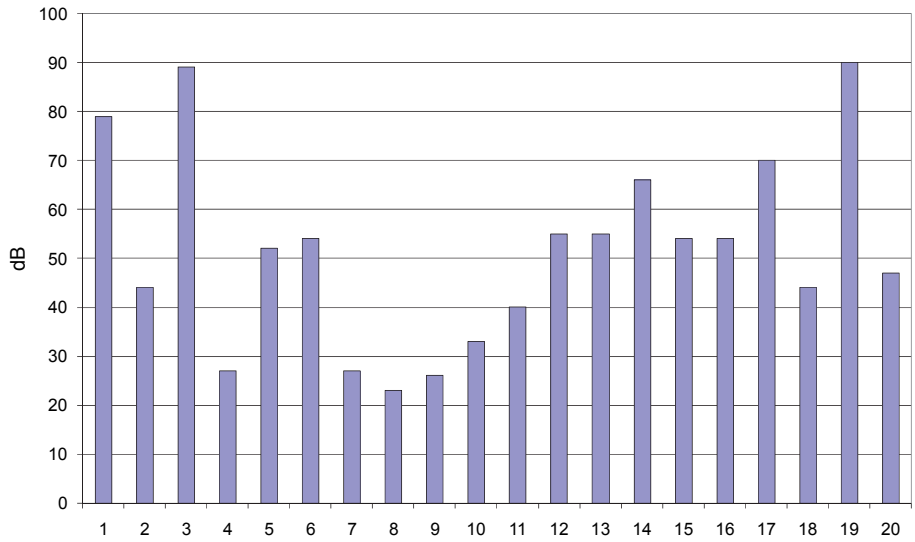

Fig. 12. Differences in acoustic pressure for twenty acceptable cases.

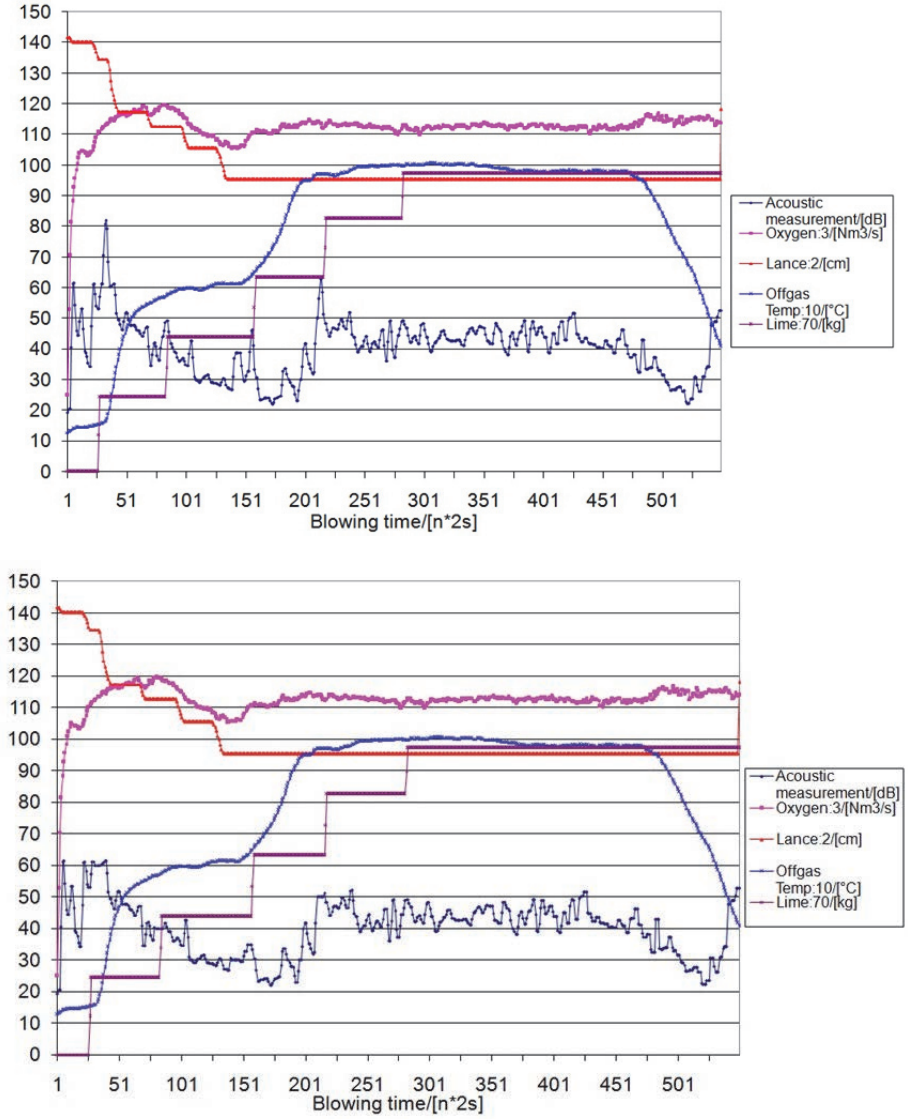

Fig. 13. The filtering of sound of lime addition from acoustic measurement.

The rise in acoustic pressure due to lime addition has been filtered away by replacing big values around the five lime additions with the surrounding acoustic pressure values (value replacement is a typical method used in outlier removal). The filtering of acoustic pressure is presented in Fig. 13. The highest values are

not present in the lower figure. The remaining variance in acoustic pressure is mainly caused by the burning rate of carbon and the behaviour of slag. The behaviour depends on, for example, the amount of lime addition, lance practice (standardised in industrial use) and the variation in oxygen flow rate that is mainly caused by the oxygen pipeline not being stable enough, which in turn can be due to multiple reasons. These reasons include two BOFs operating simultaneously when the capacity of the oxygen plant is not large enough (whole steel plant using a lot of oxygen), the performance of a regulating unit (for example valve) is not good enough or the control is not tuned properly for the simultaneous operation of two BOFs.

Fig. 14 shows two heats with acoustic measurement and other measurements: oxygen flow rate, lance height, off-gas temperature and cumulative lime addition. From the upper heat in Fig. 14 it can be seen that as the oxygen flow rate varies a lot, the acoustic measurement also has higher values. There are also other problems in the lower heat, for example the off-gas temperature is not rising properly at the early stages of the heat (difficulties with the start-up of burning). The start-up of the heat is a phase when the burning rate of carbon increases; this can be observed from the rise in off-gas temperature. The start-up phase ends as the off-gas temperature stabilises. The length of the phase is dependent on many variables, for example if the heat has a lot of coolants, sinter or scrap; or if the start-up is unstable, for instance due to difficulties in the oxygen feed. During the start-up phase there can be heavy splashing, so the optimal length of the phase is as short as possible.

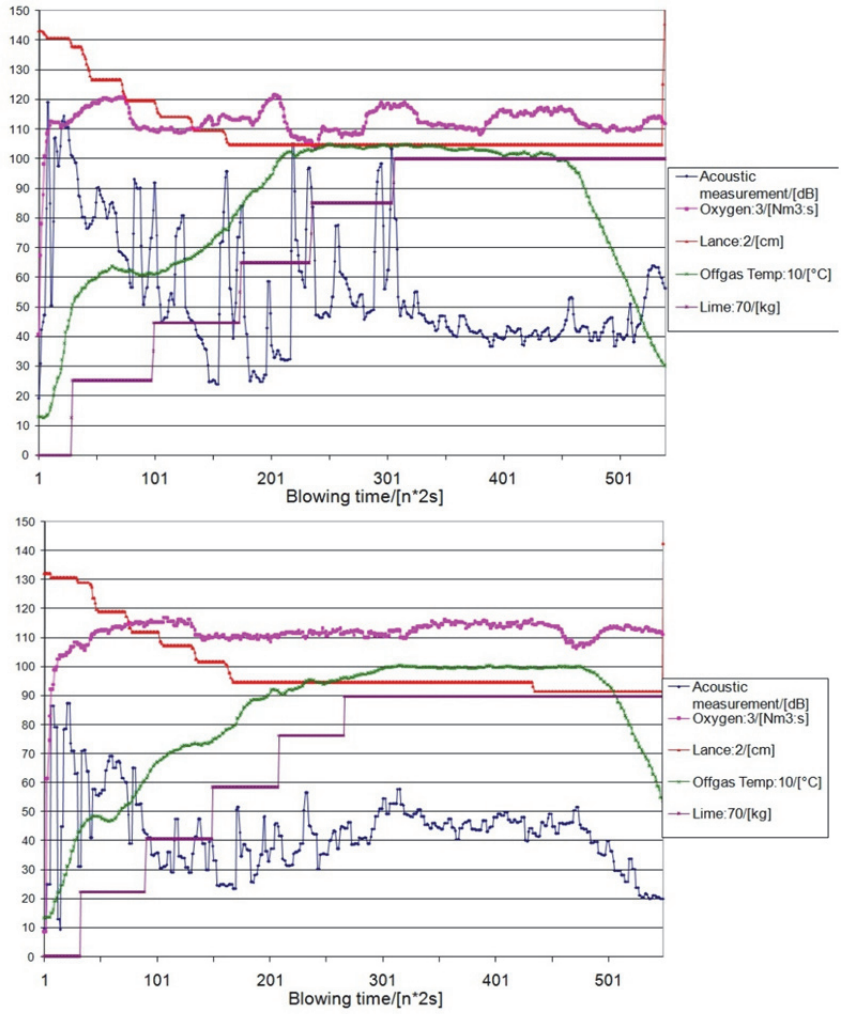

Fig. 14. Two heats with acoustic measurement.

The relationship between the variables was analysed during the ignition of the heat (increasing carbon burning rate). The variables chosen to be analysed were acoustic measurement, oxygen flow rate, lance height and off-gas temperature. The goal was to find a systematic difference during the ignition of the heats in these continuous measurements. About thirty heats were analysed, of which only three heats had difficulties during the ignition. The relationships between the variables were the same in both types of heats. Each scatter plot in Fig. 15 represents the dynamic relationship between two variables in the heat (the

direction of the process is marked with an arrow and the +/− sign shows the direction of the correlation).

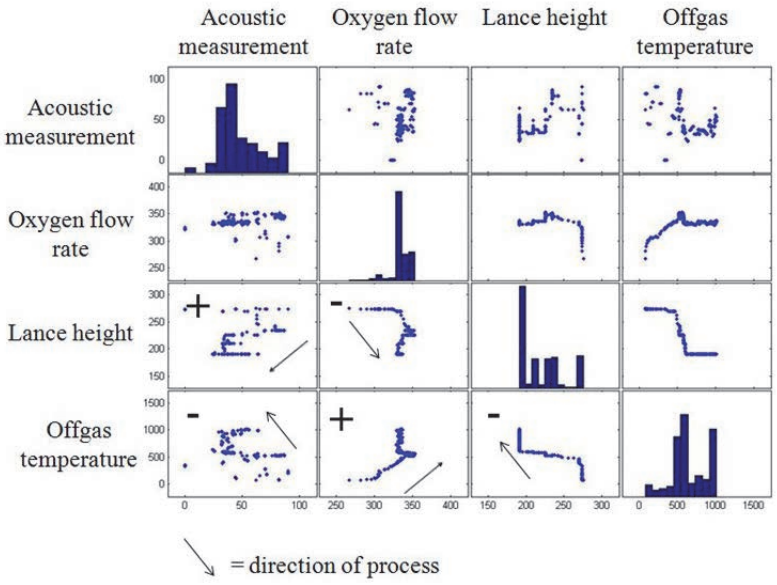

Fig. 15. Scatter plot summary of chosen variables in the ignition part of a heat.

A decreasing lance height decreases the noise recorded by the acoustic measurement. As the off-gas temperature rises, the noise decreases. The oxygen flow rate has no effect on the acoustic measurement. As the lance height decreases, the oxygen flow rate increases. Also in the ignition part of the heat the oxygen flow rate rises as the off-gas temperature rises. With a low lance height, the off-gas temperature rises as carbon oxidation is intensified. Relationships between measurements other than the acoustic measurement are a result of the normal start-up of the process. When the analysis of acoustic measurement and other measurements gives knowledge to the BOF operator that the foaming of the slag is too strong and the risk of splashing is high, he/she can use for example coke as counteraction in addition to lance practice. At this point, the further development of acoustic measurement was not considered necessary. Acoustic measurement in the process automation system was replaced with a splashing measurement, which is discussed in Chapter 3.3.

3.3 Splashing

Splashing is a serious problem in BOFs. It causes economic losses and has therefore been widely researched. The negative effects of splashing are well-known, for example lower yield, different kinds of skull formation; in the lance, upper BOF cone, BOF mouth and gas hood; hard blowing, poor dephosphorisation and desulphurisation. (Bock *et al.* 2000) To prevent splashing, the factors that cause foaming need to be known. Jung & Fruehan (2000) investigated the effects of FeO content, basicity, TiO_2, MgO and temperature of slag on foaming. The geometry of the crater formed by the impact of oxygen jets on the liquid metal surface in the converter also has an effect on splashing. Chatterjee & Bradshaw (1972) and Patjoshi *et al.* (1982) determined the critical crater depth at which splashing starts. Koch *et al.* (1993) determined the critical amount of blown gas when splashing starts, depending on the jet impulse, depth of crater and surface tension. Chatterjee & Bradshaw (1972) also stated that splashing is increased by increasing the impulse of the jet through lowering the lance and/or increasing the feed pressure. Ogawa *et al.* (1993) studied the effect of slag and metal properties on foam using a water model. They found out for example that increasing slag viscosity and/or the surface tension of the metal increase foam height and that increasing the surface tension of slag and the slag-metal interfacial tension decrease foam height. Tanaka & Okane (1987) and Okabe *et al.* (1995) stated that an increase in slag density, surface tension and viscosity decrease splashing. Also, foamy slag decreases splashing significantly (Bock *et al.* 2000).Standish & He (1989), He & Standish (1990) and Sharma *et al.* (1977) have stated that slag has an effect not on the splashing mechanisms, but on the amount of splashing. Choi *et al.* (1994) made modifications to slag in order to reduce skull formation around the mouth of the BOF. Valentino *et al.* (1997) and Tabata *et al.* (1998) reported the positive effect of a wider lance angle on the amount of splashing in the BOF. Tang *et al.* (2008) studied the effects of lance height and bottom stirring flow rate on the mixing time, the amount of splashing, the penetration depth and level fluctuation using a water model. These studies found optimum levels for the parameters in the different phases of the heat. Luomala *et al.* (2002) investigated the effect of the following variables: lance height, gas flow rate, lance nozzle angle, bottom blowing, lance position and foamy slag. The reduction of the lance nozzle angle increased the total amount of splashing. The usage of bottom blowing increased splashing on the lower parts of the converter.

Different kinds of models have been developed to predict slopping sensitivity. The model by Shakirov *et al.* (2004) is based on the calculated slag height during the blow. Some variables used in the model are slag chemistry and metallic phases, the physical properties of slag and the temperature of slag and metal. When heavy splashing occurs, they propose that the oxygen flow should be lowered. Komarov *et al.* (2000) also investigated the use of sound to suppress the foam. It was found that low frequency (90–1300 Hz) sound waves are more effective than high frequency (1300–12000 Hz) sound waves.Bock *et al.* (2000) proposed adjusting the lance height or bottom stirring or even considering the use of a different lance tip design. Iso *et al.* (1988) used images from inside the BOF to predict splashing and then used coke breeze to suppress the foam. This method meant it was possible to decrease splashing significantly. Pak *et al.* (1996) used X-ray fluoroscopy, image processing and lance vibration to predict slag foaming and an anti-foaming agent and coke were tested to suppress the foam. Evestedt *et al.* (Evestedt & Medvedev 2006), (Evestedt *et al.* 2007), (Evestedt & Medvedev 2009) developed a model-based slopping warning method. The sound signal from a microphone located in the off-gas funnel is processed to obtain an estimate of the slag level in the converter. A model describing the relationship between the off-gas flow rate, pressure and slag level estimate is updated recursively in time. The output error is fed to a change detector yielding a warning system with three alarm levels that indicate the persistence of the slopping symptom.

3.3.1 Splashing measurement at Ruukki's Raahe steel works

At Ruukki's Raahe steel works, splashing measurement has been developed and taken into use. The software development was conducted by a local company (www.altevisetec.fi). The splashing measurement is based on image analysis. At Ruukki's Raahe steel works, there are video cameras for monitoring purposes under the converters. These existing cameras were utilised when the splashing measurement was developed.

3.3.2 Analysis of splashing data

The data, process measurements and analyses were collected from the plant automation system into a database. One BOF campaign (heats done with the same lining) was chosen for analysis as it was assumed that results from different campaigns would not be comparable. In total, about thirty variables were

collected. The selection of the variables was carried out in co-operation with the steel plant personnel. Normal pre-processing was done, for example excluding of heats that did not have all the necessary measurement data. The splashing measurement is based on image analysis. The picture pixels were analysed from a snapshot captured from the camera. The amount of splashing was investigated inside a predefined area by counting the ratio of bright and dark pixels; the limiting value of brightness was predefined. The ratio of bright and dark pixels gives a numerical value for the splashing. The splashing integral for the whole blow was calculated from the momentary values. The average splashing integral was 1049.95 and its standard deviation was 506.40 for the remaining 481 heats. Fig. 16 shows the variation in the splashing integral chronologically and Fig. 17 a histogram of the splashing integral. As Fig. 17 shows, there are clearly some circumstances that cause strong splashing. Next, efforts were made to find the variables and possible variable combinations that caused strong splashing.

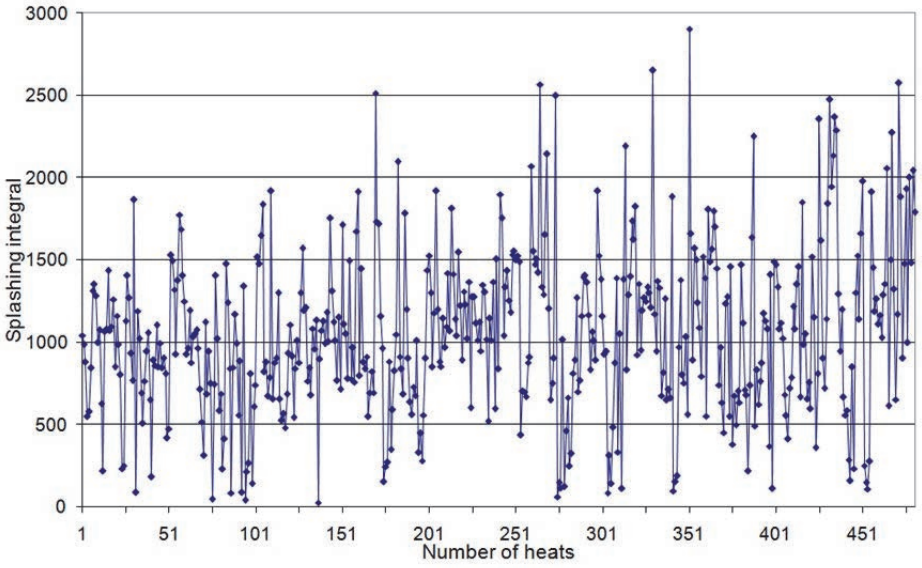

Fig. 16. Trend curve of the splashing integral.

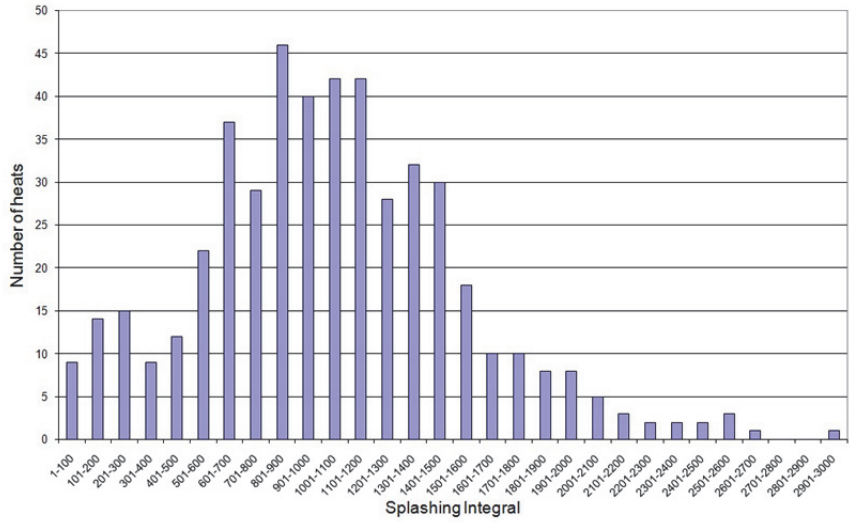

Fig. 17. Histogram of the splashing integral.

Data was collected during normal process operation and as Figures 18 and 19show there is a lot of variation in the data. Statistical correlation and models are also difficult to find because of the variable interactions. Instead of automatic data mining, a much simpler approach was chosen, taking advantage of variable grouping and elimination and expert knowledge.

Each variable was divided into two or more groups based on the variable level. For instance, the heat size was divided in two groups, big and small heat size. The average value of the splashing integral was calculated for each heat and the ratio between different groups for each variable was calculated in order to see how big a difference there was between the chosen groups. By comparing these ratios between different variables, the variables with the greatest effects on the splashing integral could be found. Later on this method was expanded to combinations of variables.

This approach puts the variables more or less in order of importance. Expert knowledge is also necessary for choosing variables and the order in which they are applied in the analysis. Results depend heavily on the selection of variable levels and this requires thorough process know-how.

After analysing the data and discussions with plant personnel, especially heat size, ferrosilicon addition, relative lime and scrap additions and the end carbon percentage were found to have an effect on splashing. Table 3 shows that the heat

size has the biggest effect on splashing, also the added ferrosilicon (called here FeSi) in the early stages of the heat has a strong effect on splashing and also the amount of charged scrap has an impact. In Table 3, Heat105k means heats where the batch size (hot metal + scrap) is less than 120 tonnes and heat120k means heats, where the batch size is more than 120 tonnes, FeSi* is the amount of added FeSi, [kg] (for example FeSi0 means that no ferrosilicon was used in the heat), Lime/Heat is the ratio showing how much lime is used to form slag and C-% is the carbon percentage at the end of the blow.

Table 3. Splashing integrals in preliminary grouping.

Group	Average	Std dev	Ratio
Heat105k (76 heats)	691.33	381.79	1
Heat120k (402 heats)	1121.01	498.19	1.62
FeSi0 (131 heats)	864.05	449.40	1
FeSi38-200 (200 heats)	932.36	487.62	1.08
FeSi200+ (197 heats)	1269.77	476.26	1.47
Lime/Heat (< 5.0%)(226 heats)	1109.61	491.58	1.11
Lime/Heat (≥ 5.0%)(256 heats)	1001.66	514.72	1
Scrap/Heat (< 22%)(209 heats)	902.79	457.51	1
Scrap/Heat (≥ 22%)(269 heats)	1169.16	512.44	1.30
C-% ≤ 0.035 (252 heats)	977.98	446.19	1
C-% > 0.035 (226 heats)	1136.01	555.02	1.16

The two following figures (Fig. 18 and 19) show how the splashing integral varies per heat size and per added FeSi. The trend lines in the figures show how the splashing integral changes as the heat size and added FeSi increase. Table 4 shows that the smaller heat size has reasonably low splashing, so research was focused on the bigger heat size. Note that the number of heats analysed later decreases from 478 heats to 402.

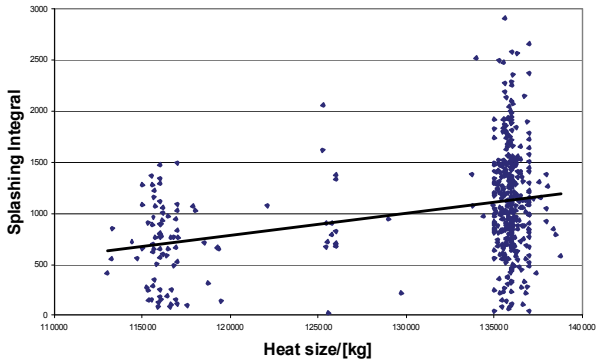

Fig. 18. Splashing integral versus heat size.

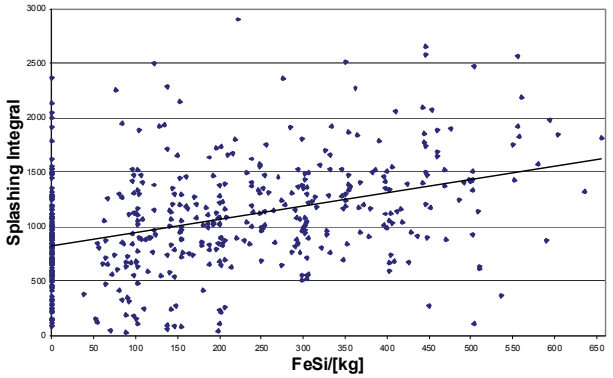

Fig. 19. Splashing integral versus FeSi.

As the research was focused only on bigger heats, it needed to be checked whether the variables used in the whole database still had the same effect on splashing. As observed from Table 4, Lime/Heat, Scrap/Heat and C-% now have a much lower ratio than earlier, which means that their effect is not so significant. It is more likely that there is a different function mode for these according to the heat size, for example a different percentage of added lime for the smaller heat size. Added FeSi still has a significant effect on splashing. After added FeSi was grouped slightly differently to have more heats in the lowest group, it was noticed that about 100 kilograms of FeSi could be added into the heat without having an effect on splashing (FeSi0 $\cong$ FeSi/Heat < 0.00075).

Table 4. Splashing integrals at Heat120k.

Group	Average	Std dev	Ratio
Lime/Heat (< 5.0%) (225 heats)	1114.33	487.51	1
Lime/Heat (≥ 5.0%) (172 heats)	1138.74	510.56	1.02
Scrap/Heat (< 22%) (130 heats)	1027.31	457.32	1
Scrap/Heat (≥ 22%) (267 heats)	1172.42	509.50	1.14
C-% ≤ 0.035 (181 heats)	1087.98	418.79	1
C-% > 0.035 (216 heats)	1155.85	553.42	1.06
FeSi0 (125 heats)	926.51	483.19	1
FeSi/Heat < 0.0015 (102 heats)	1026.67	438.45	1.11
FeSi/Heat > 0.0015 (170 heats)	1329.72	464.53	1.44
FeSi/Heat < 0.00075 (152 heats)	928.13	476.46	1
0.00075 ≤ FeSi/Heat > 0.0015(75heats)	1063.06	429.72	1.15
FeSi/Heat > 0.0015 (170 heats)	1329.72	464.53	1.43

As many of variables no longer had that much effect in the bigger heat size, new variables that affect splashing were considered. ScrapLight is the ratio that reveals how much light scrap is added to the scrap charge. Si/Mn is the ratio of how much silicon and manganese there is in the pig iron. This is an important ratio in steelmaking, which is controlled in the blast furnace. OGT_slope is the slope of the off-gas temperatures between 100 and 200 seconds and OGT is the off-gas temperature at 100 seconds. These tell us how the blowing starts, for example if OGT_slope is negative; the burning of carbon has not started properly. The effects of these variables on splashing are shown in Table 5.

Table 5. More splashing integrals at Heat120k.

Group	Average	Std dev	Ratio
ScrapLight < 50% (209 heats)	1205.37	521.98	1.16
ScrapLight ≥ 50% (188 heats)	1035.44	452.80	1
Blowing time ≤ 1060s (194 heats)	1053.26	454.76	1
Blowing time > 1060s (203 heats)	1193.38	526.57	1.13
Si/Mn < 1.14 (196 heats)	1057.81	505.52	1
Si/Mn > 1.14 (201 heats)	1190.33	481.12	1.13
OGT_slope < 0 (223 heats)	1171.11	461.19	1
OGT_slope > 0 (178 heats)	1065.69	535.27	1
OGT < 550 (185 heats)	1105.93	513.37	1
OGT > 550 (212 heats)	1141.46	483.14	1.03
OGT_slope < 0			
OGT < 550 (44 heats)	1201.02	374.55	1.03
OGT > 550 (179 heats)	1163.76	480.73	1
OGT_slope > 0			
OGT < 550 (141 heats)	1076.26	547.33	1.05
OGT > 550 (33 heats)	1020.53	485.56	1

As these variables did not have a significant effect on splashing, tests were made to see if something interesting would come up. The effect of the dominating variable was eliminated, in this case added FeSi. Research was concentrated only on heats where FeSi/Heat was less than 0.00075. Another variable was added: Si*Lime/Heat. This needs to be adjusted carefully as it seems to have a major effect on splashing. The hypothesis is that this ratio is important because if too little lime is used for higher silicon amounts in the pig iron, it will disturb the heat in a similar way as added FeSi. Fig. 20 shows that this ratio needs to be kept close to one as splashing increases rapidly as the ratio grows. According to plant personnel, the Si/Mn ratio cannot be much below one because of blast furnace practices, so there is a fairly small optimal range for this. The effects of the variables on splashing when FeSi/Heat < 0.00075 can be seen from Table 6.According to this study, the ratio of silicon and manganese is very important.

Table 6. Splashing integrals for bigger heats with FeSi/Heat < 0.00075.

Group	Average	Std dev	Ratio
OGT < 550 (62 heats)	846.68	478.15	1
OGT > 550 (90 heats)	983.04	476.13	1.16
OGT_slope < 0 (87 heats)	986.99	449.87	1.17
OGT_slope ≥ 0 (65 heats)	842.87	507.19	1
Si*Lime/Heat < 0.021 (64 heats)	751.38	348.80	1
Si*Lime/Heat > 0.021 (88 heats)	1051.89	521.17	1.4
Scrap/Heat < 22% (72 heats)	869.61	412.48	1
Scrap/Heat ≥ 22% (80 heats)	975.54	550.36	1.12
ScrapLight < 50% (68 heats)	962.70	501.98	1.08
ScrapLight ≥ 50% (84 heats)	895.14	460.31	1
C-% ≤ 0.035 (72 heats)	873.57	324.84	1
C-% > 0.035 (80 heats)	971.98	582.25	1.11
Blowing time ≤ 1060s(81 heats)	855.60	433.66	1
Blowing time > 1060s (71 heats)	1004.94	517.58	1.17
Si/Mn < 1.14 (55 heats)	643.71	300.73	1
Si/Mn > 1.14 (97 heats)	1085.06	488.63	1.69

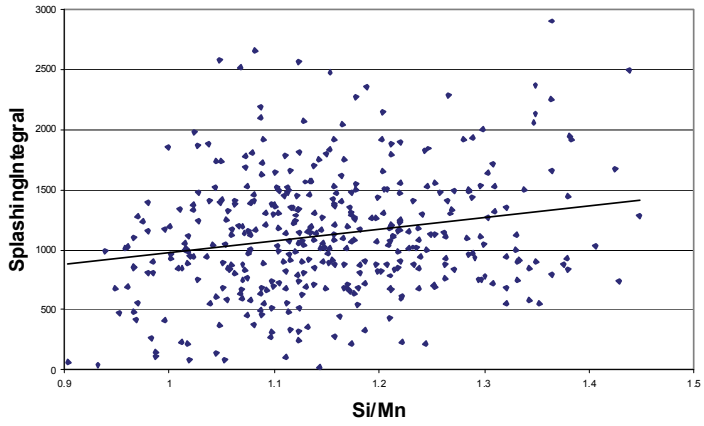

Fig. 20. Splashing integral versus Si/Mn for bigger heats with FeSi/Heat < 0.00075.

As some variables affecting splashing have now been found, the next point to be considered is how to utilise this knowledge in the control of BOFs. An example of two heats is presented: one, where FeSi is added in the early stage of the heat and another where FeSi is not added at all. We can see from Fig. 21 that adding FeSi in the early stages of the heat strongly affects the off-gas temperature. This is

natural as silicon is burnt earlier than carbon and the off-gas temperature is a function of the amount of burned carbon. The progress of the blow is disturbed and the carbon rate is not stable (off-gas temperature collapses), which leads to strong splashing as the carbon starts to burn after the FeSi has been burnt away. How to avoid this? It would be easy to say that an addition of over 100 kilograms of FeSi is not allowed in the early stages of the blow. However, it is not that simple as FeSi is always added for a reason: the batch needs extra heating. Another option would be to add less scrap, but the maximum possible amount of scrap is needed to maximise production and the usage of scrap. One possibility would be to have higher silicon content in pig iron. However, it is not always possible to operate the blast furnace so that it would give high enough silicon content in pig iron, and it is not usually economically reasonable. One further possibility would be to adjust the time when FeSi is added, for example to add it in later stages of the blow. But what kind of effects would that have on the blow as a whole? This question is not so easy to answer; it needs to be considered by steelmaking experts and via test runs.

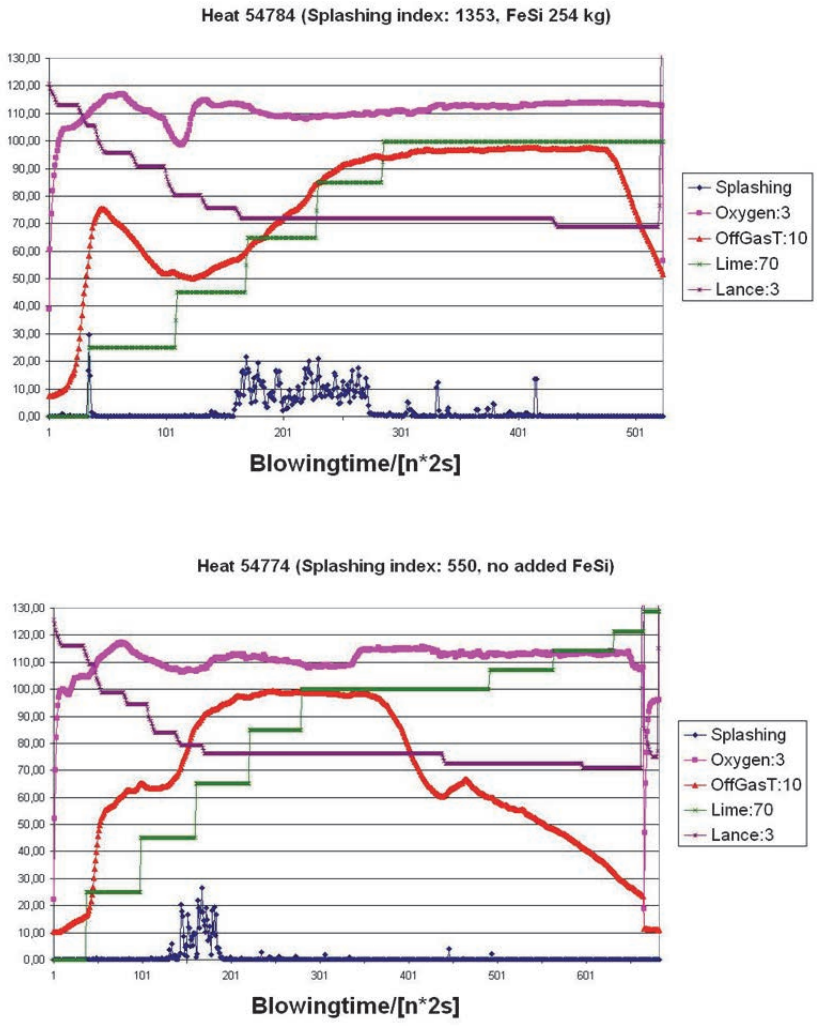

Fig. 21. Example of effect of FeSi effect on splashing integral.

In the table below, Table 7, the effects of some variables are listed and can be used as basic guidelines. It needs to be taken into account that some effects are not absolutely clear, for example the off-gas temperature. The comparison is mostly made in pairs.

Table 7. Effect of different variables on splashing.

Group	Variable range	Effect on splashing
OGT1	T < 550 °C	Lower
OGT2	T > 550 °C	Higher
OGT_slope1	Slope < 0	Higher
OGT_slope2	Slope ≥ 0	Lower
FeSi1	FeSi/Heat < 0.00075	Lower
FeSi2	0.00075 ≤ FeSi/Heat < 0.0015	Higher
FeSi3	FeSi/Heat < 0.00015	Highest
Si*Lime/Heat1 (SLH1)	Ratio < 0.021	Lower
Si*Lime/Heat2 (SLH2)	Ratio > 0.021	Higher
Scrap/Heat1(SH1)	< 22%	Lower
Scrap/Heat2(SH2)	≥ 22%	Higher
ScrapLight1(SL1)	< 50%	Higher
ScrapLight2(SL2)	≥ 50%	Lower
C1	≤ 0.035%	Lower
C2	> 0.035%	Higher
Blowingtime1(BT1)	≤ 1060 seconds	Lower
Blowingtime2(BT2)	> 1060 seconds	Higher
Si/Mn1	Ratio < 1.14	Lower
Si/Mn2	Ratio > 1.14	Higher

Some of these guidelines are hard to put into practice, for example the slope of the off-gas temperature, which is however most probably the result of added FeSi in the early stage of the heat. There are not that many actions that can be done to avoid stronger splashing in this situation. The best way to avoid stronger splashing is to avoid adding FeSi in the early stages of the blow or before the blow. Some of the guidelines are quite useful, for example keeping ratios such as silicon*lime/heat and silicon/manganese at the optimum.

Figure 17 shows that there were 58 heats with significantly higher splashing integrals than the rest of the heats. It must be assumed that there are many different variables that cause stronger splashing. Likewise, there were 37 heats with lower splashing integrals. To determine what kind of circumstances led to stronger or lower splashing, we calculated four different combinations of variables, which indicate stronger splashing in heats. From this we can see in which circumstances strong splashing is most likely to occur. A similar calculation was made for the heats with lower splashing.

Table 8 lists the combinations of variables for the heats with stronger splashing and for those with lower splashing. There are no combinations or pairs

of combinations that lead to certain splashing; this shows that the converter is a complicated process to control and that different variables have strong interactions. From this table we can find examples of the combinations of variables that should be avoided or favoured. Again, how to implement this knowledge in practice is not necessarily that simple, but at least these circumstances are now known.

Table 8. Most common combinations of variables (notations same as in Table 7.).

VariableCombination	# of heats
Strong splashing	
SLH2, SH2, BT2, Si/Mn2	23
SLH2, SH2, SL1, BT2	21
SLH2, SH2, SL1, Si/Mn2	19
OGT2, OGTS1, SH2, C2	18
SH2, SL1, BT2, Si/Mn2	18
SLH2, SH2, C2, BT2	18
FeSi3, SH2, SL1, BT2	18
SLH2, C2, BT2, Si/Mn2	17
OGTS1, SLH2, SH2, BT2	17
OGT2, OGTS1, SH2, BT2	17
SLH2, SL1, BT2, Si/Mn2	17
FeSi3, SLH2, SH2, BT2	17
SLH2, SH2, C2, Si/Mn2	17
Low splashing	
FeSi1, SLH1, SL2, Si/Mn1	13
SLH1, SL2, BT1, Si/Mn1	12
FeSi1, SLH1, BT1, Si/Mn1	12
FeSi1, SLH1, SL2, BT1	11
FeSi1, SH1, BT1, Si/Mn1	10
FeSi1, SL2, BT1, Si/Mn1	10
FeSi1, SLH1, SH1, Si/Mn1	10
OGT1, OGTS2, SLH1, Si/Mn2	10
SLH1, SH1, SL2, Si/Mn1	10
OGTS2, SLH1, BT1, Si/Mn1	10

In the literature it is often reported that the lance height has an effect on splashing. However, at least at Ruukki, the lance program is so standardised that there is no variation within the lance height and hence it does not affect splashing.

When looking at the heat size, it was noticed that if the charge size was adjusted a little, for example if the biggest heat were 135.5 tonnes, splashing

would go down by 8% (from 1125 to 1044). This would mean cutting down the heat size by a maximum of 3 tonnes. Of course, this would cut production and it assumes that the heat size is the only variable that contributes to higher splashing in these blows.

3.4 Other BOF measurements

In this chapter a few other measurement techniques are introduced briefly even though they were not used in this work.

3.4.1 Mass spectrometer

A mass spectrometer is used in analysing the off-gas flow from the BOF. Mass spectrometry is based on sampling from the off-gas duct. In the analyser the pressure of the gas sample is first decreased to very low. After that it is ionised, accelerated and measured. Analysis is done based on the mass/charge ratio. Almost any gas mixture can be broken up into its components and measured. (Morris 1993) The components of an ion beam can be isolated with many different techniques based on the mass/charge ratio. In practice there are two methods, which are used in the measuring of continuous gas flow: magnetic sector and quadruple mass analyser. (Merriman 1997)

The sampler of the mass spectrometer is normally placed in the top of the BOF in the off-gas pipe. The analysing equipment is well protected. The control computer can be located in the same room as the mass spectrometer or in the control room. (Merriman 1997)

As an example, the mass spectrometer equipment in use at Benxi Plates Co. Ltd. is presented in Hu *et al.* 2003. Their sampling equipment consists of two probes, a PLC-controlled filter and a duct leading to the mass spectrometer. Probes are installed sequentially in the vertical direction and symmetrically in the horizontal direction. One probe is in use at the time. If the probe in use is choked with dust, the operation is switched automatically to another probe. Then the choked probe can be cleaned with a high-pressure nitrogen flow, after which it stays in standby mode. The filter and mass spectrometer are installed in a small box near the off-gas pipe. After analysing, the information is sent to the computer for calibration and data transfer, which is located in the control room. The equipment also includes a gas flow rate meter, which is located in the converter gas recovery system. (Hu *et al.* 2003), (Zhi-Gang *et al.* 2003) Almost the same

configuration of off-gas analysing equipment is reported to be in use in EKO Stahl's two LD converters. (Schmidt *et al.* 2000)

Iso *et al.* (1987) examined the effect of the sampling place on the representativeness of a sample of the whole gas flow. Three sampling places before the dust remover in the upper part of the off-gas duct were tested; one in the middle of the flow, one close to the top wall and one halfway between the others. CO and CO_2 concentrations close to the top wall did not differ significantly when compared to those from the middle of the flow. This was assumed to be due to the turbulent flow (the Reynolds number was always above 3×10^5). As the composition of the gas flow is similar across the whole width of the pipe, it can be stated that the probe close to the wall is good enough to represent the whole gas flow.

3.4.2 X-ray fluorescence

A significant amount of metal is lost from the BOF in the off-gas as dust and the quantity of it can differ a lot during a blow depending on the oxygen flow rate, lance height, configuration of nozzles, slag and addition of scrap. 1–3 per cent of charged iron can be lost as iron oxide in dust. In addition to that other metals also become gasified. To improve the efficiency of the steelmaking process, a method based on X-ray fluorescence has been developed. This method measures metals from the off-gas flow on-line. Real-time information can be used to adjust the process parameters to minimise metal losses and emissions, to optimise the BOF process, for slag control and to optimise the treatment of off-gas. The location of the analyser in the off-gas system depends on its use. If the loss of iron and other metals from the BOF is measured, the analyser is placed in the early parts of the duct. If the emissions into the environment are measured, the analyser is placed in a suitable position after off-gas recovery and cleaning. (Meyer *et al.* 2001), (Thornton & Welbourn 1996), (Mink & Dye 2002)

3.4.3 Microwave radar

Microwaves are radio waves i.e. electromagnetic radiation with frequencies from 1 to 300 GHz. Their use is well-known from radar measurements, in which the distance and speed of the target needs to be measured. The advantages of microwaves are low investment and maintenance costs, ease of installation, continuous measurement, and the fact that they do not disturb the process and are

not very sensitive to temperature, pressure, dust or the medium. Researchers have shown that microwaves can also be applied successfully to the demanding conditions of the steel industry. Surface level measurement is the most important application, but it has been noticed that slag thickness can also be measured. (Bruckhaus *et al.* 2001), (Little & Lewis 2001), (Meszaros *et al.* 2001)

Microwave measurement is based on echo sounding. The microwave transmitter installed in the top of the BOF sends microwaves, which are directed into the surface of the melt. The microwaves are reflected from the surface and the receiver detects an echo. (Bruckhaus *et al.* 2001)

The reflection of microwaves is dependent on the conductivity of the material being measured. The conductivity and reflectivity of steel is much better than those of slag, so these surfaces can be separated using microwaves. The frequency of radiation has an effect on the penetrability of materials. In the patented DepthWave method, a frequency of 6.3 GHz is used for measuring. (Bruckhaus *et al.* 2001), (Meszaros *et al.* 2001)

As the reflectivity of slag is pretty poor, a more exact microwave measurement method, known as M-sequence modulated measurement, had to be developed. The microwave signal is modulated and the echo is processed. M-sequence modulated microwave measurement is being used successfully at Keihin Works in Japan. (Nagamune *et al.* 1992), (Miyahara *et al.* 1997)

3.4.4 Infrared spectrometer

The advantage in using infrared spectrometry is that it is a non-invasive measurement method. At Bethlehem Steel's Sparrows Point an optical sensor based on infrared absorption spectroscopy is in use. The hardware consists of a transmitter and detector modules. The infrared light source is a tuneable semiconductor laser diode. The diode must be cooled by liquid nitrogen to a temperature in the 80 to 120K range. The absorption spectrum of CO and CO_2 can be determined from the sensor signal using relative peak intensities. (Allendorf *et al.* 1998) An IR spectrometer is also used at SSAB Tunnplåt Works to analyse CO and CO_2. (Bergman & Hahlin 1997)

4 Development of blow-end temperature and additional material models for the BOF

The main contribution of this thesis is the development of blow-end temperature and additional material models. The target was to develop models that can be used in the BOF control system. It was also necessary to see if the model needs to be adaptive. The models are needed in every heat to predict the end time. Before there was no blow-end temperature model in use and a constant value was used for all heat types. A model for additional material had not been developed at all.

4.1 Data acquisition

Data was collected from Ruukki Raahe steel plant's Neuvo database, in which all process measurements and analyses are stored. Measurements have been collected from this database on about 50,000 heats. Altogether 36 different measurements were collected from the database. The selection of measurements was done in co-operation with specialists from Ruukki. The collected measurements from the Neuvo database contained for example amounts of the materials used, chemical contents of the product, and temperatures.

The modelling is based on heats in which a drop sensor measurement was available, as the prediction of temperature was necessary in the end of the blow. At first the drop sensor apparatus was in use only in BOF 1 and 2. Table 9 lists some features of the data sets. The drop sensors that had a temperature of 0 °C or those used to measure oxygen content were excluded.

Table 9. Content of data sets

	DBsyys00	DBtammi01	DBmaalis01
Heat numbers and	33000–40700	40701–48334	48335–51697
number of heats	(7701)	(7634)	(3363)
BOF 1	2434	2669	937
BOF 2	2580	2485	1085
BOF 3	2471	2282	1259
Sum of BOFs 1–3	7485	7436	3281
Number of drop sensors	6668	7092	2389
Number of useful drop sensors	4419	5179	1858

The database includes a little over 97% of all the heats. The reasons for being missing from the database were many; the most important one being imperfect

database operation. Some of the heats had already been excluded in the data acquisition phase.

It is worth noting that in some heats there were as many as five drop sensor measurements available and out of these the best one was chosen. The selection criteria were, for example, that the dropping time was early enough before the end of the heat (about 1 to 2½ minutes) and that the temperature of the off-gas was in a decent range (about 600–900 °C). Most of the heats had, however, only one drop sensor measurement available that was favourable. The drop sensor must be dropped early enough before the end of the blowing, in order to be able to affect the temperature of the steel with additional material, if necessary.

Data acquisition was made on a computer, from which it was possible to create a connection to the Neuvo database. The data was retrieved from this database to Microsoft Excel® using Microsoft Query®.

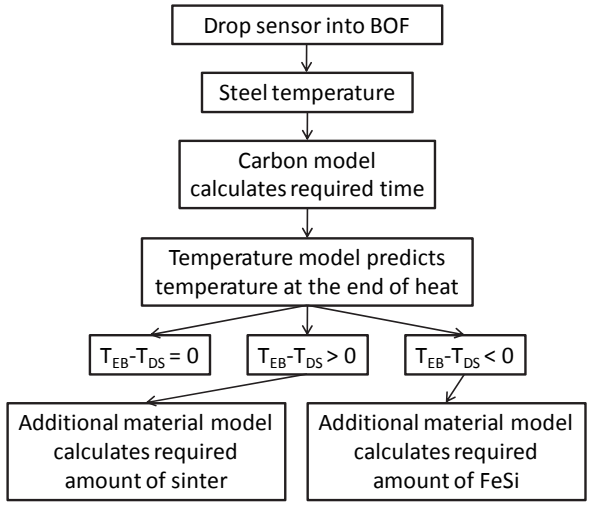

Fig. 22. Structure of blow-end temperature and additional material models.

The structure of the blow-end temperature and additional material models is presented in Fig. 22. First, a drop sensor is dropped into the BOF to get the temperature of the steel. When the temperature is available, the carbon model calculates the time required to achieve the target carbon content. When the required time is given, the blow-end temperature model calculates the temperature at the end of the heat. If the calculated temperature is the same as the target temperature, no actions are needed. If the temperature is higher than the

target temperature, the additional material model calculates the amount of sinter required to cool it down. If the temperature is lower than the target temperature, the additional material model calculates the amount of FeSi required heating it up.

4.2 Blow-end temperature model

First, the form of the model was chosen from different mathematical alternatives. The target was to keep the model as simple as possible. The alternatives were a linear model where the slope changes during the blow or a linear model where the slope is defined only on the basis of the starting values of the heat. As the time between a drop sensor measurement and the end of the blow is short, it was decided to use a constant slope, defined from the starting values of the heat. This alternative is easier to carry out and probably gives at least as good a result as the model with a changing slope. Originally, the slope was set to 0.54 °C/s so that the model adds 0.54 °C to the temperature every second after applying the drop sensor.

The calculation of the slope is carried out as follows: the temperature difference between the drop sensor temperature and the measured blow-end temperature is divided by the difference between the total blowing time and the time of dropping the sensor.

$$S = \frac{T_{EB} - T_{DS}}{t_{EB} - t_{DS}}, \tag{1}$$

where S is the slope [°C/s],

T_{EB} is the target temperature at the end of the blow,

T_{DS} is the temperature when the drop sensor is used,

t_{EB} is the total blowing time and

t_{DS} is the moment of the drop sensor from the beginning of the blow.

As mentioned earlier, the prediction of the temperature rise is necessary only after receiving the drop sensor measurement. The two main reasons for this are that the temperature rise in the early stages of the blow is more random and the moment of the drop sensor measurement can be determined from the off-gas temperature. As mentioned above, at the beginning the drop sensor apparatus was not in use in BOF 3, so the first phases of modelling were done based on the data from BOFs 1 and 2.

4.2.1 Preliminary modelling

In modelling, DBsyys00database was used as the training set and DBtammi01database as the test set. The training set contains 5014 heats done in BOF 1 or 2. From 3787 heats, in which a total number of 4979 drop sensors were used, all the necessary data for calculations was available. Next, four models were developed and tested. The models were structurally similar, but their training sets differed:

- kk-ka model. Some of the heats that had drop sensor measurement were left out as the blow-end temperature or total blowing time was not logged in the database.
- kk-ka mod model. Some heats were removed from the kk-ka model. The criteria were as follows: heats that had drop sensor measurement only after the end of the blow, heats in which the temperature had decreased after the drop sensor measurement, blows that were less than 700 seconds long and heats in which the slope was above one. In this model, 3341 heats remained and only the best drop sensor measurement was used.
- mod > 20 model. In addition, heats where the temperature change was less than 20 °C after the drop sensor measurement were filtered out.
- mod < 20 model. Heats in which the temperature change after the drop sensor measurement was less than 20 °C.

The following figures (Figs. 23, 24 and 25) and statistical features (Table 10) are to illustrate the above-mentioned models.

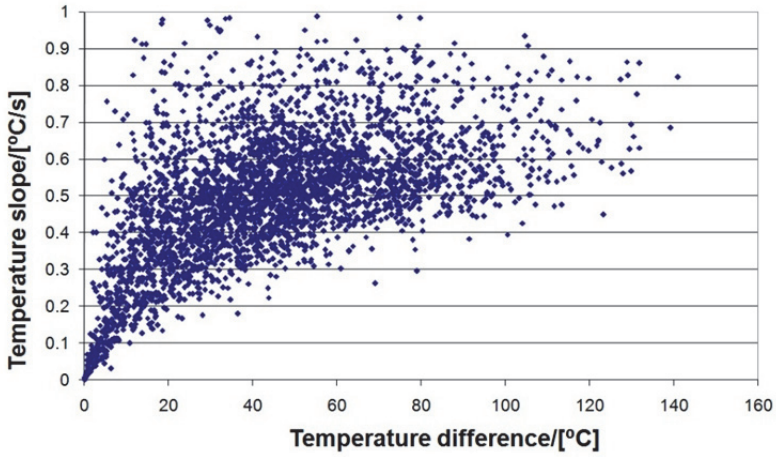

Fig. 23. Effect of time difference on temperature slope after drop sensor.

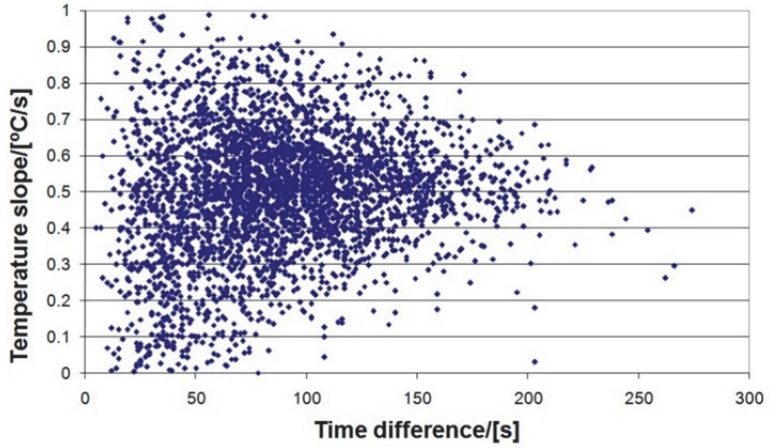

Fig. 24. Effect of temperature difference on temperature slope after drop sensor.

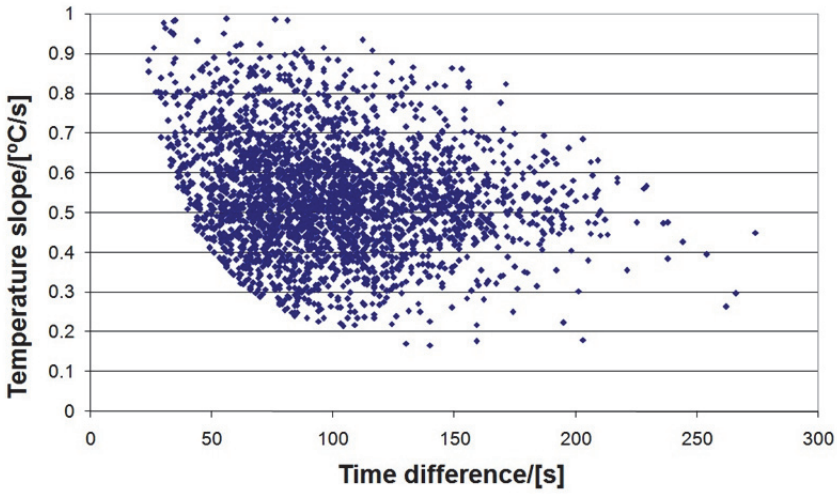

Fig. 25. Effect of time difference on temperature slope when the temperature rise is over 20 °C after drop sensor.

This filtering needed to be done as the heats with a short time between the drop sensor and the end of the blow had small temperature slope values. This is a result of dropping the drop sensor into a hot spot (local maximum temperature). These heats were removed as the modelling was meant for normal heats. The figures illustrate that by performing the filtering temperature-wise, many of the small slope values are filtered out without losing too many of the heats. If the filtering had been done time-wise, the filtered slope values would have been from the whole slope area. In this case, the objective for filtering, i.e. the removal of slopes in the wrong slope area would not have been achieved. From the chart that is filtered temperature-wise, it can be observed that there are still some heats in which the blowing lasted over three minutes after the drop sensor and, on the other hand, some heats in which the values of the slope are bigger on average as the time difference is short. It was assumed that this would not skew the training set too much compared to the benefit obtained from the filtering.

Next, the averages, variances, standard deviations and the number of heats and drop sensors in different models are presented in Table 10. Two more models were formed:

- Time30-180 is based on data formed by filtering kk-ka mod data time-wise.
- Temp+time is based on data formed by filtering mod > 20 data time-wise.

Table 10 shows that time-wise filtering does not decrease the standard deviation very much and that the standard deviation is least in the mod > 20 data. An additional time-wise filtering does not improve the result significantly, so mod > 20 data was chosen as the training set in the actual modelling. In slope calculations, two decimal digits are used, as is the case in the slope in use. The unit of the slope is °C/s.

Table 10. Statistical features of slopes in different models.

	kk-ka	kk-ka mod	mod > 20	mod < 20	Time30-180	Temp + time
average	0.372	0.500	0.543	0.316	0.504	0.544
standard deviation	1.301	0.174	0.138	0.186	0.169	0.139
number of heats	3787	3341	2700	641	3043	2599
number of drop sensors	4979	3341	2700	641	3043	2599

The test set, DBtammi01database, contains 5154 heats done in BOF 1 or 2. From 4364 heats, in which a total number of 5457 drop sensors were used, a drop sensor and other measurements required for calculating were available. Some of the heats that had the drop sensor measurement were left out as the blow-end temperature or total blowing time was not logged in the database. Heats, which had a drop sensor measurement only after the end of the blow, were left out of the test set and in addition only the best drop sensor measurement was used. Thus two test sets were formed:

- 4364m, in which more than one drop sensor measurement was available from one heat and
- 4284.

The third test set was

- 4284Temp, which was formed from 4284 by filtering the heats in which the temperature change was less than 20 °C.

With these three test sets, the functionality of the average slope given by the different models was tested. The calculated temperature is the drop sensor measurement added to the product of the slope in question and the difference between the total blowing time and the time of dropping the sensor. The calculated temperature is given by

$$T_C = T_{DS} + S(t_{EB} - t_{DS}), \tag{2}$$

where T_C is the calculated end temperature,

T_{DS} is the temperature when the drop sensor is used,

S is the slope,

t_{EB} is the total blowing time and

t_{DS} is the time when the drop sensor is used.

The error was calculated as the difference between the calculated temperature and the blow-end temperature. The error is

$$e = T_C - T_{EB}, \tag{3}$$

where e is the error,

T_C is the calculated end temperature and

T_{EB} is the target temperature at the end of the blow.

Table 11 shows the errors of the different training data sets together with some statistical features; the unit of all the values is °C. The percentage of error is calculated for every test set according to the average temperature rise. For example, the average temperature rise of 4284Temp data was 53.3 °C and the percentage of error for the current and $\mathrm{mod} > 20$ data is −4.45% ((−2.37 °C/53.3 °C) × 100%). In Fig. 26, the histograms of the errors for the different models in the test set 4284Temp are presented. Errors are divided into bins of 5 °C.

Table 11. Error tables and statistical features of test sets, 4364m, 4284 and 4284Temp.

	error(current)	error(kk-ka)	error(kk-kamod)	error(mod > 20)	error(mod < 20)
4364m					
Average	1.04	−11.44	−1.89	1.04	−15.11
Standard deviation	18.46	20.58	18.65	18.46	21.78
Mean squared error	341.94	554.21	351.36	341.94	702.38
Minimum	−379.16	−392.08	−382.20	−379.16	−395.88
Maximum	184.84	132.82	172.60	184.84	118.28
4284					
Average	1.26	−12.74	−2.04	1.26	−16.85
Standard deviation	15.03	17.33	15.34	15.03	18.42
Mean squared error	227.28	462.51	239.36	227.28	623.23
Minimum	−63.00	−89.63	−67.40	−63.00	−98.18
Maximum	90.94	67.73	80.70	90.94	63.78
4284Temp					
Average	−2.37	−18.41	−6.15	−2.37	−23.12
Standard deviation	13.46	14.10	13.39	13.46	14.73
Mean squared error	186.83	537.59	217.00	186.83	751.53
Minimum	−63.00	−89.63	−67.40	−63.00	−98.18
Maximum	90.94	47.42	80.70	90.94	34.62

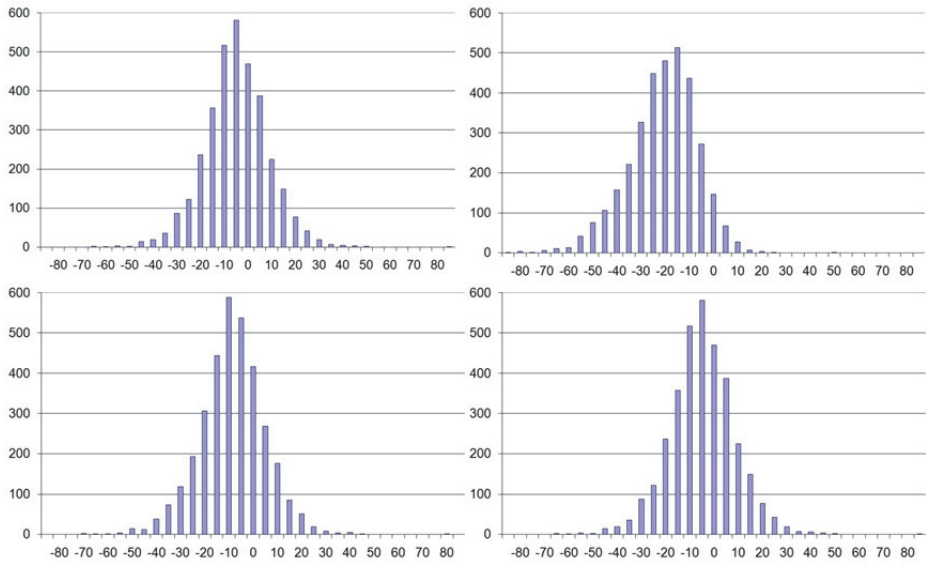

Fig. 26. Histograms of errors for different models in 4284Temp-test set (top left current, top right kk-ka, bottom left kk-ka mod and bottom right mod > 20).

It is worth noting that the standard deviation decreases when moving to smaller test sets, which shows that the filtering was done in the right direction. Diminution of the error range shows that most of the "impossible" heats have disappeared from the data and the rise of the error average shows that the training set needs to be divided into smaller parts.

4.2.2 Grouping according to converter and heat size

Based on the results gained earlier, mod > 20 was chosen for the next modelling phase. Training set mod > 20 (distribution by heat size is presented in Fig. 27) was divided into groups according to the BOF and the heat size; using the heat size, the data was divided into two groups, over 120 tons and 105–120 tons (heat size = scrap and pig iron). The largest five heats were outside the distribution, but they were included as their percentage was small. The smallest twelve heats were left out of the study, as their percentage in the smaller heat size group would have been significant.

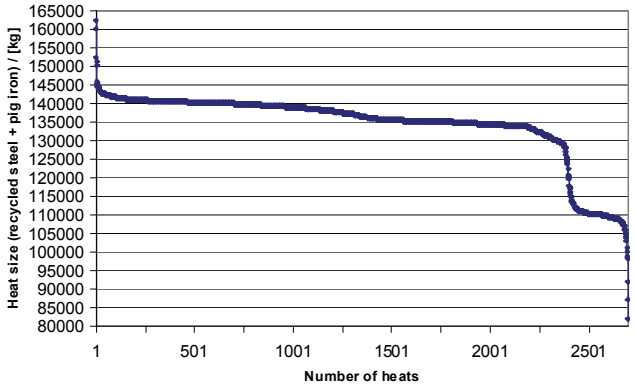

Fig. 27. Distribution of the training set by heat size.

In fact, there are three heat sizes in use at Ruukki's Raahe steel plant, but it was only regarded necessary to use two heat sizes in modelling. For modelling purposes, the original training set mod > 20 was divided into four groups: 120B1, 105B1, 120B2 and 105B2. For example, group 120B1 contains the heats of 120 tonnes in size from converter one.

The following table (Table 12) shows the modelling results.

Table 12. Calculated slopes, their standard deviations and the number of heats in the different modelling groups.

	120B1	105B1	120B2	105B2
average	0.540	0.657	0.521	0.635
standard deviation	0.134	0.129	0.132	0.136
number of heats	1181	153	1218	136

Test set 4284Temp was also divided into four groups in the way presented above. The test results for these groups are presented in the following table (Table 13). The errors for the mod < 20 model are not presented as that model was rejected. Fig. 28 presents the histograms of the errors for different models in the test set 105B1. The errors are divided into bins of 5 °C.

Table 13. Error tables and statistical features of test sets, 120B1, 105B1, 120B2, 105B2.

	error (current)	error (kk-ka)	error (kk-kamod)	error (mod > 20)	error (120B1)
120B1 (1570 heats)					
Average	−2.65	−18.49	−6.38	−2.65	−2.65
Standard deviation	11.78	12.58	11.73	11.78	11.78
Mean squared error	145.76	499.82	178.08	145.76	145.76
Minimum	−36.68	−61.85	−39.80	−36.68	−36.68
Maximum	33.58	13.73	27.20	33.58	33.58
105B1 (212 heats)					
Average	−15.19	−30.24	−18.73	−15.19	−4.56
Standard deviation	11.24	14.37	11.79	11.24	10.60
Mean squared error	356.58	1120.40	178.08	356.58	132.69
Minimum	−42.96	−66.56	−48.20	−42.96	−29.42
Maximum	13.44	−1.18	10.00	13.44	24.26
120B2 (1366 heats)					
Average	0.98	−15.34	−2.86	0.98	−0.94
Standard deviation	11.91	12.59	11.83	11.91	11.86
Mean squared error	142.82	393.75	148.10	142.82	141.33
Minimum	−32.16	−52.29	−35.70	−32.16	−33.46
Maximum	38.36	17.71	32.70	38.36	35.48
105B2 (145 heats)					
Average	−11.58	−26.89	−15.18	−11.58	−3.47
Standard deviation	13.13	15.23	13.45	13.13	12.84
Mean squared error	305.14	953.07	410.10	305.14	175.86
Minimum	−40.76	−68.13	−47.20	−40.76	−33.32
Maximum	14.40	2.68	11.00	14.40	22.99

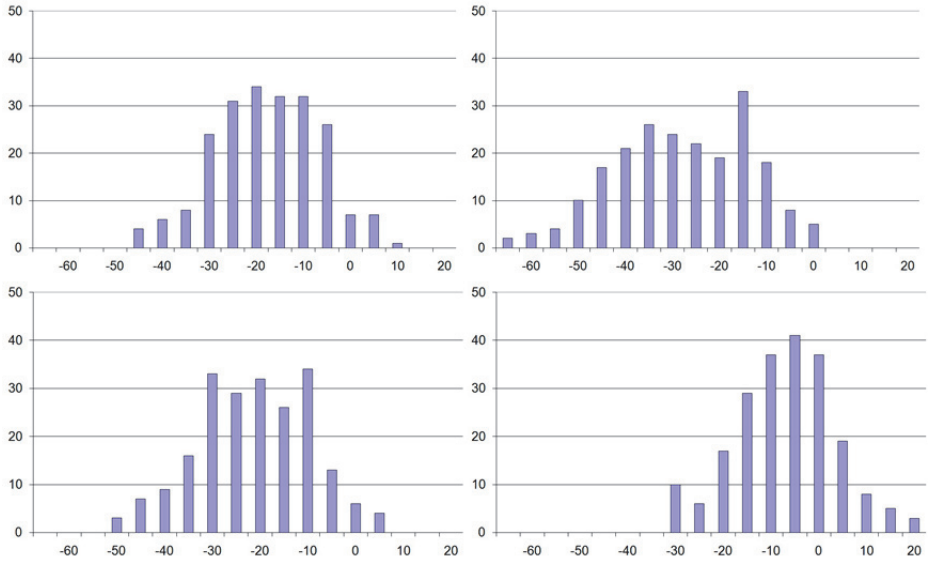

Fig. 28. Histograms of the errors for different models in the 105B1test set (top left current, top right kk-ka, bottom left kk-kamod and bottom right 105B1).

Table 13 shows a minor improvement in the groups containing big heat sizes. In the groups containing small heat sizes, the improvement is significant. The smallest improvement was in the 120B1 group, which can be explained by the fact that the bigger heats from BOF1 were used to define the slope currently in use. The percentage error in the small heat sizes is greater than in the big heat sizes, but the number of heats is smaller. Also, it is worth noting that the standard deviation has further decreased as well as the error range. The fact that the error average in all groups was negative is striking, meaning that the slope is too small on average. The reason is that both training and test sets included heats in which reblowing was done. Reblowing burns material from the heat due to oxygen feeding and this raises the temperature of the steel. When this was noticed, the heats with reblowing were removed from the data. Modelling was repeated with corrected data and these results are shown in Table 14. This table includes the calculated slopes, standard deviations and the number of heats used in modelling. The effect on the data divided into groups is shown later in Chapter 4.2.2.

Table 14. The effect of including reblown heats in modelling on the calculated slope.

	mod > 20	no reblow	reblow	mod < 20	no reblow
average	0.543	0.550	0.499	0.316	0.322
standard deviation	0.138	0.137	0.142	0.186	0.189
number of heats	2700	2335	365	641	554

In mod > 20 the filtering of reblown heats did not have a major effect; the second digit of the slope increased by one, but the change was in the right direction and the standard deviation decreased slightly. In this training set there were 13.5% reblown heats, so their share was significant. However, the original training set was large and the differences flattened out.

4.2.3 Prediction accuracy

The slope is allowed to vary within one standard deviation (as the slope average is 0.55 and the standard deviation is ~0.135, it gives slope limits of 0.415 and 0.685). Heat 40417, in which the calculated slope is near the average, was picked (see Table 15). Table 15 presents measurement values from the Neuvo database and calculated values according to the slope limits shown above.

Table 15. Information about heat 40417.

Heat	T_{DS}	t_{DS}	T_{target}	T_{EB}	t_{EB}	S
40417	1651.8	1016	1666	1702	1107	0.552

$S = 0.415$, $T_c = T_{DS} + S(t_{EB} - t_{DS}) = 1651.8 + 0.415 \times (1107 - 1016) = 1689.6$

$S = 0.685$, $T_c = T_{DS} + S(t_{EB} - t_{DS}) = 1651.8 + 0.685 \times (1107 - 1016) = 1714.1$

The temperature in question does not stay within the limits of the preset target, ±10 °C. The time difference, 91 seconds, represents the normal time difference between the drop sensor and the end point of oxygen feeding in the training set. There is still a need to decrease the standard deviation of the slope; even after filtering the reblown heats from the data divided into groups. The requirement for making an appropriate correction to the temperature, if necessary, is that the drop sensor measurement is done as early as possible. It makes sense to do the drop sensor measurement only after the burning rate of carbon starts to slow down, which is observed as a clear lowering in the off-gas temperature. If the drop sensor measurement is done earlier, the time difference is greater and thus the

error in the slope is repeated as time extends. Paying attention to the addition of additional material at the final stage of heat is discussed later on.

In addition, the modelled slopes were used to calculate the blow-end temperature and the percentage of heats within the target window were calculated. In testing it was not possible to use the target temperature, as in the training set the blow-end temperature was used. In testing the target window was adjusted around the blow-end temperature. In the following table (Table 16), the hit rate of the data used in the target window is presented. Negative values mean that the temperature is below target and positive values mean that temperature is above target. The hit rate in the target window, ±10 °C, was rather low. It was then calculated how much the target window should be above target to obtain 70% of heats in the target window. Generally speaking, it is less harmful if the steel temperature is above target rather than below target.

Table 16. The hit rate of data used in the temperature target window.

Target window	DBtammi01	DBsyys00	DBsyys00 + DBtammi01
−10 °C < Temp < 10 °C	1744 (40.2%)	1271 (33.8%)	
> 10 °C	2189 (50.5%)	2246 (59.7%)	
≤ 10 °C	400 (9.2%)	243 (6.5%)	
−10 °C < Temp < 25 °C			5744 (71.0%)
Number of heats	4333	3760	8093

Through calculation, it was determined that 70% of heats were within the target window of −10 °C ... +25 °C in the training set. The following table (Table 17) presents the number of heats and hit rates of different models in the target window in test set 2929. Test set 2929 was formed by removing the reblown heats from 4284Temp data. Table 17 also includes the target window, −25 °C ...+10 °C, which was used to estimate the correct direction of the slope. By using an asymmetric target window in relation to the average value, it can be determined how the heats are biased when using the slope in question. A table with 4284, 4284Temp and 2929 test sets can be found in Appendix 1. Fig. 29 is a graphical presentation of the number of heats in test set 2929 that hit the temperature target window.

Table 17. The number of heats and temperature target window hit rates in test set 2929.

	current	kk-ka	kk-kamod	mod > 20	mod < 20
−10 °C < x < 25 °C					
Number on target	2096	765	1822	2161	469
Share on target	71.56%	26.12%	62.21%	73.78%	16.01%
−25 °C < x < 10 °C	2400			2365	
−10 °C < x < 10 °C					
Number on target	1755	742	1600	1779	465
Share on target	59.92%	25.33%	54.63%	60.74%	15.88%

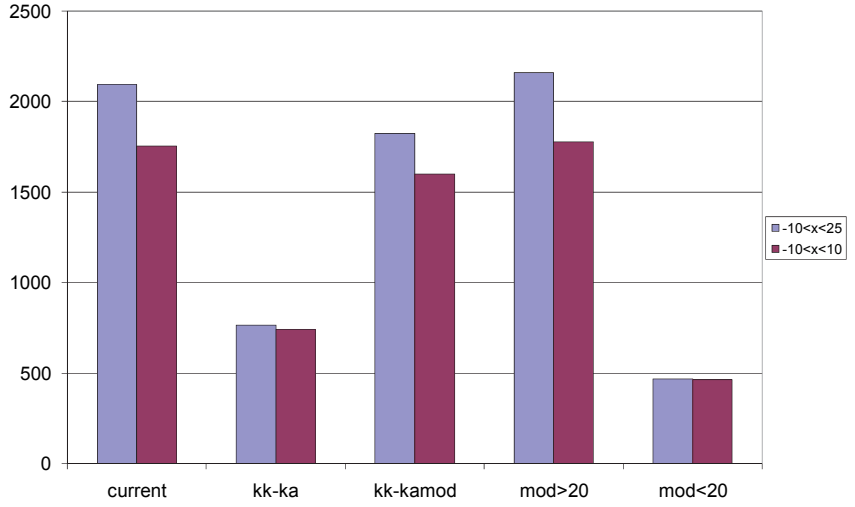

Fig. 29. The number of heats in test set 2929 inside temperature target windows.

Table 17 shows that the slopes of the current (used in plant) and best competing model (mod > 20) are almost the same and that their hit rates in the target windows are similar. The filtering of reblown heats from temperature-filtered data improved its efficiency slightly. Also, as less heats were included within the target window, −25 °C ...+10 °C, it supports the fact that the slope value, 0.55 °C/s, is closer to the correct value than the current one, 0.54 °C/s.

The following table (Table 18) shows the number of heats and hit rates in the target windows for data set 105B1. The total number of heats in data set 105B1 is 212. In this presentation, the reblown heats have not been filtered out of the groups. A table, in which the data sets divided into groups by heat size and BOF are presented, can be found in Appendix 2. Fig. 30 is a graphical presentation of the number of heats inside the temperature target windows in test set 105B1.

Table 18. The number of heats and hit rates inside different temperature target windows in test set 105B1.

	current	kk-ka	kk-kamod	mod > 20	105B1
−10 °C < x < 25 °C					
Number on target	73	13	57	73	150
Share on target	34.43%	6.13%	26.89%	34.43%	70.75%
−25 °C < x < 10 °C	169				189
−10 °C < x < 10 °C					
Number on target	72	13	57	72	134
Share on target	33.96%	6.13%	26.89%	33.96%	63.21%

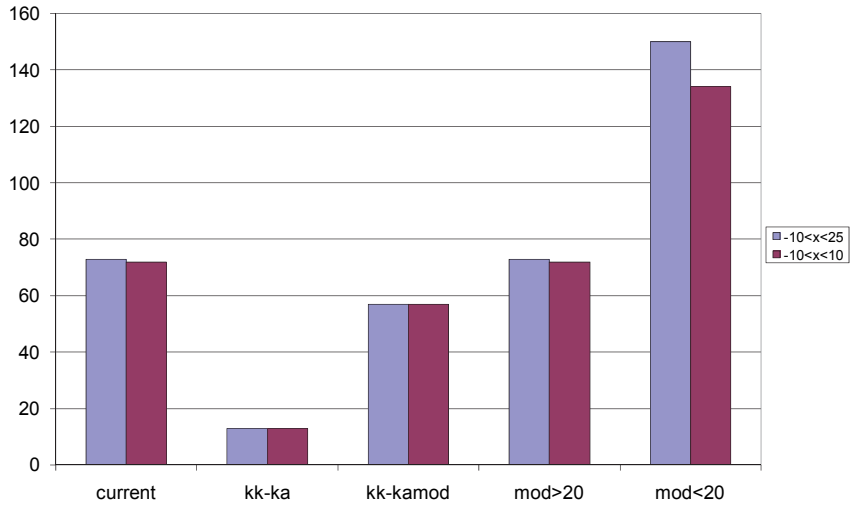

Fig. 30. The number of heats inside temperature target windows in test set 105B1.

The bigger heat size of BOF 1 now has the same slope value as that of the whole data (Appendix 2). Thus, the efficiency in this group is similar to the current and the best competing model. In the other groups, the efficiency of the new slope is better, except for BOF 2, where the wider temperature target window catches a larger number of heats. For the small heat sizes in both BOFs, the efficiency is significantly better. In each test data set, more heats are included in the target window, −25 °C ...+10 °C. This can be improved by filtering out reblown heats from the groups.

4.2.4 Final modelling

After evaluating the above-mentioned results, it was found that the grouping still needed further adjustment. In addition to heat size and the BOF, the target carbon percentage (in the training set: carbon percentage after blowing) and target temperature (in the training set: blow-end temperature) were chosen as the basis of grouping. The effect of time between the drop sensor measurement and the end of the blow on the slope value was also examined (the bottom row in the data grouping tree). As time progressed, the value of the slope and the standard deviation decreased as expected. The decreasing of the slope value is due to the fact that with a shorter time period, the "hot spot" effect dominates, whereas over a longer time period the random changes have time to normalise and therefore the standard deviation decreases. A "hot spot" means that during the blow the drop sensor lands near the oxygen jet, where the reaction is most intensive and the temperature has the local maximum. The time used here is the time period between the usage of the drop sensor and the blow-end. Even though time has an effect, it was observed that the slope of the temperature needs to be modelled with a wider time range and it was not considered possible to divide the data into new groups. It was decided that a good enough result had been reached without dividing the data again into new groups. The grouping of the data is shown in the following tree-like structure, Fig. 31. The corresponding ranges of variables are presented in Table 19.

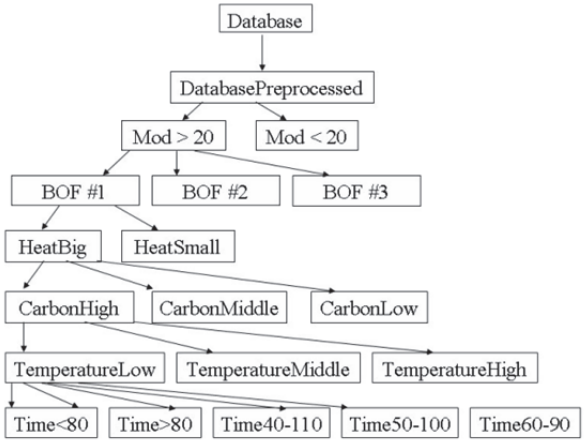

Fig. 31. Data grouping tree.

Table 19. The ranges of variables in the blow-end temperature model.

Group	Range ≤
HeatBig	≥ 120 t hot metal
HeatSmall	< 120 t hot metal
CarbonHigh (C3)	0.045 ≤ C-% < 0.08
CarbonMiddle (C2)	0.035 ≤ C-% < 0.045
CarbonLow (C1)	< 0.035 C-%
TemperatureLow (T1)	< 1660 °C
TemperatureMiddle (T2)	1660 ≤ °C ≤ 1700
TemperatureHigh (T3)	> 1700 °C
Time < 80 (t1)	< 80 s
Time > 80 (t2)	> 80 s
Time 40-110 (t3)	40–110 s
Time 50-100 (t4)	50–100 s
Time 60-90 (t5)	60–90 s

Even after classification within the chosen variables, temperature prediction remained complex. As an example, the distributions of the temperature slopes versus the heat size and carbon percentage are shown in Fig. 32. The trend lines in the figures show that as the heat size and carbon percentage increase, the slope value decreases. These trends are comparable with what happens in practice. The figures show that the scattering of slope values is huge.

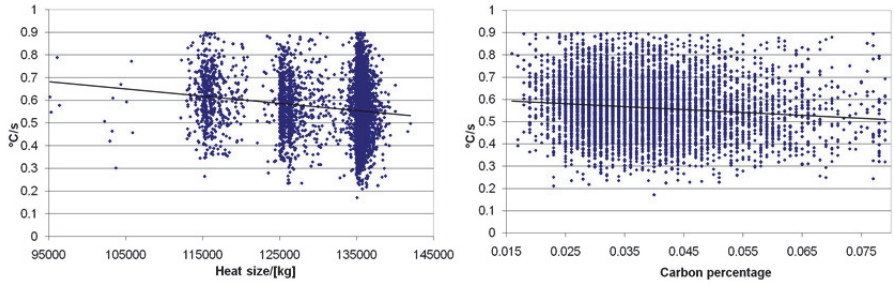

Fig. 32. Distribution of slope vs. heat size and carbon percentage.

In the following table (Table 20), the values and standard deviations of slopes in the BOF1_HeatSmall group are presented time-wise with different levels of carbon percentage. In Fig. 33 the same results are shown graphically. Slope values and standard deviations for the rest of the groups are presented in Appendix 3. A time limit of 80 seconds was chosen as it divides the data approximately in half. Groups C1 and C2 were combined because of the data

shortage; the results for a single group would not have statistical significance alone. The number of heats is also mentioned in every group.

Table 20. Values and standard deviations of slopes in the BOF1_HeatSmall group.

BOF1	HeatSmall_C1&C2		HeatSmall_C3	
	t < 80s (26 heats)	t ≥ 80s (16 heats)	t < 80s (127 heats)	t ≥ 80s (142 heats)
Average	0.64	0.62	0.69	0.65
St dev	0.140	0.115	0.142	0.093
Temp rise < 20 °C (mod < 20)	HeatSmall			
Average	0.38			
St dev	0.22			

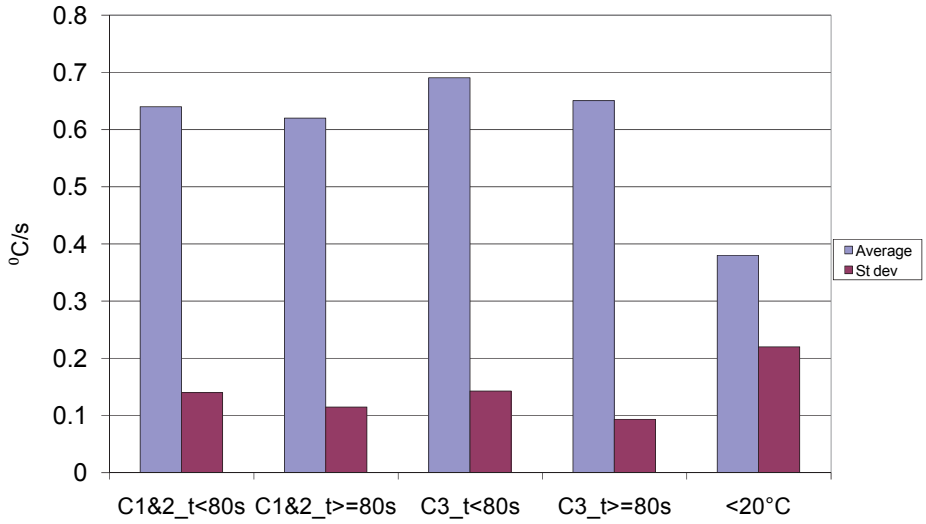

Fig. 33. Values and standard deviations of temperature slopes in BOF1_HeatSmall-group.

The carbon percentage limits were also slightly changed to make them similar to the limits used in the carbon model developed by Ruukki. New model groups are introduced in Table 21. The decision to exclude the target temperature was made in collaboration with the Ruukki experts. In the process there will be situations in which the target temperature is changed and that cannot be predicted. The target temperature may be changed during the blow, because of a change in the situation in further processing, for example in continuous casting. Due to these occasional

unpredictable situations, this kind of variable cannot be used in grouping classification for a model.

Table 21. Heat size and carbon groups of blow-end temperature model.

Group	Range
HeatBig	≥ 120 t hot metal
HeatSmall	< 120 t hot metal
CarbonHigh (C1)	0.045 ≤ C-% < 0.08
CarbonMiddle (C2)	0.035 ≤ C-% < 0.045
CarbonLow (C3)	< 0.035 C-%

Table 22 shows the results of testing the most suitable time period from when the drop sensor was dropped until the blow-end. The widest time period (40–110 seconds) gave the best results. When the widest time period is used, there is the most data available for modelling (statistically beneficial) and still the variance in slopes does not increase too much. In addition, the temperature rise for the heats is at least 20 °C from the drop sensor measurement to the first blow-end temperature measurement. The model is built between these two measurements. In Table 22 the slope values and standard deviations in the BOF1_HeatSmall group are presented time-wise. In Fig. 34 they are presented graphically. The slope values and standard deviations for the rest of the groups are presented in Appendix 4.

Table 22. Values and standard deviations of slopes in the BOF1_HeatSmall group.

BOF1	HeatSmall_C1&C2	HeatSmall_C3
	50–100s (33 heats)	50–100s (147 heats)
Average	0.61	0.67
St dev	0.124	0.115
	40–110s (40 heats)	40–110s (183 heats)
Average	0.62	0.68
St dev	0.122	0.117

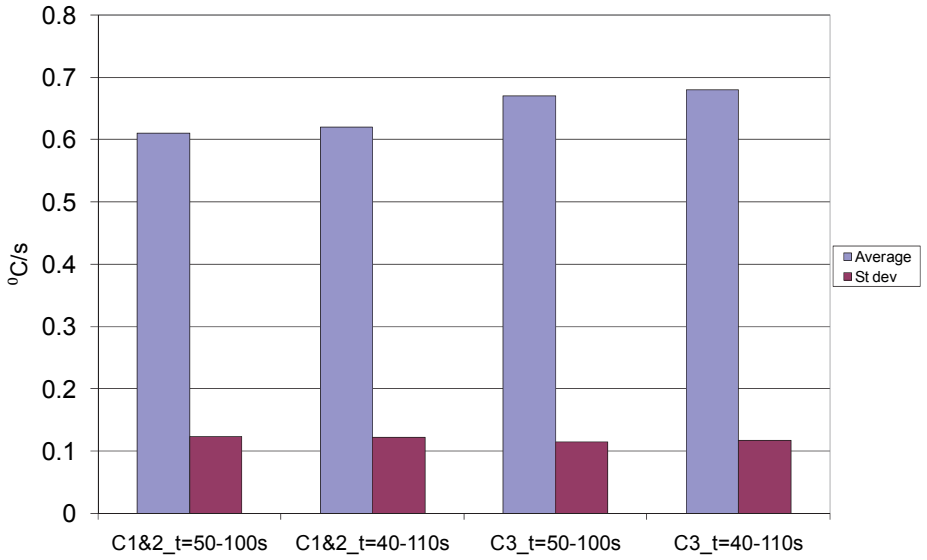

Fig. 34. Values and standard deviations of temperature slopes in the BOF1_HeatSmall group.

4.2.5 Need for adaptivity of blow-end temperature model

There is a periodic variation in the temperature slope. This was found to result from the campaign phase of the BOF, in other words how long it had been since the re-brickwork of the BOF. The variation in the temperature slope without any filtering is very random. However, if for example the moving average of 30 heats is used, the variation is easy to observe. Fig. 35 presents the variation of about 400 slopes in one BOF campaign without any filtering and with the moving average of 30 heats. Fig. 35 shows that periodic variation occurs. In the final automation solution, it is worth using adaptation for the slope. The constant slope values are allowed to follow the variation that takes place in the process equipment within the BOF campaign.

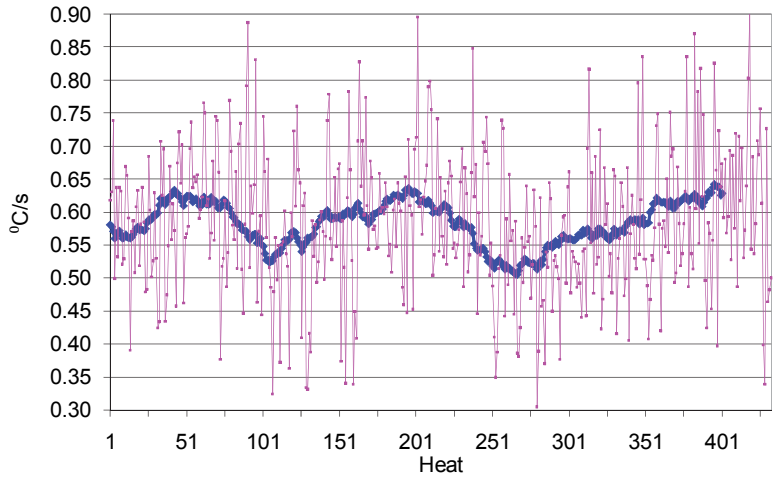

Fig. 35. Variation in temperature slope (no filtering (purple line) and moving average of 30 heats (blue line)).

The model performance was tested with two different time periods (50–100 seconds and 40–110 seconds) as well as with and without slope adaptation, in which the slope value varies within the moving average of 30 heats. During testing, the hit rate of the blow-end temperature and the calculated temperature estimate within ±10 °C limits was tested. The differences in the hit rates with and without adaptation are presented in Table 23. The hit rates for the different groups vary from 60 to 80 percent; the actual hit rates of the different groups can be seen in Appendix 5. The group of 30 heats, according to which adaptation was done, was picked from the HeatBigC2 group (the most common group). Table 23 illustrates that in BOF1 the adaptation did not improve the performance much and in some BOF2 groups an improvement of ten per cent was achieved. In spite of the potential improvement, testing was limited to without adaptation. The testing was simpler to execute and more importantly, the validation for the criteria of these 30 heats had to be done based on expertise possessed only by the plant personnel.

In the final automation solution, the adaptation in question is in use, but in the offline tests the use of adaptation was not considered essential. This testing also shows that the selected time period (40–110 seconds) was good for modelling, as the result achieved with it was almost without exception better than with the time period of 50–100 seconds.

Table 23. Differences in the hit rates with and without adaptation in BOF1 and BOF2.

	Adaptation (without-with)	
	BOF1 %	BOF2 %
HeatBigC1(50-100s)	0.00	−2.10
HeatBigC1(40-110s)	4.50	0.00
HeatBigC2(50-100s)	2.80	−12.00
HeatBigC2(40-110s)	1.80	−10.00
HeatBigC3(50-100s)	4.30	0.00
HeatBigC3(40-110s)	1.80	0.00
HeatSmallC1&C2(50-100s)	0.00	−16.60
HeatSmallC1&C2(40-110s)	0.00	−11.10
HeatSmallC3(50-100s)	0.00	5.00
HeatBigC3(40-110s)	0.00	1.90

4.2.6 Modelling BOF 3

The modelling of BOF 3 was done later after the drop sensor apparatus had been installed. Table 24 presents the slopes and standard deviations of slopes from the modelling of BOF3. In modelling, heats were used in which the drop sensor was dropped from 40 to 110 seconds before the blow-end. In this model, there is some inconsistency, the reason for which could not be explained. According to the expertise of Ruukki's personnel, most inconsistencies occur particularly in BOF 3. This may explain the slightly worse performance of the model in testing.

Table 24. Values and standard deviations of slopes of different groups in BOF 3.

	HeatBig			HeatSmall	
	C1	C2	C3	C1&C2	C3
50–100s	(247 heats)	(240 heats)	(185 heats)	(14 heats)	(30 heats)
Average	0.56	0.57	0.56	0.68	0.62
St dev	0.134	0.130	0.119	0.133	0.102
40–110s	(308 heats)	(299 heats)	(229 heats)	(19 heats)	(39 heats)
Average	0.57	0.58	0.57	0.66	0.64
St dev	0.131	0.127	0.117	0.132	0.102

4.2.7 Testing with data from all BOFs

The performance of the blow-end temperature model was tested for all three BOFs with the heats that mainly used the new charge model and other

improvements made to the plant during the project. In this testing, all heats were used. Compared to the earlier grouping, this means that:

- heats where the temperature rise is under 20 °C were also included
- the time range was not limited to 40–110 seconds
- heats with a higher slope value than 0.9 °C/s were included.

Basically, the inclusion of all the heats weakens the performance of the model, even though the effect was slight. This schema was meant to simulate the actual situation in the plant better. It was observed that improvements made to the plant made the hit rate on the temperature target window, ±10 °C, significantly better compared to the earlier testing. The improvement of the model was about ten percentage units; in the earlier testing the hit rate had been 65–70%, and later 75–80%. The results of testing are presented in Table 25 and graphically in Fig. 36 (HB = HeatBig and HS = HeatSmall). However, there are still 20–25% of the heats, which are not inside the temperature target window. The main reason for this is probably a measurement error by the drop sensor and that the representativeness of the drop sensor measurement is not always equally good. In addition, in all process conditions there is a random, unforeseen variation, which makes the slope of temperature of liquid steel differ significantly from the average. The difference between the slopes of two similar heats can be at worst as much as 0.4 °C/s and if the remaining blowing time is also fairly long, for example one hundred seconds; it means that there might be a difference of as much as 40 °C in the final temperature. This, in particular, is one of those issues where the expertise of the personnel in the control room is required. They need to be able to observe that in the on-going heat the temperature rise is not normal for some reason.

Table 25. Hit rates of different groups in BOFs 1, 2 and 3.

BOF1	BOF2	BOF3
HeatBig		
C1		
274(356) →77.0%	313(399) →78.4%	246(367) →67.0%
C2		
582(743) →78.3%	453(579)→78.2%	250(361)→69.3%
C3		
596(782)→76.2%	588(741)→79.4%	219(287)→76.3%
HeatSmall		
C1&C2		
31(41) →75.6%	24(27)→88.9%	16(20)→80.0%
C3		
165(212)→77.8%	93(132)→70.4%	34(51)→66.7%

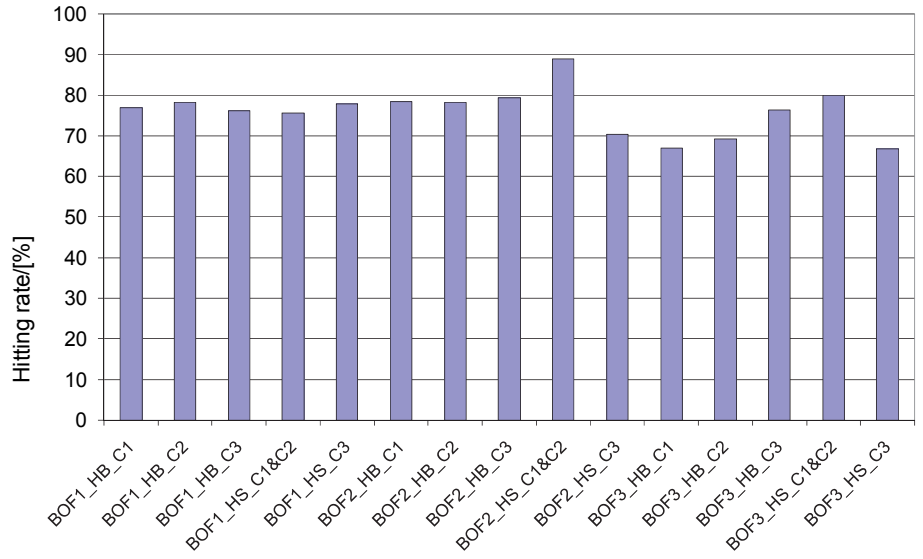

Fig. 36. Hit rates of different groups in BOFs 1, 2 and 3.

The heats, in which the temperature rise from the drop sensor measurement to the blow-end measurement was less than 20 °C, were omitted from this modelling. For these heats, the temperature slopes were formed by grouping BOF-wise only into big and small heats. In Table 26, the slopes and standard deviations of slopes are presented for different BOFs and heat sizes. In Fig. 37 they are presented graphically.

Table 26. Average values and standard deviations of slopes according to different BOFs and heat sizes.

	BOF1	BOF2	BOF3
HeatBig			
Average	0.33	0.29	0.32
St dev	0.193	0.170	0.176
HeatSmall			
Average	0.38	0.33	0.30
St dev	0.220	0.197	0.196

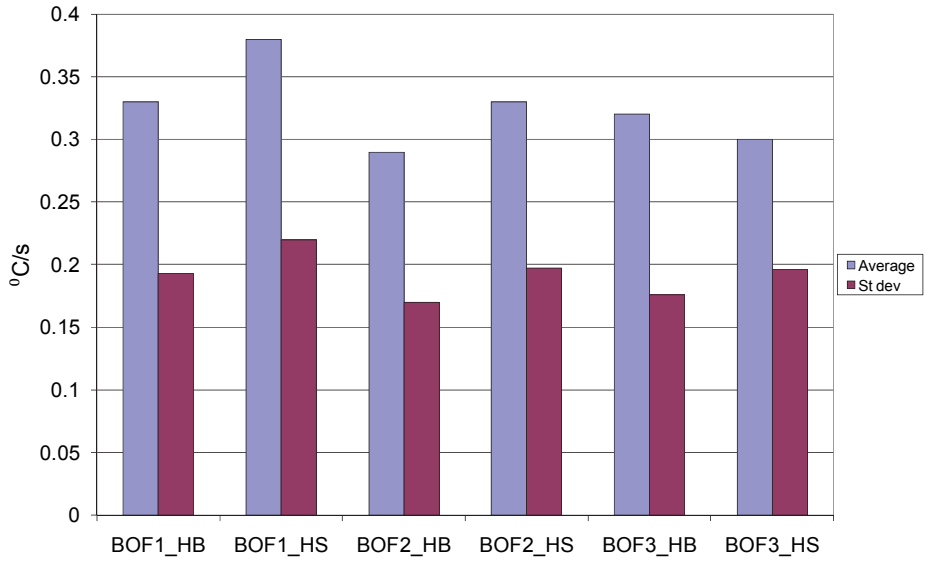

Fig. 37. Values and standard deviations of slopes according to different BOFs and heat sizes.

The testing of this group was done before the implementation of the new charge model and other improvements to BOFs 1 and 2. Table 27 shows that by using a separate slope for heats where the effect of the hot spot is big because of the short time between the measurements instead of the normal slope for the BOF and the group, a hit rate of 70–80% can be achieved instead of 40–60%. Hit rates are presented graphically in Fig. 38. In the final automation solution this cannot be implemented, because if the person in the control room for some reason decides to blow the heat for example 20 °C above the target window, the temperature rise will follow the normal slope. It is, in any case, necessary to instruct the personnel that the temperature rise is significantly lower, if the temperature is already close

to the target temperature during the drop sensor measurement. This slower temperature rise is a result of the hot spot; in other words, these two measurements are not comparable. The temperature measured from the hot spot with the drop sensor is higher than the temperature of the steel on average.

Table 27. Hit rates of different groups in BOFs 1 & 2 using newer data.

	HeatBig				HeatSmall
	Slope(T > 20 °C)	Slope(C1)	Slope(C2)	Slope(C3)	Slope(T > 20 °C)
BOF1					
Number on target	381(479)	100(162)	91(181)	67(136)	24(28)
Hit rate	→79.5%	→61.7%	→50.3%	→49.3%	→85.7%
BOF2					
Number on target	271(377)	78(147)	68(134)	38(96)	11(14)
Hit rate	→ 71.9%	→53.1%	→50.7%	→ 39.6%	→ 78.6%

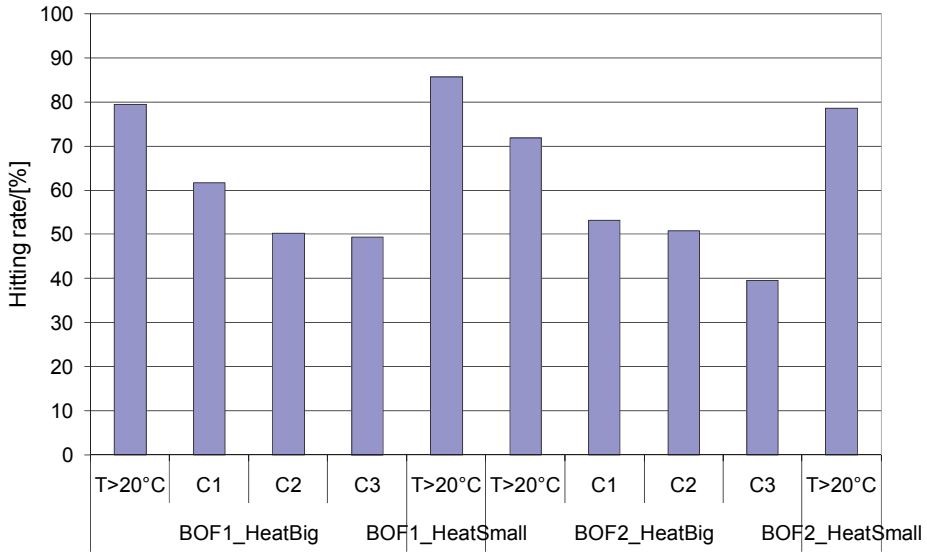

Fig. 38. Hit rates of different groups in BOFs 1 & 2 using newer data.

4.3 Development of additional material model

Generating a model for additional material was necessary as in some heats additional material is needed for temperature adjustment from the drop sensor measurement to the blow-end. Ferrosilicon and sinter are commonly used as

additional materials for temperature adjustment. Ferrosilicon is added if the temperature seems to be below the target and sinter if the temperature seems to exceed the target. In general plant practice, the carbon target is lowered to minimum before sinter is added. If the temperature is still estimated to exceed the target, the required sinter addition is calculated.

Ferrosilicon lowers the off-gas temperature, because silicon burns before carbon. In that case, less carbon monoxide is produced and the post-combustion of carbon monoxide to carbon dioxide, which mainly raises the temperature of the off-gas, decreases. This phenomenon can also be observed from the off-gas graphs. The addition of sinter introduces more oxygen into the BOF, which in principle accelerates the burning of carbon and thus the off-gas temperature should decrease slower than it would without the addition of sinter. This phenomenon cannot be clearly observed from the off-gas graphs. It is also important to determine the effect of the additional material as it affects the carbon model. The addition of ferrosilicon interrupts the burning of carbon during its effective time and the addition of sinter possibly accelerates the burning of carbon slightly because it introduces more oxygen into the process.

In the development of the additional material model, heats were used where additional material was added between the drop sensor measurement and the blow-end. The group was limited, however, so that the heats in which the addition was made less than twenty seconds before the blow-end were not used. It is assumed that in such a short time, the temperature effect of the additional material could be observed from the measurement. Additionally, the material addition cannot take place less than 200 seconds before the drop sensor measurement. This ensures that the additional material does not have any effect on the heat as the measurement is being made.

The addition should be done into the BOF as far before the blow-end as possible. If the addition is done just before the blow-end, the effect of the additional material cannot be seen in the temperature measurement. To see the effect of the addition, “turbo” is used; in other words a strong bottom-blow is done after the end of the oxygen feed. Table 28 presents the temperature effect of 100 kilograms of ferrosilicon (FeSi) and sinter and the temperature effect of 100 kilograms of FeSi and sinter per tonne of steel produced. The temperature effect of additional materials is presented graphically in Fig. 39. The value used in Ruukki’s charge model for the heating effect of 100 kilograms of FeSi in a heat of 120 tonnes of steel is 8 °C.The value used in Ruukki’s charge model for the cooling effect of 100 kilograms of sinter in a heat of 120 tonnes of steel is 4 °C.

The values used differ from the theoretical values. The main reason for the difference in the ferrosilicon effect is the simultaneously added lime to maintain the slag basicity. Some energy is used to heat up the lime. The main reason for the difference in the sinter effect is the oxygen from the sinter. The oxygen boosts the burning and therefore the cooling is not so effective. Statistically calculated values are realistic as they are in line with the values used at Ruukki.

Table 28. Temperature effects of FeSi and sinter per 100 kg and per tonne of steel produced.

	Temperature effect of 100 kg of additional material		
	FeSi		Sinter
	105k (121 heats)	120k (814 heats)	120k (236 heats)
Average	9.9 °C/100 kg	8.2 °C/100 kg	−5.0 °C/100 kg
St dev	12.8 °C/100 kg	14.8 °C/100 kg	3.6 °C/100 kg
Average		0.066 °C/(100 kg*tonne steel)	−0.041 °C/(100 kg*tonne steel)
St dev		0.12 °C/(100 kg*tonne steel)	0.055 °C/(100 kg*tonne steel)

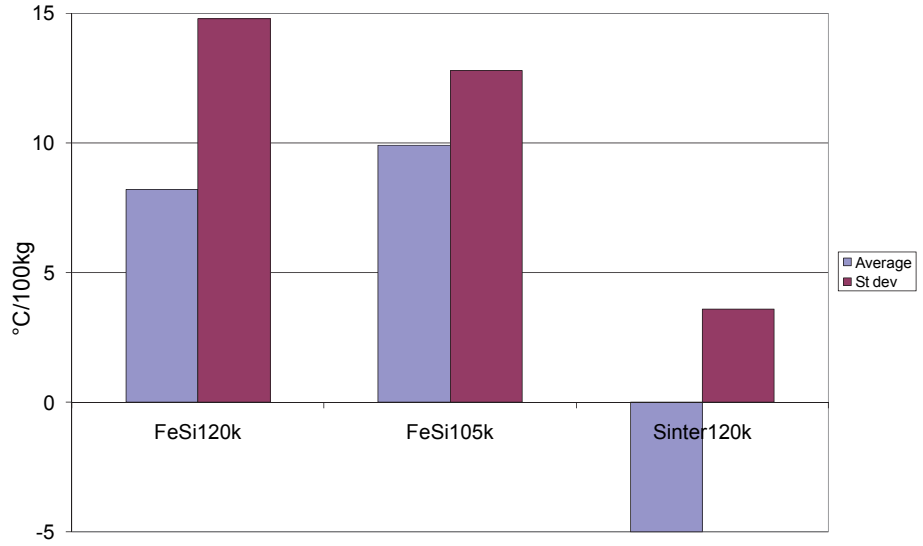

Fig. 39. Temperature effect of 100 kg of additional material.

Tables 29 and 30 show the effect of the usage of the additional material model, when it was tested for hitting the temperature target window; ±10 °C. In Fig. 40 and 41, the hit rates are presented graphically. The hit rates improved as the

temperature effect was used. In ferrosilicon heats, the effect of the additional material model is significant and in sinter heats even more crucial.

Table 29. Hit rates of ferrosilicon heats in different groups.

	Without FeSi effect	With FeSi effect
120B1		
C1	117(249) → 47.0%	159(249) → 63.9%
C2	75(144) → 52.1%	99(144) → 68.6%
C3	24(42) → 57.1%	26(42) → 61.9%
105B1		
C1&C2	14(32) → 43.8%	16(32) → 50.0%
C3	21(44) → 47.7%	33(44) → 75.0%
120B2		
C1	103(232) → 44.4%	151(232) → 65.1%
C2	46(74) → 62.2%	49(74) → 66.2%
C3	21(27) → 77.8%	20(27) → 74.1%
105B2		
C1&C2	6(25) → 24.0%	12(25) → 48.0%
C3	9(20) → 45.0%	10(20) → 50.0%

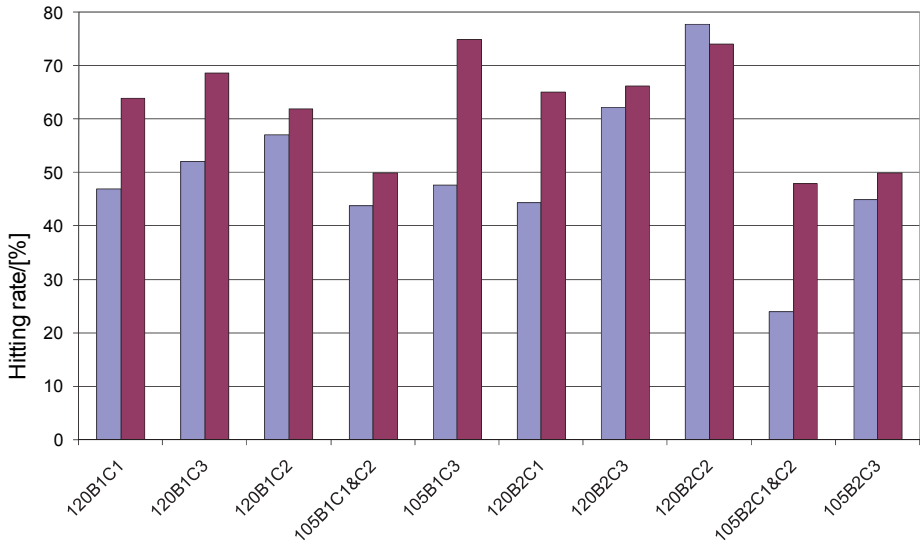

Fig. 40. Hit rates of ferrosilicon heats with and without the effect of temperature.

Table 30. Hit rates of sinter heats in different groups.

	Without sinter effect	With sinter effect
120B1		
C1	8(46) → 17.4%	26(46) → 56.5%
C2	9(30) → 30.0%	16(30) → 53.3%
C3	4(19) → 21.1%	12(19) → 63.2%
105B1		
C1&C2	0(1) → 0%	1(1) → 100%
C3	1(2) → 50.0%	2(2) → 100%
120B2		
C1	16(64) → 25.0%	39(64) → 60.9%
C2	10(34) → 29.4%	16(34) → 47.1%
C3	2(32) → 6.3%	21(32) → 65.6%
105B2		
C1&C2	2(2) → 100%	1(2) → 50.0%
C3	1(3) → 33.3%	2(3) → 66.6%

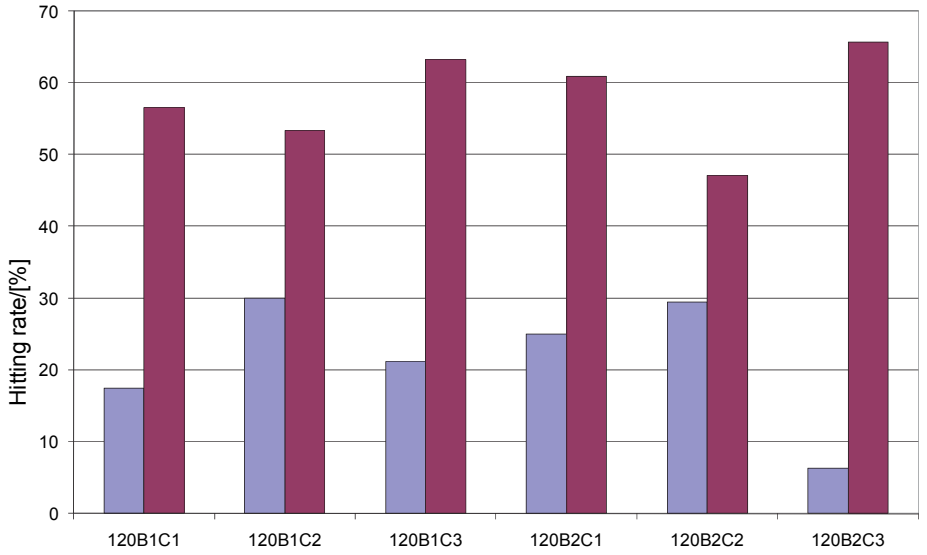

Fig. 41. Hit rates of sinter heats with and without the effect of temperature.

In later testing, the heats with additional material were only tested using the additional material model; it was assumed that the usage of a defined temperature effect is beneficial. Table 31 and Fig. 42 present the target temperature window hit rate of the heats with additional material for the different BOFs.

Table 31. Hit rates of ferrosilicon heats in bigger heat size for different BOFs.

	BOF1	BOF2	BOF3
C1	28(42) → 66.7%	24(38) → 63.2%	39(69) → 56.5%
C2	43(55) → 78.2%	38(55) → 69.1%	44(63) → 69.8%
C3	45(64) → 70.3%	35(50) → 70.0%	27(34) → 79.4%

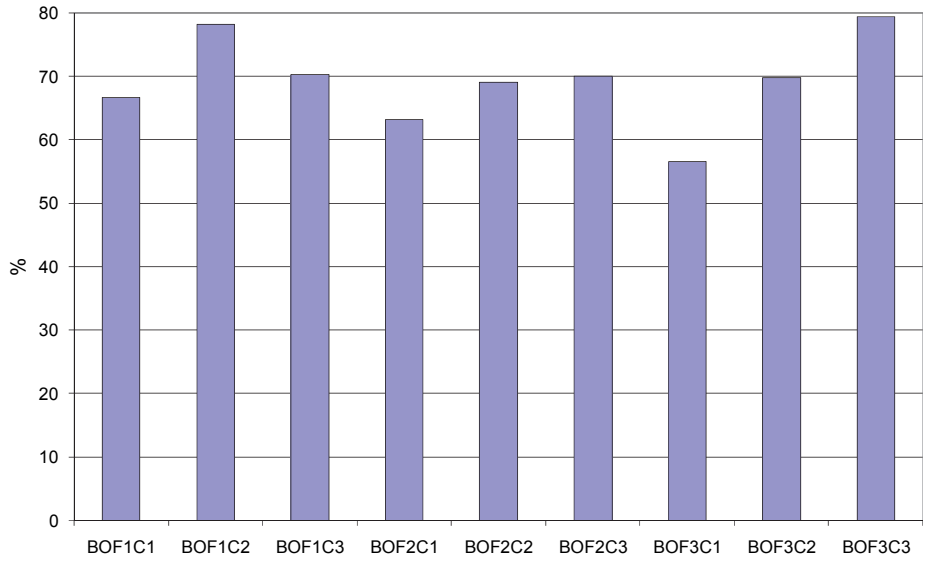

Fig. 42. Ferrosilicon heats with temperature effect.

The testing data was relatively small and the number of heats remained small. There were not enough ferrosilicon heats for the smaller heat size or for any sinter heat group. The hit rate of the heats with additional material was in the same range in BOF 2 and slightly better in BOF 1 than in earlier testing. In BOF 3, the performance was slightly better because of the inaccuracy in the blow-end temperature model.

5 Discussion

The development of special measurements and models and therefore better monitoring is important for any process. Productivity and quality will improve as the process operation is monitored more efficiently. Also, energy savings and improved work safety are benefits achieved from investments in the development work of measurements and models.

Three different special measurements in a BOF were studied in this thesis. These measurements were radio wave interferometer (RWI), acoustic measurement and splashing measurement. RWI and acoustic measurement are more direct measurements than splashing measurement, but there are also more challenges in using them. Acoustic measurement is sensitive to noises from the surroundings other than the actual desired noise from the oxygen jet hitting the surface of the steel–slag interface. The RWI measurement device is sensitive to splashes within the BOF, which easily make the visibility to the steel-slag surface problematic. This causes problems with the functionality of RWI measurement; it may give the wrong result or no result at all. RWI measurement can handle the slag-steel emulsions during the blow and separate slag and steel surfaces. The signal from the acoustic measurement can be filtered and used with the help of expert knowledge. The skulling problem in RWI is decreased by smart placement. One possible place is in the pipeline of the drop sensor. The analysis of RWI measurement was presented in Chapter 3.1.

Splashing measurement provided knowledge about the conditions that cause heavy splashing. For example, ferrosilicon added in the early stages of the heat is the most significant variable to cause splashing. Adding ferrosilicon causes heavy splashing and makes the rest of the blow less stable. Also, the ratio of silicon to manganese of the hot metal and the amount of scrap are important variables that have an effect on splashing. Adding a lot of scrap, especially light scrap, in the heat causes splashing. By using the knowledge gained from the splashing measurement, it is possible to make guidelines for the operators about the conditions that need to be avoided to improve the blowing strategy. The analysis of splashing measurement is introduced in Chapter 3.3.

The development of the blow-end temperature model provided knowledge of the variables affecting the temperature rise. The blow-end temperature model was developed using grouping of variables, which was done using the expert knowledge of the plant personnel. In many cases production limits led to a natural distribution between the groups, for example in the heat size. In addition, trial and

error was used to identify limits for other variables. Therefore, no systematic data-based algorithm or method for identifying variable limits was used, but the expert knowledge led to a tree-like structure. The BOF, heat size and carbon target were chosen as variables for different model groups. The development of the blow-end temperature model was introduced in Chapter 4.2. By using these model groups it was possible to increase the temperature hit rate. The modelling was done for different converters. A bigger heat size has a slower temperature increase than a smaller heat size. A heat with a lower carbon target also shows faster temperature growth than a heat with a higher carbon target.

The additions of ferrosilicon and sinter are made to a heat in the later stage of blowing in order to reach the target temperature when the carbon content is at the desired level. Ferrosilicon is added to accelerate the temperature increase and sinter is added to slow down the temperature growth. The development of the additional material model provided more understanding of the effect of the additional materials, for example that the addition has to be done as soon after using the drop sensor as possible. There will then be enough time for the additional material to react in the steel and have its effect on the temperature. The development of the additional material model is introduced in Chapter 4.3.The development provided numeric values for the effects of additional materials and these values could then be used in the process control system. Additional research should be done, for example the duration of the effect of additional material should be analysed; at present there are only assumptions.

A more effective way to use process data, expert knowledge, special measurements and different models would be to integrate them in a BOF monitoring system. Below, a possible structure of such a monitoring system is discussed.

When designing a monitoring system, the key points to take into account include the following. Measurements that are used must be robust and repeatable and easy to calibrate. To achieve maintainability the models must be precise, understandable and adaptive. To achieve modularity the new sub-models must be flexible. The system needs to be able to deal with different kinds of information (numeric data, models, expert knowledge, etc.). It is important to design a monitoring system carefully in consultation with different experts in order to make it understandable for different types of users.

In Fig. 43 the proposed monitoring system consists of three subsystems: modelling, visualisation and an Expert System. Further, the modelling subsystem itself has three parts. The first part is *Before the blow*, which includes the charging

model, the second part is *During the blow*, including RWI and the splashing indicator and the third part is *End point estimation*, consisting of the carbon, blow-end temperature and additional material models. The first and third parts are currently in use at Ruukki's Raahe Steel Works, and are more or less part of the automation system. The RWI measurement was tested, but is not currently in use at the steel plant. The splashing measurement is in use, but does not contain a database that would give information to the personnel. Thus it is not in use as a splashing indicator. It would take extra work to construct that database, so it is not merely a matter of implementing the system.

The first part, the charging model, is already in good shape. Having it combined in a monitoring system would be a good place to keep a large database and detailed information about raw materials. It would also contain expert knowledge about them, for example if some raw material is likely to cause difficulties in reaching the target for some chemical element. These guidelines are known to the BOF personnel, but it would be useful to collect them as an expert knowledge database to avoid loss of knowledge as the personnel changes. In addition, these guidelines could be shown as on-screen messages, so it would reduce human error as people tend to forget things when in a hurry.

The second part, the RWI measurement and splashing indicator, does not yet exist, so making it functional would take the most work. Having dynamic monitoring during the blow would be useful, as it would give the personnel the possibility of making changes to the process according to problems observed by the monitoring system. In terms of the possibilities offered by RWI measurement, the main one is that it would predict splashing. Personnel would therefore have time to take action to avoid splashing, for example to add some material to reduce foam. Combining information from the RWI measurement and splashing measurement, it would be possible to generate a database that would contain information about circumstances when action is required. The main advantage of this part would naturally be higher yield.

The third part, the carbon, blow-end temperature and additional material models, are in use. Putting them in a monitoring system would be a good place to keep a large database and expert knowledge could also be kept there. Expert knowledge would contain for example information about cases when there is a risk that the blow-end temperature model is wrong or even better it would contain a different case for temperature behaviour in those situations and assist the personnel to achieve the target temperature. At the very least, the system would offer an easier platform for updating and adapting the system.

The structure of the monitoring system is illustrated in Fig. 43. The monitoring section itself includes a user interface, which gives warnings, alarms and possible actions. It should also facilitate updating operations.

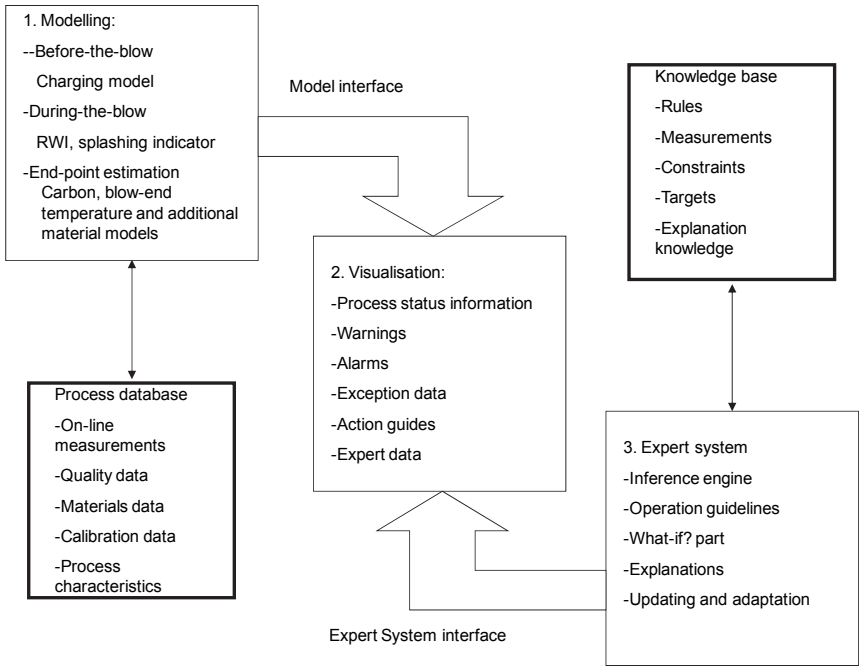

Fig. 43. Monitoring system of basic oxygen furnace.

In this case, maintainability and modularity are easier to achieve than transportability. The system should be planned so that there are standard interfaces between different parts, so it is easy to add new modules within the system. One issue in making maintainability easy is to construct a flexible development user interface, so it is easy to change different parameters and add new expert knowledge. This kind of monitoring system would not be very easy to transport to a different plant as it contains a lot of plant-specific information and its structure is so tailor-made that it would not give any advantage to other plants. (Ruuska *et al.* 2007)

6 Conclusions

In this thesis some special measurements and blow-end temperature modelling of a basic oxygen furnace (BOF) have been studied. The target of the research was to increase knowledge of measurements and phenomena in the converter and thus way improve the opportunities for more efficient monitoring and control of the process. The applicability of three special measurements for monitoring a BOF was investigated and models were developed for the blow-end temperature and for additional material at the end of the blow.

Special measurements were investigated to obtain more knowledge about their usability in a BOF. In addition, analysing these measurements resulted in new process knowledge. The usage of RWI was seen as beneficial as it would be possible to see the rising trend of the liquid surface level in advance and to perform some corrective actions to avoid excessive foaming and eventual splashing. The advantage of acoustic measurement was also to foresee vigorous foaming in advance, but it was noted that it is sensitive to disturbing noise from the surroundings. The analysis of the splashing measurement revealed several factors that usually increase splashing. It does not, however, give information in advance. It would be best to use the information from two different measurements, for example RWI and the splashing measurement, to predict an increase in splashing, as splashing causes significant iron losses.

The development of blow-end temperature and additional material models provided a lot of knowledge about the factors affecting the temperature. Factors that were used in grouping were the BOF number, heat size and end carbon content. It was also noticed that there are still many heats that do not reach the target, while using the current models.

There are other factors affecting the temperature that are not included in the models. Some of them are measurable and some are not. For example, the oxygen flow rate and lance height might have an effect on temperature. Also, very stiff slag presents a challenge for measuring temperature. There is still a need for further research in this area, which strengthens the impression that this process is complex. It would be useful to research further the effect of additional materials. For example the duration of the effect of additional material should be analysed; at present there are only some assumptions available.

It was noticed, as always in process development, that continuous monitoring and more research needs to be done to observe the changes in process conditions, raw materials, procedures and so on. Otherwise the benefit of the improvements

and models will decrease. However, it would be possible to set acknowledged routines and warnings in the improved monitoring system to help operators to notice the need for system tuning. Having a monitoring system would give financial benefit in terms of having fewer reblowings, better yield and quality of final product and also savings in raw materials as the controllability of the process would be improved. As a monitoring system contains a database of guidelines, it would also result in making a good basis for new employees to become familiar with the process and therefore make their training smoother.

References

Allendorf S, Ottesen D, Hardesty D, Goldstein D, Smith C & Malcolmson A (1998) Laser-based sensor for real-time measurement of off-gas composition and temperature in BOF steelmaking. AISE Steel Technology 4: 31–35.

Béranger G, Henry G & Sanz G (eds) (1996) The Book of Steel. Paris France; Intercept, Chapter 57.

Bergman D & Hahlin P (1997) Experience of waste gas analysis based control system for the LD-LBE-process at SSAB Tunnplåt AB, Luleå, Sweden. 2nd European Oxygen Steelmaking Conference, Taranto, Italy: 303–312.

Birk W, Arvanitidis I, Jönsson P & Medvedev A (2000) Physical modelling and control of dynamic foaming in an LD-converter process. IEEE Industry Applications Conference: 35th IAS Annual Meeting and World Conference on Industrial Applications of Electrical Energy, Roma, Italy: 2584–2590.

Birk W, Arvanitidis I, Jönsson P & Medvedev A (2001) Physical Modeling and Control of Dynamic Foaming in an LD-Converter Process. IEEE transactions on industry applications 37: 1067–1073.

Birk W, Arvanitidis I, Jönsson P & Medvedev A (2003) Foam level control in a water model of the LD converter process. Control Engineering Practice 11: 49–56.

Bock M, Schoop J & Oehler C (2000) The Influence of Blowing Techniques, Bottom Stirring and Lance Design in the LD-processes on Slag Formation, the Formation of Lance and Converter Skulls and Converter Lining Life. 3rd European Oxygen Steelmaking Conference, Birmingham, United Kingdom: 163–177.

Boom R (2003) Mastering the heat in the Fe-C-O converter: Evolution of process control in fifty years of oxygen steelmaking. 4th European Oxygen Steelmaking Conference, Graz, Austria: 1–19.

Brooks SGA & Coley KS (2002) Interfacial area in top blown oxygen steelmaking. 61st Ironmaking Conference Proceedings, Nashville, USA: 837–850.

Bruckhaus R, Fiedler V & Lachmund H (2001) Improvement of the BOF process by use of a radar measurement at the Dillinger Hutte steel plant. Revue de Metallurgie Cahiers d'Informations Techniques 6: 553–559.

Bååth, L (1996) A method for simultaneously measuring the positions of more than one surface in metallurgic processes. Patent Number EP0697108, USA.

Bååth L (2003) Radio wave interferometer measurements of slag depth. Proceedings of Iron & Steel Society International Technology Conference and Exposition, Indianapolis IN, USA: 875–882.

Chatterjee A & Bradshaw AV (1972) Break-up of a liquid surface by an impinging gas jet. Journal of the Iron and Steel Institute: 179–187.

Choi H, Ryu J, Kim M, Lee H, Kim C & Chung Y (1994) Modification of lance nozzle to increase productivity and BOF lining life at No. 2 Steelmaking Plant in Pohang Works. 77th Steelmaking Conference Proceedings, Chicago IL, USA: 93–99.

Deo B & Boom R (1993) Fundamentals of Steelmaking Metallurgy. London UK, Prentice-Hall.

Evestedt M& Medvedev A (2006) Model-based slopping monitoring by change detection. Proceedings of the 2006 IEEEInternational Conference on Control Applications, Munich, Germany: 2492–2497.

Evestedt M, Medvedev A, Thorén M & Birk W (2007) Slopping warning in the LD converter process – an extended evaluation study. 12th IFAC Symposium on Automation in Mining, Mineral and Metal Processing, Quebec, Canada: 267–272.

Evestedt M& Medvedev A (2009) Model-based slopping warning in the LD steel converter process. Journal of Process Control 19: 1000–1010.

Fileti AMF, Pacianotto TA & Cunha AP (2005) Neural modeling helps the BOS process to achieve aimed end-point conditions in liquid steel. Engineering Applications of Artificial Intelligence 19: 9–17.

Fruehan RJ, Editor (1998) The Making, Shaping and Treating of Steel. 11th Edition, Steelmaking and Refining Volume. Pittsburgh PA, AISE Steel Foundation.

Graveland-Gisolf E, Mink P, Overbosch A, Boom R, Gendt G & Deo B (2003) Slag droplet model, a dynamic tool to simulate and optimize the refining conditions in BOF. Steel Research International 74: 125–130

Grethe U, Kempken J, Schramm R & Klingenberg R (1996) BloCon – Modularized and adaptable BOF process model of high performance. 79thSteelmaking Conference Proceedings: 359–367.

Guzela DDN, Oliveira JG, Staudinger G & Müller J (2003) The ultimate LD steelmaking converter: The synthesis of 50 years of development. 4th European Oxygen Steelmaking Conference, Graz, Austria: 1–14.

Hahlin P, Carlsson G & Ångström S (1986) MefCon – Mefos converter control system. Process control in the steel industry 1: 233–246.

Hahlin P (1993) Dynamic control of metal analysis and bath temperature in a steel converter. 1stEuropean Oxygen Steelmaking Conference, Düsseldorf, Germany: 154–158.

Han M & Huang X (2008) Greedy kernel components acting on ANFIS to predict BOF steelmaking endpoint. 17thIFAC World Congress, Seoul, Korea: 1–6.

Han M & Wang X (2011) BOF oxygen control by mixed case retrieve and reuse CBR. 18thIFAC World Congress, Milano, Italy: 1–6.

He QL & Standish N (1990) A model study of droplet generation in the BOF steelmaking. ISIJ International 30: 305–309.

Healy GW & McBride DL (1977) The Mass-Energy Balance. BOF Steelmaking 4: 101–170.

Higuchi Y & Tago Y (2001) Effect of Lance Design on Jet Behavior and Spitting Rate in Top Blown Process. ISIJ Int 41: 1454–1459.

Hoorn AI, Konijnenburg JT & Kreijger PJ (1976) Evolution of Slag Composition during the Blow. Proceedings McMaster Symposium on Iron and Steelmaking No. 7, The Role of Slag in Basic Oxygen Steelmaking. Hamilton (Ont.), Canada: McMaster University: 2.1–2.26.

Hu Z, He P, Tan M & Liu L (2003) Continuous determination of bath carbon content on 150 t BOF by off-gas analyser. Journal of University of Science and Technology Beijing 6: 22–25.

Iso H, Jyono Y & Kanemoto M (1987) Dynamic Refining Control by Analysis of Exhaust Gas from LD Converter. Trans Iron Steel Inst Jpn 5: 351–359.

Iso H, Arima K, Kanemoto M, Ueda Y & Yamane H (1988) Prediction and Suppression of Slopping in the Converter. Transactions ISIJ 28: 382–391.

Jalkanen H, Suomi M-L & Wallgren M (1998) Simulation of oxygen converter process (BOF). Joint Finnish-South African Symposium on Metallurgical Research, Johannesburg: 1–21.

Jalkanen H (2007) Challenge of modelling of high-temperature materials process; oxygen converter process (LD, BOF) as an example. Acta Metallurgica Slovaca 3: 434–446.

Jun T, Xin W, Tianyou C & Shuming X (2002) Intelligent control method and application for BOF steelmaking process. 15thIFAC World Congress, Barcelona, Spain: 1–6.

Jung S & Fruehan RJ (2000) Foaming Characteristics of BOF Slags. ISIJ International 40: 348–355.

Jämsä S-L (1977) LD-konvertterin panostusmalli. Oulu, Finland.

Kattenbelt C & Roffel B (2008a) Hierarchical two layer statistical slop prediction model. Scanmet III, Luleå, Sweden: 1–9.

Kattenbelt C & Roffel B (2008b) Dynamic Modeling of the Main Blow in Basic Oxygen Steelmaking Using Measured Step Responses. Metallurgical and materials transactions B 39B: 764–769.

Kim J, Sim E & Jung S (2005) An automated blowing control system using the hybrid concept of case based reasoning and neural networks in steel industry. Proceedings of 2nd International Symposium on Neural Networks, Chongqing, China 3: 807–812.

Koch K, Falkus J & Bruckhaus R (1993) Hot metal experiments of the metal bath spraying effect during the decarburization of Fe-C melts through oxygen top blowing. Steel Research 64(1): 15–21.

Kreijger PJ, Boer JH de, Reints J & Snoeijer AB (1975) Development of Dynamic Converter Control at Hoogovens. Proceedings CIM Symposium on Control of Basic Oxygen Steelmaking, Toronto, Canada: 1–27.

Krieger W (2003) 50 years LD steelmaking – 50 years of innovation. 4th European Oxygen Steelmaking Conference, Graz, Austria: 1–15.

Kitamura S, Shibata H & Maruoka N (2008) Simulation model of dephosphorization by liquid and solid coexisting slag. Scanmet III, Luleå, Sweden: 1–10.

Kivelä P (1982) LD-konvertterin staattisen mallin laatiminen. Oulu, Finland.

Kivelä S (2000) Konvertteriprosessin hiilipitoisuuden hallinta sumealla. Oulu, Finland.

Komarov S, Kuwabara M & Sano M (2000) Suppression of slag foaming by a sound wave. Ultrasonics Sonochemistry 7: 193–199.

Laine K (1998) Pudotussondien käyttö konvertterin lämpötilanhallinnassa. Oulu, Finland.

Lange KW (1981) Physical and Chemical Influences during Mass Transfer in Oxygen Steelmaking Process. Lingerich Germany, West Deutscher Verlag.

Lassila I, Holappa L & Valovirta, E (2004) Investigation on post combustion phenomena in BOF by in-situ gas analysis. Scanmet II, Luleå, Sweden: 225–232.

Lilja J, Ollila S & Nevala H (2006)Decade of development in steelmaking at Ruukki Production, Raahe Steel Works. 5thEuropean Oxygen Steelmaking Conference, Aachen, Germany: 494–500.

Little S & Lewis C (2001) Radar level measurement in the steel industry. 2001 Ironand Steel Exposition and AISE Annual Convention, Cleveland, OH, USA: 1–41.

Luomala M, Fabritius T, Virtanen E, Siivola T & Härkki J (2002) Splashing and spitting behaviour in the combined blown steelmaking converter. ISIJ International 42(9): 944–949.

Malmberg D & Bååth L (1995) Radio-wave technology in metallurgical and mining industry. Scaninject VII, Luleå, Sweden 2: 245–255

Malmberg D & Bååth L (1999) Slag level detection in EAFs using microwave technology. Scandinavian Journal of Metallurgy 28(6): 266–276.

Merriman D (1997) Mass spectrometry for oxygen steelmaking control. Steel Times 11: 439–440.

Meyer G, Westerdale B & Nicolosi J (2001) Real time monitoring of specific metalfume in high temperature furnace exhaust by X-ray fluorescence. Proceedings of EPD Congress, New Orleans, LA, USA: 579–586.

Meszaros G, Kemeny F, Walker D, Zaranek R & Mannion F (2001) Degasserguide. Patent Number US6255983, USA.

Millman MS, Bååth L, Malmberg D & Price E (2001) Radio Wave Interferometry for BOS Slag Control. ICS 2001, 2ndInternational Congress on the Science & Technology of Steelmaking, University of Wales, Swansea, UK: 309–320.

Mink P & Dye S (2002) Reducing vessel fume losses and recycling of BOF residuals. 85thSteelmaking Conference, Nashville, TN, USA: 639–651.

Miyahara H, Hatanaka T, Arai Y, Ikeda M, Okimoto S & Kato N (1997) Electrical instrumentation computer (EIC) integrated system for labor saving in the basic oxygen furnace operation. NKK Technical Review 76: 1–8.

Mizuta M, Kanai T & Miyamoto M (2000) Development of new temperature control system in the steelmaking process. 83rd Steelmaking Conference Proceedings, Pittsburgh, PA, USA: 381–385

Molloy NA (1970) Impinging jet flow in a two-phase system: the basic flow pattern. J Iron Steel Inst 208: 943–950.

Morris AS (1993) Principles of measurement and instrumentation. New York, Prentice Hall.

Nagamune A, Tezuka K, Mori T & Fujiwara H (1992) Development of the M-Sequence Signal Modulated Microwave Level Meter. NKK Technical Review 65: 54–60.

Oeters F (1989) Metallurgy of Steelmaking. Düsseldorf Germany, Verlag Stahleisen mbH.

Okabe S, Sakai T, Miayzawa T & Kimura E (1995) Physical modeling of splashing of top blown gas injection onto liquid bath. Proceedings of EPD Congress: 313–320.

Ollila S, Kelchtermans R & Stone RP (1999) Implementation of an automated drop in sensor system at Rautaruukki Steel Raahe Steel Works. 82nd Steelmaking Conference Proceedings, Chicago, Il, USA: 385–391.

Ollila S & Lilja J (2004) Development of BOF blowing control at Rautaruukki Steel, Raahe Works. Scanmet II, Luleå, Sweden 1: 215–224.

Pak J, Min D & You B (1996) Slag foaming phenomena and its suppression techniquesin BOF steelmaking process. 79thConference of the Steelmaking Divisionof the Iron and Steel Society, Pittsburgh, Pennsylvania, USA: 763–769

Patjoshi AK, Behera RC, Sarangi A & Misra S (1982) Cold model investigation with inclined multinozzles. Iron and Steel International: 27–32.

Pehlke RD (1973) Unit Processes of Extractive Metallurgy. New York, American Elsevier.

Rautell T (2000) Jälkipalaminen konvertteriprosessissa. Espoo, Finland.

Roininen J (1999) Konvertterin tuotantokapasiteetin lisäys toteuttamalla suorakaato-praktiikka pudotushappisondilla. Oulu, Finland.

Russell RO, Donaghy N, Meyer EC & Goodson KM (1993) Everlasting BOF linings at LTV Steel. Proceedings 1st European Oxygen Steelmaking Congress: 220–225.

Ruuska J, Ollila S & Leiviskä K (2003) Temperature model for LD-KG converter. IFAC Workshop on New Technologies for Automation of the Metallurgical Industry, Shanghai, China: 69–74.

Ruuska J, Ollila S & Leiviskä K (2004) Temperature and Additional Material Models for LD-KG converter. Materia 2: 38–42.

Ruuska J, Ollila S & Leiviskä K (2005) Data Classification in Temperature Modelling of LD-KG Converter. 16thIFAC World Congress, Prague, CzechRepublic: 1–6.

Ruuska J, Ollila S, Bååth L & LeiviskäK (2006a) Possibilities to use new measurements to control LD-KG-converter. 5th European Oxygen Steelmaking Conference, Aachen, Germany: 210–217.

Ruuska J, Ollila S & Leiviskä K (2006b) Splashing in LD-KG-converter and variables having effect on it. IFAC Workshop – MMM'2006, Cracow, Poland: 32–37.

Ruuska J, Ollila S & Leiviskä K (2007)Model-based monitoring of basic oxygen furnace. 12th IFAC Symposium on Automation in Mining, Mineral and Metal Processing, Quebec, Canada: 47–51.

Shakirov S, Boutchenkov A, Galperine, G & Schrader B (2004) Prediction and Prevention of Slopping in a BOF. Iron & Steel Technology: 38–44.

Sharma SK, Hlinka JW & Kern DW (1977) The bath circulation, jet penetration and high-temperature reaction zone in BOF steelmaking. Iron and Steelmaker: 7–18.

Schmidt H, Opitz A, Muller J & Pirklbauer W (2000) Experience with an off-gas analysis system for process control in the LD converter. Metallurgical Plant and Technology International 5: 60–62, 66–67.

Standish N & He QL (1989) Drop generation due to an impinging jet and the effect of bottom blowing in the steelmaking vessel. ISIJ International 29: 455–461.

Stroomer-Kattenbelt C (2008) Modeling and optimization of slopping prevention and batch time reductionin basic oxygen steelmaking. Netherlands, Enschede.

Tabata Y, Marsh R, Kelly P & Masaoka T (1998) Improvement of BOP steel refining blowing control using wide angle lance nozzles. 81st Steelmaking Conference Proceedings, Toronto, Canada: 451–457.

Tanaka T & Okane K (1987) Interaction between gas and liquid by means of jet of top lance. Transactions ISIJ 27: B–7.

Tang P, Yu Y, Wen G, Zhu M, Zhou L, Long Y & Liang Q (2008) Study on the optimization of the combined blown converter process in Chongqing Iron and Steel company. Journal of University of Science and Technology Beijing, 15: 5–9.

Thornton G & Welbourn B (1996) Reduction in BOS fume losses by the applicationof x-ray fluorescence measurements. 79thConference of the Steelmaking Divisionof the Iron and Steel Society, Pittsburgh, Pennsylvania, USA: 123–127.

Turkdogan ET (1996) Fundamentals of Steelmaking. London United Kingdom, Institute of Materials.

Valentino G, Mancano G & Cesare A (1997) A use of new lance tips in Steel-shop No. 1 at Ilva Taranto. 2nd European Oxygen Steelmaking Conference, Taranto, Italy: 79–84.

Viana JF & Castro LFA (2004) Converter oxygen blowing model based on neural networks. Scanmet II, Luleå, Sweden 1: 205–214.

Wang X, Wang ZJ & Tao J (2006) Multiple neural network modelling method for carbon and temperature estimation in basic oxygen furnace. 3rd International Symposium on Neural Networks, Chengdu, China 1: 870–875.

Yang L, Liu L & He P (2002) [%P] prediction and control model for oxygen-converter process at the end point based on adaptive neuro-fuzzy system. Proceedings of the 4th World Congress on Intelligent Control and Automation, Shanghai, China: 1901–1905.

Ylönen H, Jauhola M, Marttio S & Ollila S (1999a) The use of novel technologies at a steel plant to improve process control and performance. 82nd Steelmaking Conference Proceedings, Chicago, Il, USA: 199–210.

Ylönen H, Jauhola M, Marttio S & Ollila S (1999b) The use of novel technologies at a steel plant to improve process control and performance. Scanmet I, Luleå Sweden 1: 361–377.

Zhao H, Yuan Z, Wang W, Pan Y & Li S (2010) A novel method of recycling CO_2 for slag splashing in converter. J Iron and Steel Research International 17(12): 11–16.

Zhi-Gang H, Liu L, Ping H & Ming-Xiang T (2003) A dynamical off-gas model on a 150t BOF. Steel Times International 3: 11–12.

Appendix 1 The number of heats and temperature target window hit rates in 4284, 4284Temp and 2929 test sets

−10 °C ... 25 °C, −25 °C ... 10 °C and −10 °C ... 10 °C are different temperature target windows. Current, kk-ka, kk-kamod, mod > 20 and mod < 20 are models presented in Chapter 4.2.1.

4284 (4284 heats)	current	kk-ka	kk-kamod	mod > 20	mod < 20
−10 °C < x < 25 °C					
Number on target	3152	1798	2901	3152	1443
Share on target	73.58%	41.97%	67.72%	73.58%	33.68%
−25 °C < x < 10 °C	3040			3040	
−10 °C < x < 10 °C					
Number on target	2317	1481	2228	2317	1216
Share on target	54.08%	34.57%	52.01%	54.08%	28.38%

4284Temp (3364 heats)	current	kk-ka	kk-kamod	mod > 20	mod < 20
−10 °C < x < 25 °C					
Number on target	2409	960	2133	2409	600
Share on target	71.61%	28.54%	63.41%	71.61%	17.84%
−25 °C < x < 10 °C	3122			3122	
−10 °C < x < 10 °C					
Number on target	1958	923	1822	1958	591
Share on target	58.20%	27.44%	54.16%	58.20%	17.57%

2929	current	kk-ka	kk-kamod	mod > 20	mod < 20
−10 °C < x < 25 °C	2096	765	1822	2161	469
Number on target	71.56%	26.12%	62.21%	73.78%	16.01%
Share on target					
−25 °C < x < 10 °C	2400			2365	
−10 °C < x < 10 °C					
Number on target	1755	742	1600	1779	465
Share on target	59.92%	25.33%	54.63%	60.74%	15.88%

Appendix 2 The number of heats and temperature target window hit rates in 120B1, 105B1, 120B2 and 105B2 test sets

120B1, 105B1, 120B2 and 105B2 are models presented in Chapter 4.2.2.

120B1 (1570 heats)	current	kk-ka	kk-kamod	mod > 20	120B1
−10 °C < x < 25 °C					
Number on target	1142	392	991	1142	1142
Share on target	72.74%	24.97%	63.12%	72.74%	72.74%
−25 °C < x < 10 °C	1310				1310
−10 °C < x < 10 °C					
Number on target	954	386	858	954	954
Share on target	60.76%	24.59%	54.65%	60.76%	60.76%

105B1 (212 heats)	current	kk-ka	kk-kamod	mod > 20	105B1
−10 °C < x < 25 °C					
Number on target	73	13	57	73	150
Share on target	34.43%	6.13%	26.89%	34.43%	70.75%
−25 °C < x < 10 °C	169				186
−10 °C < x < 10 °C					
Number on target	72	13	57	72	134
Share on target	33.96%	6.13%	26.89%	33.96%	63.21%

120B2 (1366 heats)	current	kk-ka	kk-kamod	mod > 20	120B2
−10 °C < x < 25 °C					
Number on target	1094	505	1004	1094	1057
Share on target	80.09%	36.97%	73.50%	80.09%	77.38%
−25 °C < x < 10 °C	1051				1097
−10 °C < x < 10 °C					
Number on target	844	485	838	844	847
Share on target	61.79%	35.51%	61.35%	61.79%	62.01%

105B2 (145 heats)	current	kk-ka	kk-kamod	mod > 20	105B2
−10 °C < x < 25 °C					
Number on target	74	24	56	74	104
Share on target	51.03%	16.55%	38.62%	51.03%	71.72%
−25 °C < x < 10 °C	115				114
−10 °C < x < 10 °C					
Number on target	70	24	54	70	82
Share on target	48.28%	16.55%	37.24%	48.28%	56.55%

Appendix 3 Average values and standard deviations of slopes of different groups in BOF 1 and BOF 2

Presented in Chapter 4.2.4.

BOF1	HeatBig			HeatSmall
	C1Temp1&2	C2Temp1&2	C3Temp1&2	C1&C2
t < 80s	(114 heats)	(451 heats)	(252 heats)	(26 heats)
Average	0.60	0.60	0.64	0.64
St dev	0.145	0.138	0.124	0.140
t ≥ 80s	(84 heats)	(417 heats)	(229 heats)	(16 heats)
Average	0.50	0.55	0.58	0.62
St dev	0.089	0.104	0.086	0.115
	C1Temp3	C2Temp3	C3Temp3	C3
t < 80s	(27 heats)	(201 heats)	(83 heats)	(127 heats)
Average	0.48	0.54	0.54	0.69
St dev	0.105	0.130	0.125	0.142
t ≥ 80s	(32 heats)	(205 heats)	(87 heats)	(142 heats)
Average	0.43	0.48	0.52	0.65
St dev	0.098	0.106	0.081	0.093
Temp rise < 20 °C	HeatBig			HeatSmall
Average	0.33			0.38
St dev	0.193			0.220

BOF2	HeatBig			HeatSmall
	C1Temp1&2	C2Temp1&2	C3Temp1&2	C1&C2
t < 80s	(173 heats)	(372 heats)	(163 heats)	(35 heats)
Average	0.56	0.58	0.58	0.58
St dev	0.144	0.136	0.121	0.136
t ≥ 80s	(142 heats)	(467 heats)	(192 heats)	(26 heats)
Average	0.50	0.53	0.56	0.57
St dev	0.076	0.097	0.083	0.108
	C1Temp3	C2Temp3	C3Temp3	C3
t < 80s	(37 heats)	(128 heats)	(39 heats)	(101 heats)
Average	0.47	0.52	0.52	0.67
St dev	0.138	0.118	0.112	0.139
t ≥ 80s	(53 heats)	(153 heats)	(46 heats)	(121 heats)
Average	0.45	0.47	0.51	0.66
St dev	0.094	0.118	0.112	0.102
Temp rise < 20 °C	HeatBig			HeatSmall
Average	0.29			0.33
St dev	0.170			0.197

Appendix 4 Average values and standard deviations of slopes of different groups in BOF 1 and BOF 2

Presented in Chapter 4.2.4.

	HeatBig			HeatSmall	
	C1	C2	C3	C1&C2	C3
BOF1					
50–100s	(544 heats)	(412 heats)	(341 heats)	(33 heats)	(147 heats)
Average	0.53	0.55	0.58	0.61	0.67
St dev	0.127	0.120	0.108	0.124	0.115
40–110s	(658 heats)	(530 heats)	(431 heats)	(40 heats)	(183 heats)
Average	0.54	0.56	0.58	0.62	0.68
St dev	0.127	0.119	0.108	0.122	0.117
60–90s	(346 heats)				
Average	0.52				
St dev	0.127				
BOF2					
50–100s	(525 heats)	(325 heats)	(205 heats)	(46 heats)	(128 heats)
Average	0.52	0.54	0.55	0.58	0.66
St dev	0.119	0.124	0.109	0.141	0.136
40–110s	(658 heats)	(422 heats)	(269 heats)	(54 heats)	(163 heats)
Average	0.52	0.54	0.56	0.58	0.67
St dev	0.120	0.120	0.106	0.133	0.130

Appendix 5 Hit rates of different groups in BOF 1 and BOF 2

Presented in Chapter 4.2.5.

BOF1	Without adaptation	With adaptation
Heat Big		
C1		
50–100s	11(17) heats → 64.7%	11(17) heats → 64.7%
40–110s	14(22) heats → 63.6%	13(22) heats → 59.1%
C2		
50–100s	140(213) heats → 65.7%	134(213) heats → 62.9%
40–110s	183(273) heats → 67.0%	178(273) heats → 65.2%
C3		
50–100s	176(262) heats → 67.2%	169(262) heats → 62.9%
40–110s	239(340) heats → 70.3%	233(340) heats → 68.5%
HeatSmall		
C1&C2		
50–100s	6(8) heats → 75.0%	6(8) heats → 75.0%
40–110s	8(10) heats → 80.0%	8(10) heats → 80.0%
C3		
50–100s	34(45) heats → 75.6%	34(45) heats → 75.6%
40–110s	47(61) heats → 77.0%	47(61) heats → 77.0%
BOF2		
Heat Big		
C1		
50–100s	30(48) heats → 62.5%	31(48) heats → 64.6%
40–110s	51(70) heats → 72.9%	51(70) heats → 72.9%
C2		
50–100s	167(258) heats → 64.7%	198(258) heats → 76.7%
40–110s	205(311) heats → 65.9%	236(311) heats → 75.9%
C3		
50–100s	89(132) heats → 67.4%	89(132) heats → 67.4%
40–110s	118(176) heats → 67.0%	118(176) heats → 67.0%
HeatSmall		
C1&C2		
50–100s	4(6) heats → 66.7%	5(6) heats → 83.3%
40–110s	6(9) heats → 66.7%	7(9) heats → 77.8%
C3		
50–100s	25(40) heats → 62.5%	23(40) heats → 57.5%
40–110s	34(54) heats → 63.0%	33(54) heats → 61.1%

401. Huttunen, Sami (2011) Methods and systems for vision-based proactive applications

402. Weeraddana, Pradeep Chathuranga (2011) Optimization techniques for radio resource management in wireless communication networks

403. Räsänen, Teemu (2011) Intelligent information services in environmental applications

404. Janhunen, Janne (2011) Programmable MIMO detectors

405. Skoglind-Öhman, Ingegerd (2011) Participatory methods and empowerment for health and safety work : Case studies in Norrbotten, Sweden

406. Kellokumpu, Vili-Petteri (2011) Vision-based human motion description and recognition

407. Rahko, Matti (2011) A qualification tool for component package feasibility in infrastructure products

408. Rajala, Hanna-Kaisa (2011) Enhancing innovative activities and tools for the manufacturing industry: illustrative and participative trials within work system cases

409. Sinisammal, Janne (2011) Työhyvinvoinnin ja työympäristön kokonaisvaltainen kehittäminen – tuloksia osallistuvista tutkimus- ja kehittämisprojekteista sekä asiantuntijahaastatteluista

410. Berg, Markus (2011) Methods for antenna frequency control and user effect compensation in mobile terminals

411. Arvola, Jouko (2011) Reducing industrial use of fossil raw materials : Techno-economic assessment of relevant cases in Northern Finland

412. Okkonen, Jarkko (2011) Groundwater and its response to climate variability and change in cold snow dominated regions in Finland: methods and estimations

413. Anttonen, Antti (2011) Estimation of energy detection thresholds and error probability for amplitude-modulated short-range communication radios

414. Neitola, Marko (2012) Characterizing and minimizing spurious responses in Delta-Sigma modulators

415. Huttunen, Paavo (2012) Spontaneous movements of hands in gradients of weak VHF electromagnetic fields

416. Isoherranen, Ville (2012) Strategy analysis frameworks for strategy orientation and focus

Book orders:
Granum: Virtual book store
http://granum.uta.fi/granum/

UNIVERSITY OF OULU P.O.B. 7500 FI-90014 UNIVERSITY OF OULU FINLAND

ACTA UNIVERSITATIS OULUENSIS

ISBN 978-951-42-9801-1 (Paperback)
ISBN 978-951-42-9802-8 (PDF)
ISSN 0355-3213 (Print)
ISSN 1796-2226 (Online)

UNIVERSITY of OULU
OULUN YLIOPISTO